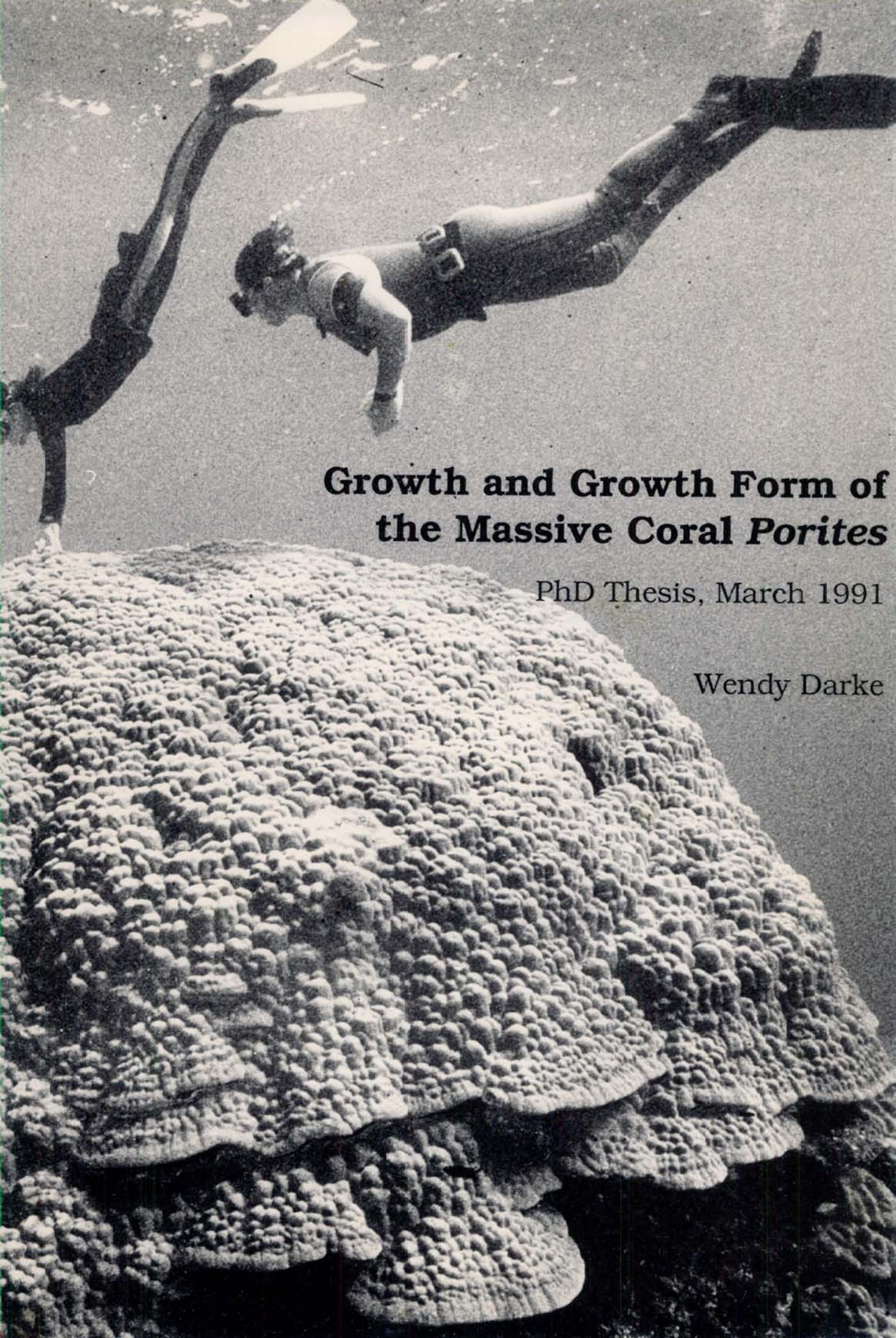

Growth and Growth Form of the Massive Coral *Porites*

PhD Thesis, March 1991

Wendy Darke

GROWTH AND GROWTH FORM OF THE MASSIVE CORAL *PORITES*

Thesis submitted by
Wendy Marilyn DARKE BSc(Hons) (Bristol, UK)
in March 1991

for the degree of Doctor of Philosophy in
the Marine Biology Department, School of Biological Sciences
at James Cook University of North Queensland

I, the undersigned, the author of this thesis, understand that James Cook University of North Queensland will make it available for use within the University Library and, by microfilm or other photographic means, allow access to users in other approved libraries. All users consulting this thesis will have to sign the following statement:

> "In consulting this thesis I agree not to copy or closely para-phrase it in whole or in part without the written consent of the author; and to make proper written acknowledgement for any assistance which I have obtained from it."

Beyond this, I do not wish to place any restriction on access to this thesis.

..... 25/3/91

(signature) (date)

ABSTRACT

Massive *Porites* colonies develop a bumpy growth surface as they increase in size. Development of a bumpy growth surface occurs when skeletal growth no longer provides the necessary increase in surface area to accommodate tissue growth. A massive *Porites* colony becomes bumpy when it reaches a critical size determined by the ratio of its tissue growth to its skeletal growth. This ratio also determines the degree of bumpiness which develops at the growth surface.

X-radiographs of skeletal slices cut from the vertical growth axis of massive *Porites* colonies display annual density banding and skeletal architecture associated with corallites, that is, skeleton deposited by individual polyps. Density bands outline former positions of the growth surface. Examination of X-radiographs of *Porites* shows that new corallites are initiated on, or towards, the summit of bumps, whilst older corallites are compressed and ultimately occluded at the bottom of valleys formed between bumps. X-radiographs show that it takes 4 to 7 years from the formation of a corallite to its occlusion. Polyps on the growth surface of a bumpy *Porites* colony must, therefore, be continually lost. All polyps are lost and replaced during a 4 to 7 year period. Consequently, tissue covering the growth surface of a massive *Porites* colony can be no older than 7 years, even though the colony may have been growing for several centuries.

Computer models designed to simulate growth of a massive *Porites* colony indicated that the growth form displayed by a *Porites* colony is determined by the ratio of tissue growth to skeletal growth. Models having a relatively faster tissue growth compared with skeletal growth developed a bumpy surface sooner, and the amount of bumpiness developed was greater, than for models having a relatively slower tissue growth compared with skeletal growth. Predictions from computer models accorded with observations and measurements made on actual colonies and on X-radiographs of skeletal slices cut from colonies. Thus, the ratio of tissue growth to skeletal growth determines important aspects of the growth form displayed by massive *Porites* colonies.

The ratio of tissue growth to skeletal growth was shown to significantly affect the rate of polyp loss and replacement in *Porites* colonies. The longevity of polyps is less in *Porites* colonies displaying a well developed bumpy growth surface than in colonies displaying a smoother growth surface. Hence, the age of polyps, and therefore the tissue, covering a bumpy growth surface is less than polyps and tissue covering a smooth growth surface.

Skeletal surface area in massive *Porites* colonies was shown to be a useful indicator of tissue biomass. Measurements of change in surface area of *Porites* colonies with increasing size show that the rate of tissue growth must decrease as the colony grows. Development of a bumpy growth surface alleviates this geometric restriction for only months to a couple of years. Development of a bumpy growth surface is an indication that tissue growth is becoming constrained by skeletal growth. Once a colony becomes bumpy, the tissue growth is almost totally constrained by the rate by skeletal extension.

Significant differences in growth and growth form characterised massive *Porites* colonies collected from different reef environments. Measurements made on the colonies suggested that differences in environmental conditions probably altered the ratio of tissue growth to skeletal growth and caused the colonies to grow in different ways. Differences in growth were reflected in the resulting growth form. Information about relative rates of tissue and skeletal growth within a massive *Porites* colony gained from observations and measurements of the growth form can be used to provide further information about coral growth and details of environmental conditions obtaining during growth.

CONTENTS

PLATES

FIGURES

Figure **Page**

DECLARATION

I declare that this thesis is my own work and has not been submitted in any form for another degree or diploma at any university or other institution of tertiary education. Information derived from the published or unpublished work of others has been acknowledged in the text and a list of references is given.

W M Darke
25 March 1991

ACKNOWLEDGEMENTS

Many people have given their time, understanding and expertise to enable me to convert an assortment of ideas, into the scientific research presented in this thesis. I hope that this work does justice to all of the people who have contributed to my project.

Thanks and appreciation to Dr. David Barnes and Dr. John Collins who have provided never-ending support, enthusiasm and encouragement. I consider myself to have been very fortunate in having such a complementary set of supervisors. Their guidance, wealth of knowledge and kindness has played a major role in the culmination of this work. A special thank you to David Barnes for his patience and dedication to the improvement of my writing skills, and to John Collins for his understanding of the difficulties associated with embarking on new research.

I was also very fortunate to have Barry Tobin tutor me in computers and computer programming when I first arrived at the Australian Institute of Marine Science (AIMS). I am especially grateful to Barry for relaying his expertise of computing and for his assistance and patience with computer problems encountered during this study. Thanks to Dr. Janice Lough for her helpful comments with many aspects of this research, but particularly for her advice and expertise on statistical matters associated with this work.

I have been extremely impressed with the outstanding level of technical support that Monty Devereux has given me with many of the experimental procedures performed in this study; particularly with the painstaking task of processing over 500 protein and chlorophyll samples. I am also especially grateful to Monty for the kindness and moral support he has shown me during the past three years. Jane Wu Won has also provided excellent assistance with experimental aspects of this work for which I am very grateful. I would also like to thank, the staff of the computer section at AIMS, Nick Harcock, Malcolm McKenzie, Bob McDonald and Coral

Graham, who have all provided help with computer problems. Monty and Jane, along with all of the other AIMS staff who have helped me with aspects of this research have never failed to impress me with their willing attitude to help and their dedication to their work.

There have been many people who have stepped in at various stages of this research and provided much needed and valuable contributions to the work; Dr. Bruce Chalker provided the necessary equations required for the chlorophyll determination, and very helpful comments on several parts of the research. Dr. Michel Pichon provided assistance with the difficult task of *Porites* species identification. In addition to Dr. Janice Lough, Dr. Glen De'arth, Dr. Ross Alford and Debbie Rae provided help and advise with statistical procedures used. Hua Wang helped me with the mathematical equations used for the computer models. Dr. John Chisholm and Dr. Jean-Pierre Gatusso have both provided very useful comments and criticisms relating to several aspects of this work. I am especially grateful to all of these people for the contributions they have made to this thesis.

I was very impressed with the excellent quality of photographic plates and figures presented in this thesis. Thanks to Karen Handley for producing the photographic plates and to Marietta Eden for helpful suggestions for improving and for drawing the figures. I would also like to thank Dr. Peter Moran for the frontispiece photograph and Dr. Peter Isdale for initiating the idea. Thanks also to Steve Clarke for arranging the text on the frontispiece.

I wish to thank the crews of the AIMS research vessels, R.V. *Lady Basten*, R.V. *Sirius*, R.V. *Pegasus* and especially the crew of the R.V. *Harry Messel* who have provided such a high standard of logistical support. I would also like to thank John Hardman of the AIMS marine operations unit for his help with supplying of equipment used for field work.

I wish to thank the Science and Engineering Research Council, U.K. for providing a 3 year PhD scholarship which has enabled me to undertake this research.

I am very grateful to Dr. Joe Baker, the Director of AIMS, for giving me the opportunity to carry out research at AIMS where I have been able to make full use of the excellent research facilities and expertise of the AIMS staff. I would also like thank Prof. Howard Choat, of the Marine Biology Department James Cook University, and the Science and Engineering Research Council for contributing to the cost of field trips and conferences I have been fortunate enough to attend.

Finally, there are many people who I would very much like to thank, who have cared about me, and have provided very important personal encouragement. These people have helped me to keep everything in perspective, so that I have enjoyed life and enjoyed doing my research. Very special thanks to my parents, family and friends back in England who have maintained close supportive links via correspondence. I would also especially like to thank Patricia Crowle, Pornsook Chongprasith and Kay Johnston for their friendship, kindness and invaluable personal support and encouragement, particularly when it was most needed. I wish to thank Chris Platt for his encouragement throughout this research and to thank Steve O'Reilly and Danielle Johnston for providing personal support and encouragement during the final stages of the thesis write-up.

CHAPTER 1

BACKGROUND AND OBJECTIVES

1.1. INTRODUCTION TO THESIS.

Coral reefs are unique ecosystems in that they leave behind a record of their growth and activity which may extend far back into geological times. The coral reef literature is permeated by the notion that the form and shape of colonial reef corals alters with environmental conditions. Certain links between growth form and environment are well established. What has been lacking is an understanding of the biology which links a coral's growth form to its environment. There have been few attempts to link coral biology with colonial growth form so that it becomes possible to decipher the record of environment inherent in colonial form. The work presented here arose from attempts to understand the mechanisms involved in coral growth which might modify colonial growth form. The goal with which this work began was to be able to better understand a coral's environment from some of the records it creates by growing.

1.1.1. Tissue growth to skeletal growth relationships in massive corals.

Coral growth involves both an increase in tissue and an increase in skeleton. This feature of growth has received little attention. Obviously, skeleton cannot be generated without tissue. Equally, in hard corals, tissue requires skeleton as a substrate and for support. Barnes (1973) pointed out that differentials between tissue growth and skeletal growth may profoundly affect the form of the colony produced.

He also examined ways in which different modes of asexual division and associated skeletal growth might affect the relationship between tissue growth and skeletal growth. Barnes' ideas have their simplest expression in a coral such as *Porites*, in which small polyps sit in small skeletal cups, the calices, which share common walls (Plate 1.1). *Porites* is a common genus of coral with a word-wide distribution. It can grow for centuries and form massive colonies several metres high (Veron and Pichon, 1982; Potts *et al.*, 1985; Veron, 1986). It appears to have an exceptionally plastic growth morphology (Roos, 1967; Brakel, 1976, 1983). Massive colonies range from plate-like through hemispherical to columnar, several species have a branching growth form and certain species appear to bridge the gap between massive and branching forms. *Porites* was the genus chosen for work on growth form described here. The work was limited to massive, rounded growth forms belonging to species that have the potential to form colonies over 500 mm high (Page 26).

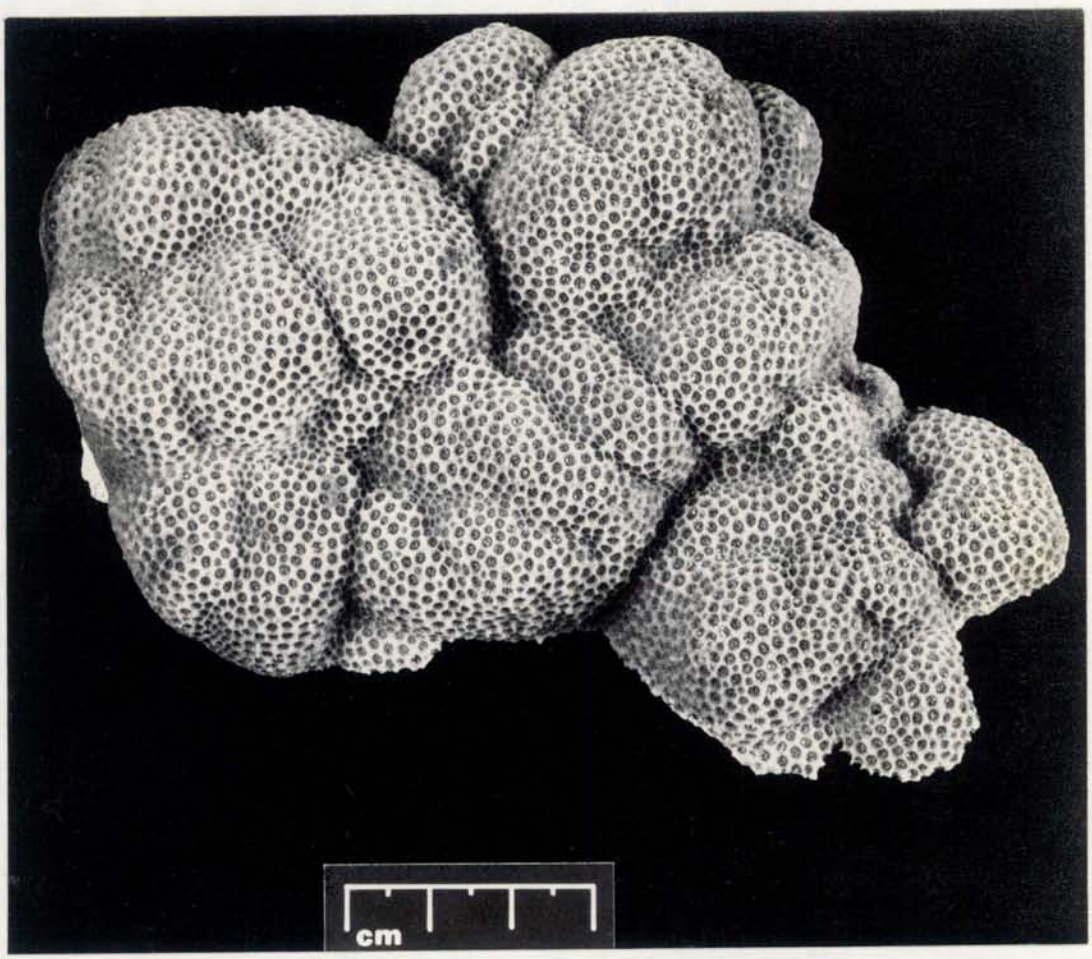

Plate 1.1. Specimen of *P.lobata* displaying calices on the upper growth surface.

Coral colonies are an accumulation of interconnected polyps lying roughly side by side. Each polyp is a tissue sack with only one entrance, the mouth, at the upper surface. The mouth is surrounded by a ring of tentacles. The tentacles, and internal divisions within the polyp are arranged in multiples of 6. This distinguishes the hard corals, the hexacorallia, from the soft corals, the octocorallia, in which the tentacles and internal polypary compartments are arranged in multiples of 8.

The wall of the sack is made up of two layers of cells, the ectodermis and endodermis separated by a connective layer, usually considered to be acellular, called the mesoglea. The endodermis is sometimes called the gastrodermis because it lines the internal, digestive cavity of the sack, the coelenteron. The ectodermis is divided into 2 parts. The free ectodermis covers those parts of the sack which are in contact with the environment. The free ectodermis is histologically distinct from the calicoblastic ectodermis, which invests and secretes the calcium carbonate skeleton. Thus, skeletal deposition in hard corals is usually considered to occur outside the animal, beneath this lower, calicoblastic layer of tissue.

Johnston (1980) provides a very clear review of the processes of skeletal deposition of scleractinian corals. Histological and histochemical aspects of calcification form a central part of this review. Barnes and Chalker (1990) provide another, excellent review which is more centred on physiological and biochemical aspects of calcification. Johnston comes from a school which believes that an organic matrix has a controlling role in the precipitation of calcium carbonate, and the shape, form and arrangement of the precipitated crystals. Barnes and Chalker belong to a school which maintains that, if there indeed exists a matrix, it does not play a central role in controlling the orientation in which crystals are precipitated.

Massive *Porites* colonies increase in size by the extension of existing polyps and the addition of new polyps. New polyps are formed by extratentacular budding from existing polyps (Wells, 1956). This simply means that existing polyps remain "intact" and new polyps develop by rearrangement of the tissues connecting adjacent polyps. For growth of new polyps to occur in a massive *Porites* colony, the skeleton

surface area must be increased (Fig. 1.1). Thus, tissue growth and skeletal growth are mutually inter-dependant in *Porites*, as in all corals.

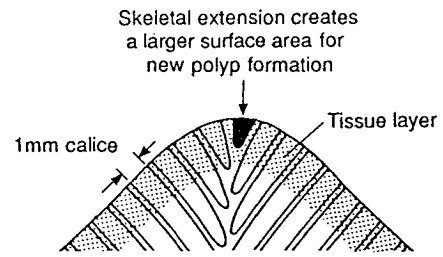

Fig. 1.1. Diagrammatic representation of a longitudinal section through a bump on the growth surface of a massive *Porites* colony.

Barnes (1973) showed, using mathematical models, that a hemispherical, colonial coral growth form would need to increase its rate of linear extension with each doubling of the tissue growth surface. Figure 1.2. illustrates this idea. The figure illustrates that, if a massive, hemispherical colony is to maintain a smooth growth surface and constant tissue growth, skeletal extension must increase as a colony becomes bigger.

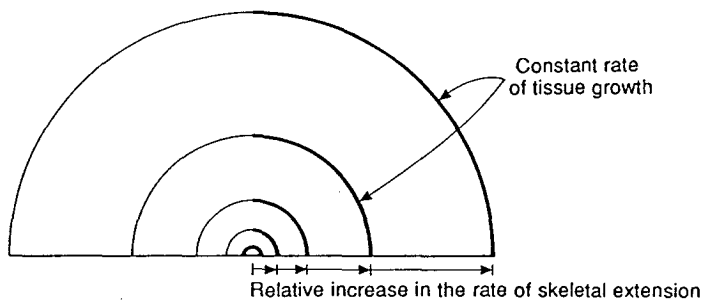

Fig. 1.2. Hemispherical, coral growth form model displaying a constant rate of tissue growth.

Alternatively, if a massive, hemispherical coral maintains a smooth growth surface and constant skeletal extension, then tissue growth must decrease as the colony grows. Figure 1.3 illustrates that tissue growth must decrease with increasing colony size if skeletal extension remains constant.

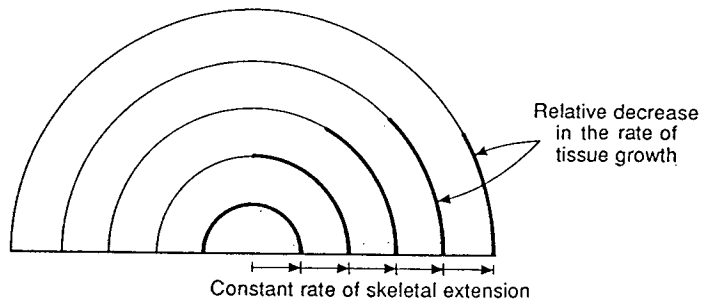

Fig. 1.3. Hemispherical, coral growth form model displaying a constant rate of skeletal extension.

On the basis of the theoretical models described above, and the presumption that massive corals display a constant rate of skeletal extension as they increase in size, Barnes (1973) suggested that, as massive corals increase in size, they encounter problems with accommodation of tissue growth [a first description of skeletal density banding in corals (Knutson *et al.*, 1972) appeared when Barnes' paper was in press and Barnes refers to the implications for his models of density banding in an addendum added before publication]. It was apparent to Barnes that the rate of tissue growth would become constrained by the rate of skeletal extension once a colony reached a certain size. This size he suggested would be determined by the relative rates of tissue growth to skeletal growth within a colony i.e., the ratio of tissue growth:skeletal growth. Thus, he envisaged that colonies with a relatively fast tissue growth, compared with skeletal growth, would encounter this constraint sooner than colonies with lower tissue growth to skeletal growth ratios.

Barnes (1973) suggested that the development of a bumpy growth surface, a characteristic displayed by all massive *Porites* colonies, offered a means of increasing the skeletal surface area for accommodation of tissue growth as a colony increased in size and tissue growth became constrained. It was implied by Barnes that the development of a bumpy growth surface overcame this constraint. To test this implied hypothesis, a technique was developed to estimate surface area presented by a bumpy *Porites* colony. The technique was used to assess the extent to which development of a bumpy growth surface provides a larger surface area for accommodation of tissue growth as *Porites* colonies increase in size (Chapter 5).

1.1.2. Relationships between tissue growth:skeletal growth ratios and colonial growth form.

It appeared to Barnes (1973) that tissue growth and skeletal growth within a coral may be controlled, to some extent, independently of each other by external factors. This idea is based on the understanding that different environmental factors influence tissue growth and skeletal growth in slightly different ways. According to Barnes it is more appropriate to express coral growth as the ratio of tissue growth to skeletal growth. He suggests that, if variations in the ratio of tissue growth:skeletal growth occur between coral colonies of the same species, then the differences in the ratio are likely to have their greatest affect on the rate of polyp division. This, in turn, affects the growth form of the colony.

It can be inferred from observation of overall growth forms displayed by massive *Porites* colonies that differences in the ratio of tissue growth to skeletal growth between colonies must exist. Massive *Porites* colonies display a variety of growth forms ranging from hemispherical through to columnar to plate-like (Roos, 1967; Brakel, 1976, 1983). These variations in growth form result from differentials in rates of skeletal extension over the growth surface of a colony (Fig. 1.4).

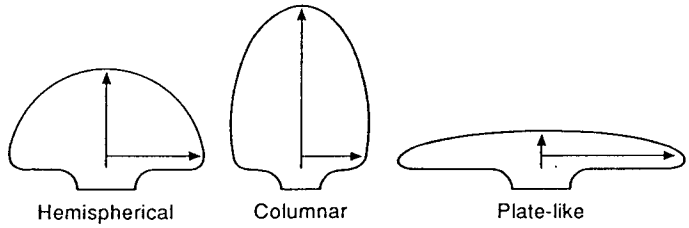

Fig. 1.4. Massive coral growth forms displaying different relative rates of skeletal extension.

The ratio of tissue growth to skeletal growth in these three growth forms (Fig. 1.4) must be different. Figure 1.5. shows that, although the amount of tissue covering both the hemispherical and plate-like colony is the same, the amount of skeletal growth necessary to support this amount of tissue was very different between the 2 colonies. Hence, very different ratios of tissue growth to skeletal growth were associated with formation of these different growth forms.

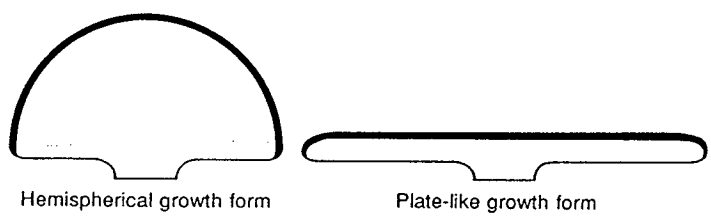

Fig. 1.5. Hemispherical and plate-like growth forms displaying the same amount of tissue but considerably different amounts of skeleton.

This study investigates whether differences in the ratio of tissue growth:skeletal growth amongst *Porites* colonies are reflected by the growth form displayed by a colony. Initially, computer simulations of massive *Porites* growth and growth forms were used to discover aspects of *Porites* growth and growth form which would otherwise have taken years of field work. Very simple models were

constructed in which growth involved iterative addition of new "corallites" and in which the ratio of tissue growth to skeletal growth could be changed (Chapter 3). Predictions from these models about colonial growth form developed using different tissue growth to skeletal growth ratios are tested against reality (Chapter 5).

1.1.3. Relationships between the environment of a *Porites* colony and aspects of its growth and growth form.

The importance of integrating environmental factors with measurements of coral growth and growth form to compile a complete picture of coral growth was emphasised by Buddemeier and Kinzie (1976) in an extensive review of coral growth. Despite this, work on growth form has continued to draw upon correlations between colony shape and environmental conditions. There have been few attempts to develop a mechanistic understanding of the relationship between growth form and environment. Such mechanistic understanding must, inevitably, be based upon measurements of the way in which growth alters with environment. Here too, workers developing such understanding have seldom attempted to relate physiological responses to growth form.

Techniques used to measure skeletal growth.

Various techniques to estimate skeletal growth or calcification are described in the review on coral growth by Buddemeier and Kinzie (1976). A substantial amount of data on rates of skeletal growth in various coral species, from around the world, is presented in this review. Techniques most commonly used for estimating skeletal growth include: direct measurements of increase in linear dimension or surface area (Loya, 1976; Gladfelter, 1984; Brown *et al.*, 1985; Muscatine *et al.*, 1985); alizarin staining (Barnes, 1972, Macintyre and Smith, 1974; Dustan, 1975; Lamberts, 1978; Brown *et al.*, 1985); annual density banding (Knutson *et al.*, 1972; Macintyre and Smith, 1974; Hudson *et al.*, 1976; Stearn *et al.*, 1977); increase in

mass (or weight) of coral skeletons, (Jokiel *et al.*, 1978; Davies, 1989); radioactive tracers (Goreau, 1959; Clausen and Roth, 1975; Barnes and Crossland, 1977, 1982); alkalinity anomaly techniques (Smith and Kinsey, 1978; Dennison and Barnes, 1988), and radiometric dating techniques (Moore and Krishnaswami, 1972, 1974; Moore *et al.*, 1973; Dodge and Thomson, 1974; Noshkin *et al.*, 1975).

Environmental factors which affect skeletal growth.

It is apparent from the literature that light, acting through the symbiotic zooxanthellae present in the gastrodermal coral tissue layer, is the major environmental factor which influences skeletal growth. Kawaguti and Sakumoto (1948) first proposed that light enhances calcification in reef-building corals. Goreau (1959; see also 1961, 1963; Goreau and Goreau, 1959, 1960) first conclusively demonstrated this effect. Vandermuelen *et al.* (1972) demonstrated that light-enhanced calcification results from photosynthesis by the zooxanthellae, and Chalker (1981) and Barnes (1982) showed that the light response curve for calcification essentially follows that for photosynthesis (see also Johnston, 1980; Barnes and Chalker, 1990). The process by which light enhances calcification, has not yet been established. Possible mechanisms to account for light-enhanced calcification are discussed in the review by Barnes and Chalker (1990).

Since light affects skeletal growth, several workers have been able to show that relationships exist between skeletal growth and other environmental factors which affect the ambient light intensity. These include; depth of water and turbidity (Dodge and Vaisnys, 1977; Huston, 1985; Kendall *et al.*, 1985).

Although some workers have shown that variations in skeletal growth are correlated with variations in sea temperature (e.g. Dodge and Vaisnys, 1975, 1980; Weber *et al.*, 1975a; Hudson *et al.*, 1976; Dunbar and Wellington, 1981; Dodge and Lang, 1983), it has not proved easy to isolate the effects of temperature on skeletal growth from the effects of light intensity. The temperature response curve for

calcification may be more complicated than the light response curve. In certain corals, temperatures outside an optimum range of 18°C to 31°C causes a reduction in coral respiration, zooxanthellar photosynthesis and calcification (Coles and Jokiel, 1977, 1978; Jokiel and Coles, 1977). However, the extent to which temperature controls skeletal growth has not been fully established.

Coral growth and calcification have been shown in laboratory studies to be significantly affected by water motion (Jokiel, 1978; Dennison and Barnes, 1988). Increased water motion appears to increase coral calcification. Dennison and Barnes (1988) suggested that water motion affects coral metabolism and calcification by altering the thickness of the boundary layer adjacent to the coral tissue. They envisaged that a change in the thickness in this boundary layer would affect the rate of diffusion of dissolved substances necessary for calcification.

Techniques for measuring tissue growth.

An early technique used to monitor tissue growth of a newly settled, massive *Porites* colony involved repeated photography. Counts were then made of polyps on the growth surfaces seen in consecutive photographs (Stephenson, 1931). This technique was applicable to massive *Porites* colonies because the polyps are not separated by coenosteal tissue (i.e., they are directly adjacent) and they are small and evenly spaced. This tedious technique is less feasible with large colonies where significant growth would take months to years to become apparent. It is also less applicable in genera having large, less evenly distributed polyps than does *Porites*.

It has proved much simpler to equate tissue biomass to the surface area of colonies covered by tissue and, hence, relate tissue growth to changes in surface area. Surface area has been estimated from linear dimensions and by the amount of aluminium foil or liquid latex required to cover the growth surface (Marsh, 1970; Loya, 1976; McCloskey and Muscatine, 1984; Muscatine *et al.*, 1985; Meyer and Schultz, 1985). All these methods are based on the assumption tissue biomass is directly proportional to skeletal surface area. This assumption has not been tested.

Surface area was used to estimate tissue biomass in studies described here. An investigation was carried out to assess whether measurements of the surface area of a massive *Porites* colony covered by tissue could be used to estimate tissue biomass (Chapter 4).

Environmental factors that affect tissue growth.

A coral's nutritional requirements may be met from both heterotrophic and autotrophic modes of nutrition (Muscatine, 1973, Sebens, 1987). Heterotrophic feeding habits displayed by corals include: capturing of zooplankton using nematocysts (stinging cells) and tentacles (Porter, 1974), trapping of particulate organic matter with mucus secreted on to the upper tissue growth surface (Lewis, 1975, 1976), absorption of bacteria and dissolved organics (Sorokin, 1973) and absorption of inorganic nutrients such as phosphorus, nitrogen and calcium (D'Elia, 1977). The relative importance of heterotrophic feeding has not yet been established and probably varies considerably between different species (see, for instance, Porter, 1976; Muscatine and Porter, 1977, Porter, 1985). Corals may depend upon heterotrophic nutrition to satisfy essential dietary requirements for organic materials containing nitrogen, phosphorus, calcium and vitamins (Sorokin, 1980, 1981).

Autotrophy has the potential to satisfy a considerable proportion of the energetic requirements of reef-building corals. It was first shown by Smith *et al.,* (1969) that carbon, photosynthetically fixed by zooxanthellae, is transported to, and used by, the coral host. Several workers have shown that light intensity affects the amount of carbon translocated to the coral host (e.g., McCloskey and Muscatine, 1984; Porter *et al.,* 1984). The importance of photosynthetically fixed carbon for coral tissue growth has yet to be established (Muscatine and Porter, 1977, Porter, 1985).

It seems that the nutritional requirements of corals may be met from zooxanthellae and several heterotrophic sources. In contrast, the literature suggests that the rate of calcification is almost entirely controlled by light intensity. Thus,

variations in environmental conditions may alter differently rates of tissue growth, calcification and skeletal growth. This study examines massive *Porites* colonies from different reefal environments to see if differences in growth form can be related to systematic differences in environment. In an attempt to develop a mechanistic, as well as correlatory link between growth form and environment, this examination was carried out with the idea that relative differences in tissue and skeletal growth would have a major role in determining colonial growth form (Chapter 5).

1.1.4. The choice of massive *Porites* for growth and growth form studies.

Porites forms the largest of all coral colonies. A very large, rounded *Porites* colony, 6.9 m in diameter, living on the Great Barrier Reef (G.B.R.) was found by Potts *et al.*, (1985) to be at least 677 years old. Veron (1986) describes some colonies living on the G.B.R. to be 8 m high, which, given an approximate growth rate of 10 mm yr^{-1} (see Isdale, 1977; Chivas *et al.*, 1983; Barnes and Lough, 1989; Lough and Barnes, 1990a), roughly corresponds to 800 years of growth. Thus, an intriguing question which might be asked of massive *Porites* colonies is; "what is the average age of polyps on the growth surface of such very large colonies?" This study uses observations and measurements of skeletal features displayed by X-radiographs of skeletal slices to determine the age of polyps covering the growth surface of massive *Porites* colonies (Chapter 2).

Other aspects of the choice of massive *Porites* for this study include the basic hemispherical growth form of shallow water, massive species and the uniform, cerioid arrangement of polyps on the growth surface (see 1.1.1; also Barnes, 1973). Polyps are added to the growth surface in the coenenchyme created between existing polyps as colonies increase in size. Thus, polyps are added, overall, in an iterative fashion. These features make massive *Porites* colonies well suited to computer simulations of growth and allow easy comparisons of the resultant growth forms with growth form in actual colonies (Chapter 3, Chapter 5).

Variations in the overall growth form displayed by massive *Porites* colonies have been related to differences in the environmental conditions surrounding the coral. For example, changes in growth form of *Porites asteroides*, from hemispherical to plate-like colonies, with increasing depth on a reef slope in the Caribbean were shown by Roos (1967) to be related to decrease in ambient light. Subsequent studies on variations in growth form of *P.asteroides* in the Caribbean (Brakel, 1983) showed that flattened growth forms were also present in shallow water as well as at depth. Brakel suggested that flattened colonies were present in shallow water due to high turbulence, and in deep water due to low light intensity. Thus, relationships between colonial growth form and environment are not necessarily direct and simple. A mechanistic account of a similar, non-linear response to a major environmental gradient is detailed here (Chapter 5).

1.2. GROWTH AND GROWTH FORM CHARACTERISTICS OF MASSIVE *PORITES.*

Porites belongs to the Phylum Cnidaria, Order Scleractinia and is represented by at least 16 species on the G.B.R. Six of these species have massive growth forms and grow to over 200 mm in diameter (Veron and Pichon, 1982; Veron, 1986). Massive *Porites* are some of the most important reef-building corals and often constitute the major proportion of the reef frame-work (Guzman and Cortes, 1989). *Porites* is a common reefal genus with abundant colonies on all the major reef systems of the world, including those of the Caribbean, and the Indian and Pacific Oceans.

Massive *Porites* colonies can be recognised under water from their shape (Plate 1.1), characteristic bumpy growth surface and small polyp diameter (averaging about 1 mm; Plate 1.2). Colour in *Porites* colonies varies from pink, purple-blue, through green, to brown and to cream. Colour does not seem to be related to species.

Plate 1.2. Massive *Porites* colony at Myrmidon Reef, central G.B.R.

Plate. 1.3. Specimen of *P. lobata* displaying the tissue layer within the skeleton.

Tissue covering the growth surface of a massive *Porites* colony forms a thin uniform veneer over the skeletal surface. This veneer is usually less than 10 mm thick (Plate 1.3).

1.3. SITES SELECTED FOR COLLECTION OF *PORITES*.

Environmental conditions associated with reefs situated across the entire shelf width of the central G.B.R vary considerably from near-shore to offshore reef localities (Wilkinson and Cheshire 1988). Near-shore reefs are exposed to extensive terrigenous input, particularly during the tropical wet season. During the summer wet season which runs from November to April, these reefs experience increased sedimentation, turbidity and nutrient availability, and decreased salinity. These conditions diminish with distance offshore. Reefs situated on the outer edge of the Barrier Reef are affected by oceanic conditions. The oceanic influences decrease towards the shore. Gradients in light transmittance, turbulence, nutrient availability and salinity, therefore, exist between reefs across the width of the central G.B.R (see Wilkinson and Cheshire 1988).

Massive *Porites* colonies collected for the major part of this study were selected from three reefs located across the central G.B.R. Samples used in the study included several species from a range of environments (Page 26, 27). Colonies were collected from Pandora Reef (18.49°S, 146.26°E), Rib Reef (18.29°S, 147.53°E) and Myrmidon Reef (18.16°S, 147.23°E) (Fig. 1.6). These were at, respectively, near-shore, mid-shelf and shelf-edge sites. Pandora and Myrmidon Reefs are planar reefs and Rib Reef is a crescentic reef (see Hopley, 1983 for details of morphological classifications).

Tissue samples used in analyses of tissue biomass per unit skeletal surface area were removed from *Porites* colonies growing at 2 reefs. These reefs were located at opposite ends of the G.B.R.: Yonge Reef, near Lizard Island, in the northern section of the G.B.R. (35.58°S, 135.63°E) and Reef 21/141 situated in the

north of the Swain Reefs group, at the south end of the G.B.R. (21.52°S, 151.5°E; Fig. 1.6). These reefs are subject to very different environmental conditions (see Maxwell, 1968, Hopley, 1983).

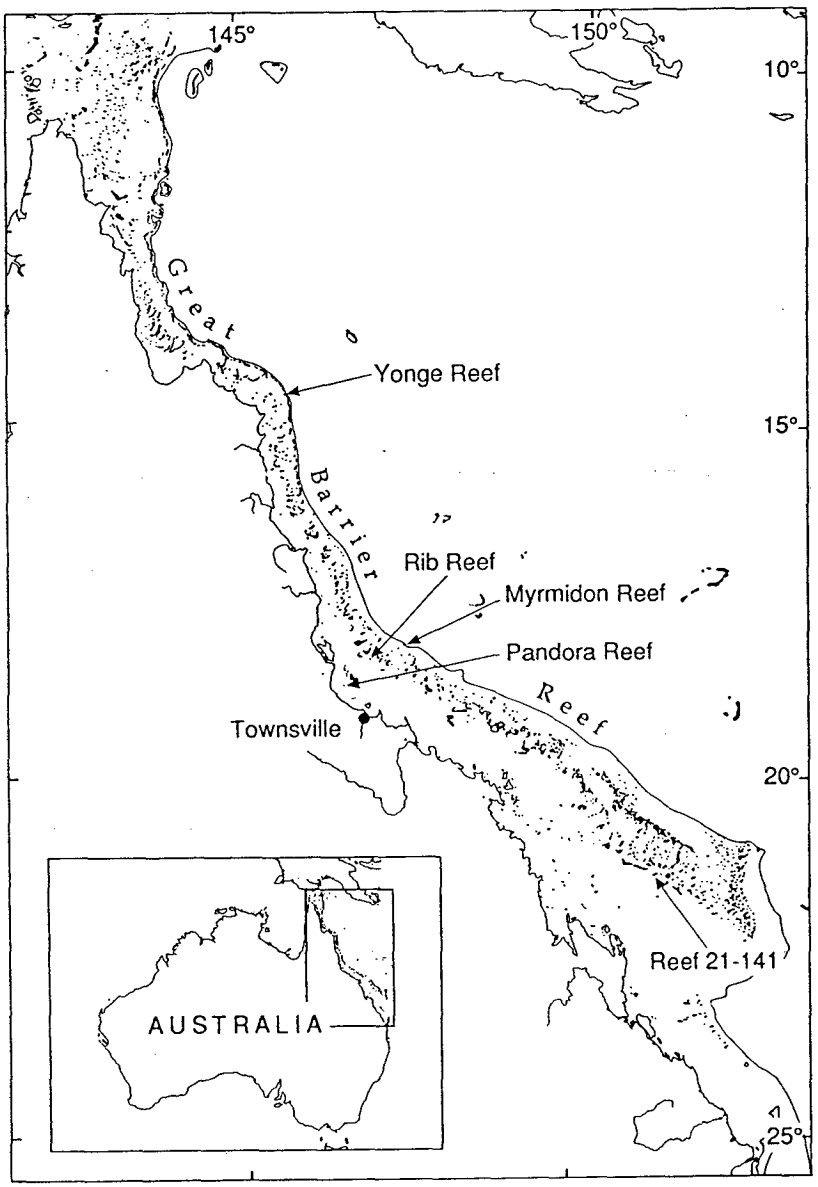

Fig. 1.6 Map of the North Queensland coast and Great Barrier Reef showing reefs selected for collection of *Porites* colonies (Chapters 2 & 5) and collection of tissue samples (Chapter 4).

1.4. MASSIVE *PORITES* COLONIES AS ENVIRONMENTAL RECORDERS.

Much of the current research on massive *Porites* colonies is directed towards extraction of climatic and other important environmental records that may be contained within the skeleton. The most important record is the characteristic annual skeletal density banding pattern revealed by X-radiographs of skeletal slices cut from a skeletal growth axis. The annual density banding pattern has attracted considerable attention because it may provide records of tropical marine environments in much the same way that tree rings provide records of temperate and sub-polar terrestrial environments (see Lough and Barnes, 1990a; see also section 2.1.5.). Unlike tree rings, understanding of density banding in coral skeletons is not yet sufficiently evolved to allow development of techniques for extraction of reliable proxy environmental records. Indeed, such records may not exist in coral skeletons or it may prove impossible to extract them. Nevertheless, the annual nature of the basic banding pattern means that useful information about coral growth - skeletal density, colonial growth rate and annual calcification - is recorded as information which can be dated (Lough and Barnes, pers. comm.). Appropriately used, such information may reliably indicate changes in the coral's environment over periods of several decades (Barnes and Lough, pers. comm.). The point here is that annual density banding does provide the means for dating various records and inclusions in coral skeletons. This is, perhaps, the most important feature of the coral density banding pattern.

A range of materials are included in coral skeletons during growth. For example, *Porites* colonies living on near-shore reefs in the central G.B.R. incorporate into their skeletons fluorescent compounds that are associated with river discharge (Isdale, 1984; Boto and Isdale, 1985). These fluorescent compound generally occur as discrete bands within the skeleton and provide a record of river discharge and, hence, a record of rainfall. Fluorescent bands in fossil *Porites* from late Quaternary reef terraces in the south of the Sinai Peninsula were recently used as evidence that, during the late Quaternary, the climate was much wetter than the present, extreme desert conditions (Klein *et al.*, 1990). Variations in isotopic ratios of oxygen and

carbon present in skeletons of massive *Porites* colonies have been used to provide information on seasonal variation in sea temperature and the concentration of atmospheric carbon, respectively (Weber *et al.*, 1975b; Emiliani *et al.*, 1978; Fairbanks and Dodge, 1979; Schneider and Smith, 1982; Druffel, 1987; Chivas *et al.*, 1983; Carriquiry *et al.*, 1988). Massive *Porites* colonies also incorporate into their skeletons radioactive isotopes which were generated by nuclear tests. They can, thus, be used as recorders of such environmental change (Knutson *et al.*, 1972; Moore *et al.*, 1973; Buddemeier *et al.*, 1974; Moore and Krishnaswami, 1974; Noshkin *et al.*, 1975, Benniger and Dodge, 1986). Similarly, other contaminants become incorporated into the skeletons. Concentrations of cadmium, lead, phosphorus and other trace metals have risen as a result of activities of our industrial society and coral skeletons provide a record of such increases (Dodge and Gilbert, 1974; Dodge *et al.*, 1984; Shen and Boyle, 1987, 1988; Shen *et al.*, 1987).

Work described here was aimed at providing a better understanding of how massive *Porites* corals grow, and of the factors controlling growth form. Growth form itself provides an integrated record of environmental conditions. A major objective of the work was, then, to enable better deciphering of the environmental records encoded as colonial growth form. The work was carried out alongside a major investigation of environmental information encoded in coral skeletons as density variations. It was hoped that this research would contribute to better understanding of such records (Barnes and Lough, 1989; Barnes *et al.*, 1989; Barnes and Lough, 1990; Lough and Barnes, 1990a, b, c) - indeed it already has (see, for example, Barnes and Lough, 1990, p.147 & p. 163).

CHAPTER 2

PATTERNS OF SKELETAL GROWTH *IN PORITES* REVEALED BY X-RADIOGRAPHS

2.1. INTRODUCTION.

Growth processes of massive *Porites* colonies are described in this chapter. The description is based on observations and measurements of the annual density banding pattern and corallites displayed in X-radiographs of skeletal slices removed from the vertical growth axis of massive *Porites* colonies. X-radiographs described here, refer to the X-radiograph positive produced from the X-ray negative. The annual density banding pattern displayed by massive *Porites* corals, which has been widely documented (see below), is used as a chronological marker for determining the longevity of corallites and thus the polyps covering the growth surface of massive *Porites* colonies.

2.1.1. The annual nature of the banding pattern.

X-radiographs of skeletal slices cut from a growth axis of massive coral colonies display concentric dark and light bands which correspond to regions of high and low density skeleton (Plate 2.1). The bands outline former positions of the growth surface of a colony. Coral skeletal density banding patterns were first described by Knutson *et al.* (1972) who demonstrated that the basic banding pattern -

Plate 2.1. X-radiograph positive of a 7 mm thick skeletal slice cut from the vertical growth axis of a *P. solida* colony collected from Rib Reef, central G.B.R. The annual skeletal extension rate, determined from the number of annual density band couplets along the X-Y line, was 11.1 mm yr^{-1}. The longevity of the apparent corallite marked was 5½ years. Refer to plate 2.3 for enlarged section.

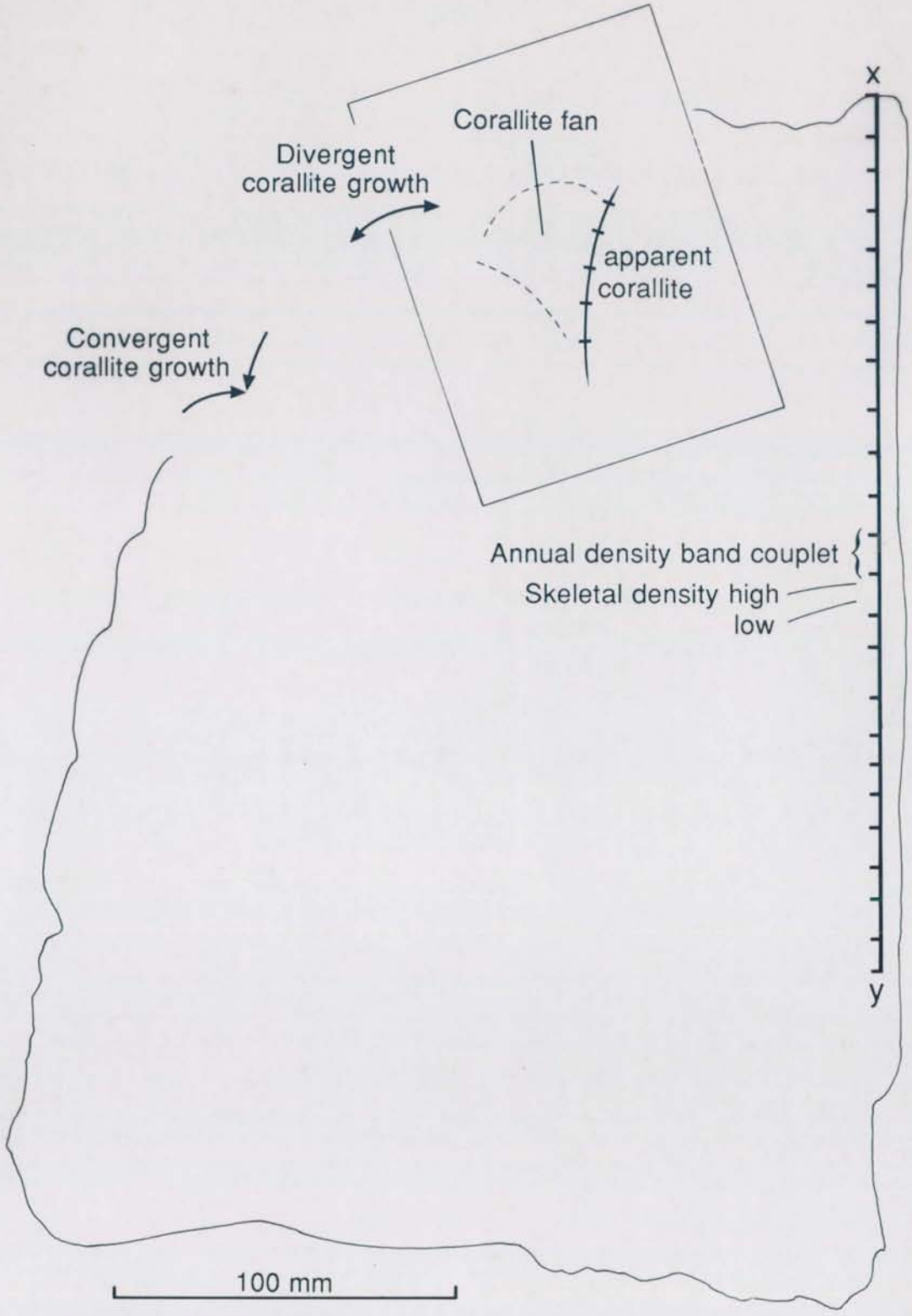

Plate 2.1. X-radiograph positive of a 7 mm thick skeletal slice cut from the vertical growth axis of a *P. solida* colony collected from Rib Reef, central G.B.R. The annual skeletal extension rate, determined from the number of annual density band couplets along the X-Y line, was 11.1 mm yr^{-1}. The longevity of the apparent corallite marked was 5½ years. Refer to plate 2.3 for enlarged section.

one dense band plus one less dense band, was formed over a year. This they demonstrated by referring the density banding pattern to radioactive bands introduced, at known dates, into the skeletons of corals from Enewetak Atoll as a result of the testing of nuclear weapons during the period, 1948-58 (see also, Buddemeier *et al.*, 1974; Noshkin *et al.*, 1975).

The annual nature of the density banding pattern has since been confirmed by a variety of workers, for a range of massive coral species, from sites around the world, using several different dating techniques. Dating procedures used for density bands include, radiometric techniques (Moore and Krishnaswami, 1974; Macintyre and Smith, 1974; Dodge *et al.*, 1974; Noshkin *et al.*, 1975), alizarin staining (Macintyre and Smith, 1974; Buddemeier and Kinzie, 1975; Hudson *et al.*, 1976; Stearn *et al.*, 1977; Wellington and Glynn, 1983; Glynn and Wellington, 1983), variations in the carbon and oxygen stable isotopic composition (Weber *et al.*, 1975a; Goreau, 1977; Emiliani *et al.*, 1978; Fairbanks and Dodge, 1979; Dunbar and Wellington, 1981; Weil *et al.*, 1981; Schneider and Smith, 1982; Wellington and Glynn, 1983; Chivas *et al.*, 1983; Pätzold, 1984; Druffel, 1985, 1987; Carriquiry *et al.*, 1988) and fluorescent inclusions in the skeleton resulting from coastal run-off (Isdale, 1984; Boto and Isdale, 1985). The literature now contains a range of papers in which density bands are used to date various skeletal inclusions such as, lead, cadmium and phosphates (eg., Dodge and Gilbert, 1984; Dodge *et al.*, 1984; Benninger and Dodge, 1986; Shen *et al.*, 1987; Shen and Boyle, 1987, 1988). Although, none of these papers question the annual nature of the density banding pattern, it is universally agreed that massive coral skeletons contain and present an annual density banding pattern.

2.1.2. The appearance of density bands in massive corals.

The literature includes few descriptions of annual banding in corals which differ from the simple couplet pattern of one dense band and one less dense band. There are some papers which provide a different account of the banding pattern but do not provide supporting evidence (eg., Druffel, 1985; Charachinda and Chansang,

1985; Brown *et al.*, 1986). Schneider and Smith (1982) argue that corals from the Hawaiian Archipelago show only one band per year, with one abrupt change in density and one more gradual change in density giving the appearance of two bands per year. Their analysis is based on X-ray densitometry rather than X-radiograph positives. Barnes and Lough (1989) suggest that the couplet pattern is built up from much finer bands (see below). These papers present the only exceptions to an otherwise ubiquitous couplet pattern. However, there are very wide variations in the descriptions of the couplet pattern. These range from a very narrow dense band coupled with a broad, less dense band through to a narrow, less dense band coupled with a wide dense band (Webber *et al.*, 1975b; Hudson, 1981a,b). Interestingly, it has only very recently been pointed out that there exists a fundamental discrepancy between descriptions of a "square wave" density banding pattern and densitometer profiles (see also Schneider and Smith, 1982). Barnes *et al.* (1989) demonstrate that densitometry does not provide profiles consistent with a "square wave". As will be seen, the commonly presented, couplet description for density bands is one of many examples in which an apparently clear and agreed picture of density banding becomes uncertain and confused when examined in detail.

The presence of a pattern of fine bands within the annual couplet pattern adds further confusion to the basic picture. These were first described by Buddemeier (1974) and investigated by Buddemeier and Kinzie (1975); see also Houck (1978). These authors considered the bands to represent an additional, lunar banding pattern imposed over a basic annual pattern. Barnes and Lough (1989) on the other hand, presented evidence to suggest that the annual pattern is built up from fine bands. While not embracing the idea that the fine bands have a lunar periodicity, they proposed that fine bands are the fundamental density pattern in massive coral skeletons.

2.1.3. Skeletal architecture associated with density bands.

Buddemeier *et al.* (1974) noted that the variations in skeletal density represented by density bands could arise from three possible sources. These were,

variations in skeletal chemistry, differences in crystal packing making up skeletal elements, and differences in the thickness and spacing of skeletal elements. However, they discounted variations in skeletal chemistry because published values for organic and inorganic variations in skeletal composition were too low to account for the sorts of difference in density recorded by X-radiographs. Instead they proposed that density variations were most likely caused by variations in crystal packing. This contrasts with Buddemeier and Kinzie (1975) who suggested that variations in the packing of skeletal elements cause the density variations which supported the observations of Macintyre and Smith (1974). Despite the relevance of variations in architecture to a mechanistic understanding of coral density band patterns, no further work on this topic was carried out for more than a decade. Barnes and Devereux (1988) demonstrated experimentally that most of the density variations associated with density banding in *Porites* could be explained solely in terms of the packing of skeletal elements. Crystal packing within these elements contributed little, if anything, to density variations associated with annual banding patterns.

2.1.4. Sub-annual timing of density band formation.

Considerable confusion is apparent in the literature concerning seasonal timing of density band formation. The literature includes about 20 papers describing work aimed at finding the times of formation of high and low density bands, often involving the various skeletal markers listed above, but also including the nature of the banding pattern at the outer margin of the skeleton at the time of collection (see Lough and Barnes, 1990b). A slight majority of these papers supports the view that a dense band is formed in summer, or during periods when sea water is warmest. Most of the remaining papers support the opposite view. Although a certain degree of error may be attributed to techniques used for dating the banding pattern (see Barnes *et al.*, 1989; Lough and Barnes, 1990b), the possibility that the banding pattern may differ between different environments and different locations does not seem to have been given serious consideration (but see Buddemeier *et al.*, 1974;

Buddemeier and Kinzie, 1975; Lough and Barnes, 1990a). Barnes and Lough (1990a) confirm Dodge's (1978) suggestion that this is an important aspect of density band research that requires further investigation.

2.1.5. Environmental correlates of density banding.

The annual nature of the density banding pattern strongly suggests environmental controls over skeletal deposition. Although various environmental factors have been suggested as causes or controls of the density banding pattern, no clear relationship between density bands and environmental factors has emerged. Several authors have suggested that banding is primarily controlled by, or primarily a response to, seasonal changes in light intensity (Knutson *et al.*, 1972; Buddemeier and Kinzie, 1975; Wellington and Glynn, 1983). As detailed earlier, light plays a major role in skeletal deposition in reef building coral (Chapter 1, 1.1.3.). Other authors have suggested that seasonal variation in water temperature is the key factor controlling density band formation (Dodge and Vaisnys, 1975, 1980; Weber *et al.*, 1975b; Hudson *et al.*, 1976; Dodge and Lang, 1983). The relative importance of light and temperature to coral density bands remains a subject for debate and speculation (see, especially, Highsmith, 1979). Other factors have been implicated in the control of density band formation. Such secondary contributors include; reproductive periodicity, nutrient availability, turbidity, sedimentation and wave action (Buddemeier and Kinzie, 1975; Dodge and Vaisnys, 1977, 1980; Highsmith, 1979; Wellington and Glynn, 1983).

Significant correlations between fluctuations in environmental conditions and density band patterns in coral skeletons have often been accepted as evidence for a causal link. In only a few cases, for instance, Dodge and Thomson, 1974; Dodge and Lang, 1983; Glynn and Wellington, 1983, have the mathematical analyses been carried out in a rigorous manner that eliminates the positive results that must inevitably arise when one annual cycle is correlated with another - regardless of whether they are linked. Thus, evidence for linkages between coral density patterns

and particular environmental signals is often ambiguous and sometimes tenuous. Barnes and Lough (1989) point out that the pursuit of empirical and numerical linkages has occupied much of the research on density bands without providing a clear picture as to causative or controlling environmental factors.

2.1.6. X-radiographs as records of coral colonial growth.

Annual density bands displayed by X-radiographs of skeletal slices removed from massive corals can be used to determine the growth rate of coral skeletons retrospectively (Macintyre and Smith, 1974; Buddemeier and Kinzie, 1976; Highsmith, 1979; Dodge, 1978, 1981; Hudson, 1981a, 1981b, 1985; Pätzold, 1984; Huston, 1985). Since the bands outline former positions of the growth surface, X-radiographs also present information about the shape and form of colonies over their lifetimes. It is possible to use the annual banding pattern to relate colony shapes to colony ages, and colony outlines to colony sizes and ages. Thus, X-radiographs of skeletal slices present considerable information about the growth history of massive corals.

The possibility that X-radiographs of skeletal slices would provide information about a coral's growth history was realized from the first (Knutson *et al.*, 1972). Few authors mention that X-radiographs present images of the corallites within a skeletal slice (Plate 2.1 & 2.3), although the presence of such images in X-radiographs is often implicit in the text (e.g., Pätzold 1984). Moreover, few authors seem to have appreciated that annual density bands might be combined with the growth histories of individual corallites to provide more information about colonial growth histories. This thesis makes considerable use of the growth history of individual corallites (and thus polyps), and groups of corallites, in combination with the annual density banding pattern, to determine aspects of the life and growth of massive colonial corals that have not previously been available.

2.2. MATERIALS AND METHODS.

2.2.1. Collection of *Porites* colonies.

Thirty-six massive *Porites* colonies were collected from three reefs; Pandora Reef, Rib Reef and Myrmidon Reef (see section 1.3 & Fig. 1.6 for details of reef locality and morphology). Twelve colonies were collected from each reef. *Porites* on the G.B.R. grows about 10 mm yr^{-1} (Isdale, 1977; Chivas *et al.*, 1983; Barnes and Lough, 1989; Lough and Barnes, 1990a). Rounded, more-or-less hemispherical, specimens at least 200 mm in height were collected in an attempt to provide specimens presenting growth records extending over the last 20 years. In general, colonies greater than 500 mm in height were too large for collection. All colonies were collected from back reef areas on each reef at depths between 3 to 5 m (relative to MLWS). Details of species collected from different reefs are listed in Table 2.1.

Table 2.1.

Number of specimens collected at different reefs

Species	Reef		
	Pandora	Rib	Myrmidon
P. lobata	4	9	4
P. lutea	3	2	4
P. solida	2	1	4
P. mayeri	3	-	-

According to Veron (1986), only 6 species of *Porites* form massive, rounded colonies greater than 200 mm in diameter on the G.B.R. These include *P. australiensis* and *P. myrmidonensis* in addition to those listed in Table 2.1. The intention was to

collect several specimens of each species from reefs across an inshore-offshore transect in the central section of the G.B.R.

At each reef locality divers wearing self-contained underwater breathing apparatus (SCUBA) attached marker floats to each *Porites* colony of approximately the correct size and shape. Between 20-30 colonies were tagged at each reef. A hand-sized sample was chiselled from each tagged colony and taken back to the research vessel for identification using a binocular microscope. Species were identified according to Veron and Pichon (1982) and Veron (1986). The intention was to collect 3 specimens of each species growing on each reef. Failure to maintain this collection plan (see Table 2.1) was caused partly because insufficient numbers of colonies were tagged at certain reefs to provide the full range of samples, and partly because some identifications were altered after samples were re-examined using the facilities and expertise at the Australian Institute of Marine Science (AIMS).

The twelve colonies selected from each reef, from the initial set of 20-30 hand specimens, were prised off the reef substratum using a hammer, chisel and crow bar. Each colony was rolled into a strong, nylon net bag which was attached to an inflatable boat via a rope. The boat crew lifted colonies to the water surface in the nylon bags using the rope. The colonies were returned the research vessel and left in the sun to dry. Each colony was given an identification number based upon the reef from which it was collected and the number of the 200 mm diameter buoy which originally marked its position (eg. PAN-12, RIB-22, & MYR-B28). The height and width of each colony was measured.

2.2.2. Slicing of coral colonies and X-radiography of slices.

Each colony was cut in half along a vertical growth axis using a chain saw fitted with tungsten-tipped teeth. Colonies were initially cut in half to provide small enough pieces of coral from which slices of skeleton could be removed using a more precise stone masons diamond saw. Although the diameter of the diamond saw was

600 mm, the drive mechanism reduced its effective cutting depth to about 250 mm. Cutting colonies in half with a chain saw also provided a flat surface which could be placed on the movable table of the stone-mason's saw. Each colony half was secured to the table with a chain and was cut in half again to provide two coral quarters from the original colony. Care was taken to ensure that this cut passed through, or close to, the origin of the colony and normal to its growth axis. The blade was lubricated with a stream of fresh water. One of the resulting coral quarters was left in place on the cutting table. The saw blade was repositioned to remove a slice of skeleton, 6-7 mm thick, from the face left by the initial pass with the diamond blade.

Slices were cut 6-7 mm thick as a compromise between the recommendation that slices be cut 3 calices thick (Buddemeier *et al.,* 1974) - which, for *Porites*, would be 2-3 mm thick - and obtaining reasonably robust slices that could be easily handled and transported (see also Barnes and Lough, 1989; Barnes *et al.,* 1989). Each slice removed from a colony represented one half of a vertical section through a complete colony (e.g., plate 2.1). Two slices were removed from each colony and X-radiographed. X-radiographs of the first slice removed were analyzed in preference to those of the second slice because the first slice was usually closest to the vertical growth axis of a colony.

X-radiographs of the coral slices were produced using the X-ray facilities at a local hospital. The X-ray machine was a Toshiba Rotanode type DRX-190H and a Toshiba beam-limiting device model TF-6TL-3. Different focus to film distances (FFD) were tested. It was found that, by increasing the distance between the X-ray source and a slice (i.e., increasing the FFD with the slice laying on a cassette holding the X-ray film), features associated with skeletal architecture were displayed more clearly in the X-ray images (see Barnes and Lough, 1989; Barnes *et al.,* 1989). As the distance between the X-ray source and the subject increased, the angle at which the electrons penetrated the subject was decreased. As a result, the X-ray image was clearer. The FFD was set to the maximum convenient distance for the X-ray machine, which was 1.0 m. X-ray film was Kodak T-mat G double-sided emulsion film (TMG-1). Exposures were made using a Fuji G-8 screen to improve image quality.

Single-sided emulsion film produces clearer images than double-sided emulsion. However, single-sided emulsion film was not available in sizes that covered the entire slices. Exposure times were varied until images displaying the best resolution were produced. The most satisfactory exposure times for the 6-7 mm slices, using the double-sided emulsion film with the Fuji screen, were 46 kVp at 50 Ma for 0.16 s or 0.20 s. Contact prints were made for all X-radiographs. X-radiographs are negative images and, consequently, the contact prints were positive images. X-ray positives of skeletal slices show dense bands as darker regions than less dense bands (Plate 2.1).

2.2.3. Measurements of annual skeletal extension rates from X-radiographs of skeletal slices.

The annual banding pattern seen in X-radiographs was used to determine the average annual skeletal extension rate for each colony. Each X-radiograph was covered with transparent film. A straight line was drawn on the film as close to the main vertical growth axis of each colony displayed by the X-radiograph. The line was drawn so that it crossed the density bands normally, or was as close to normal as possible (e.g., line X-Y, Plate 2.1). The line began at the outer surface of the colony. The banding pattern seen at this outer surface was noted and the line was terminated at an equivalent point in the banding pattern close to the origin of the colony. Thus, the line crossed a complete set of annual band couplets. In most X-radiographs, the banding pattern was not clearly displayed towards the origin of the colony because, despite care in cutting slices, many slices were not cut through the exact origin of the colony. If the slice was not cut through the exact origin of a colony, the bands became increasingly blurred as the cut became more tangential to them.

The number of annual band couplets crossed by the line was counted. It was then possible to divide the number of annual bands by the length of the line to determine an average annual extension rate for that colony.

This annual rate of skeletal extension was used to calculate the age of each colony from the overall height of the colony. Extension rate was used in preference to counting the number of band pairs along the entire vertical growth axis because, as mentioned above, it was often difficult to distinguish band pairs close to the origin of the colony.

2.2.4. Measurements on corallites apparent in X-radiographs.

Corallites displayed in the X-radiographs did not remain parallel to each other. Rather, they tended to be organised into discrete fans; each fan terminating in a bump at the outer surface of the colony (e.g., Plate 2.1 & 2.3). This arrangement of corallites is discussed below in detail. Any single corallite could be traced from its apparent origin on or close to the central fan axis to the point at which it disappeared at the margin of the fan (see Plate 2.1 & 2.3).

Six large, well developed corallite fans associated with bumps on the outer surface were selected on each X-radiograph. Fans were selected as close to the vertical growth axis as possible. This meant that fans terminating on the uppermost surfaces of the colony were preferred. Two corallites were selected within each corallite fan. These corallites originated at about the same point in each fan but diverged to the opposite margins of the fan. Lines were drawn on the transparent overlay which traced the tracks of these 12 corallites on each X-radiograph. The number of annual bands crossed by each track was counted and expressed to the nearest half year. A mean value was calculated for each colony. This value is, in effect, the mean corallite longevity for that colony.

2.2.5. Comparisons of corallites on slices with those in X-radiographs.

Four coral slices and corresponding X-radiographs were selected from samples from Rib Reef. Two colonies with fairly bumpy growth surfaces and 2 with fairly smooth growth surfaces were selected. One of the smooth-surfaced colonies was *P. lutea* and the remaining colonies were *P. lobata*. A 100 mm long section was

marked out on the outer growth surface of each colony seen in the 4 X-radiographs. The section was close to the vertical growth axis on the X-radiograph. The section was marked by tracing along the outline of the growth surface with a K & R map measurer (K & R manufacturers, 1933 Premier Row, Orlando, Florida 32809, U.S.A.). This instrument is normally used for tracing along roads on maps to determine distances between points. The corresponding 100 mm long section on each skeletal slice was also marked.

The number of corallites apparent at the colony growth surface were counted along the 100 mm section on each X-radiograph. Counting was made much easier because the corallites extended back into the skeleton from the outer edge. The number of calices was counted in corresponding regions of the growth surface present on the skeletal slices. The slice was 6-7 calices thick and, hence, the number of calices that intersected one of the sawn surfaces was counted along the 100 mm long section.

2.2.6. Statistical procedures.

The growth measurements taken from the 36 coral slices and corresponding X-radiographs were analyzed using a Macintosh SE personal computer equipped with the statistical package *Statview*. The mean and standard deviations (± S.D.) for annual skeletal extension rate and corallite longevity were determined for colonies from different reefs and species. The effect of species and reef on annual skeletal extension and corallite longevity were assessed by one-way analysis of variance (ANOVA) tests using the ANOVA routine in *Statview* package. The ANOVA test which examined possible differences in annual skeletal extension rate and corallite longevity between species included data for *P.lobata, P.lutea* and *P.solida* colonies which were represented by each reef. *P.mayeri* was only collected on Pandora reef and was, consequently, excluded from the species test on the grounds that it was not found at each reef locality. ANOVA tests for differences in annual skeletal extension rates and corallite longevity on colonies between reefs were performed including and excluding data for *P. mayeri.*

A simple correlation analyses was performed using the *Statview* package on data for annual skeletal extension rates and corallite longevity in all 36 *Porites* colonies collected from the inshore-offshore transect.

A paired *t*-test was used to compare the number of actual corallites counted along 100 mm long sections marked on four skeletal slices with the number of apparent corallites counted along equivalent 100 mm sections displayed in corresponding X-radiographs.

2.3. RESULTS.

All colonies collected from the inshore-offshore transect were roughly hemispherical and displayed the bumpy growth surface characteristic of large, massive colonies of *Porites*. Some colonies were slightly broader than they were high, that is, dome-shaped; while others were slightly higher than they were wide, that is, helmet-shaped. Values for mean colony heights, widths and ages are given in Table 2.2.

Table 2.2.

Mean ± standard deviation (± S.D.) for the height, width and age of 36 *Porites* colonies collected from the central G.B.R.

Reef	Number of colonies	Height (mm) Mean ± S.D.	Width (mm) Mean ± S.D.	Age (years) Mean ± S.D.
Pandora	12	398 ± 79	450 ± 65	40.5 ± 12.0
Rib	12	348 ± 83	450 ± 82	32.0 ± 6.4
Myrmidon	12	391 ± 64	457 ± 56	50.6 ± 8.6
All	36	381 ± 70	452 ± 67	41.0 ± 12.0

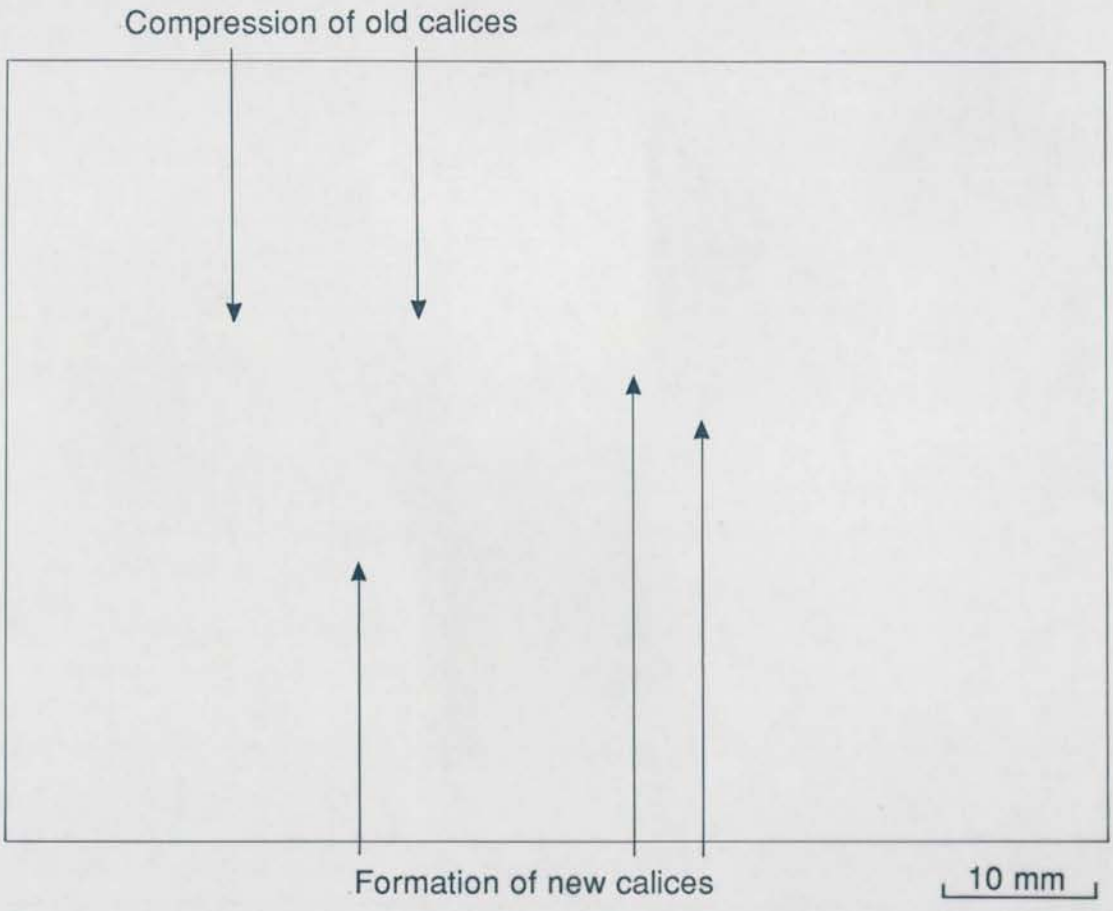
Compression of old calices
Formation of new calices
10 mm

2.3.1. Appearance of calices at the growth surface of colonies.

The shape and size of calices were examined in both colonies and slices cut from colonies for X-radiography. Very small, but regular calices, less than 0.5 mm in diameter, were observed on the tops of walls between adjacent, fully developed calices (Plate 1.2 & 2.2). These calices represented the newly forming calices arising from extratentacular division of the tissue. These small calices were, almost always, found at the summit of bumps on the colony growth surface. New calices were seldom found forming on the sides of bumps.

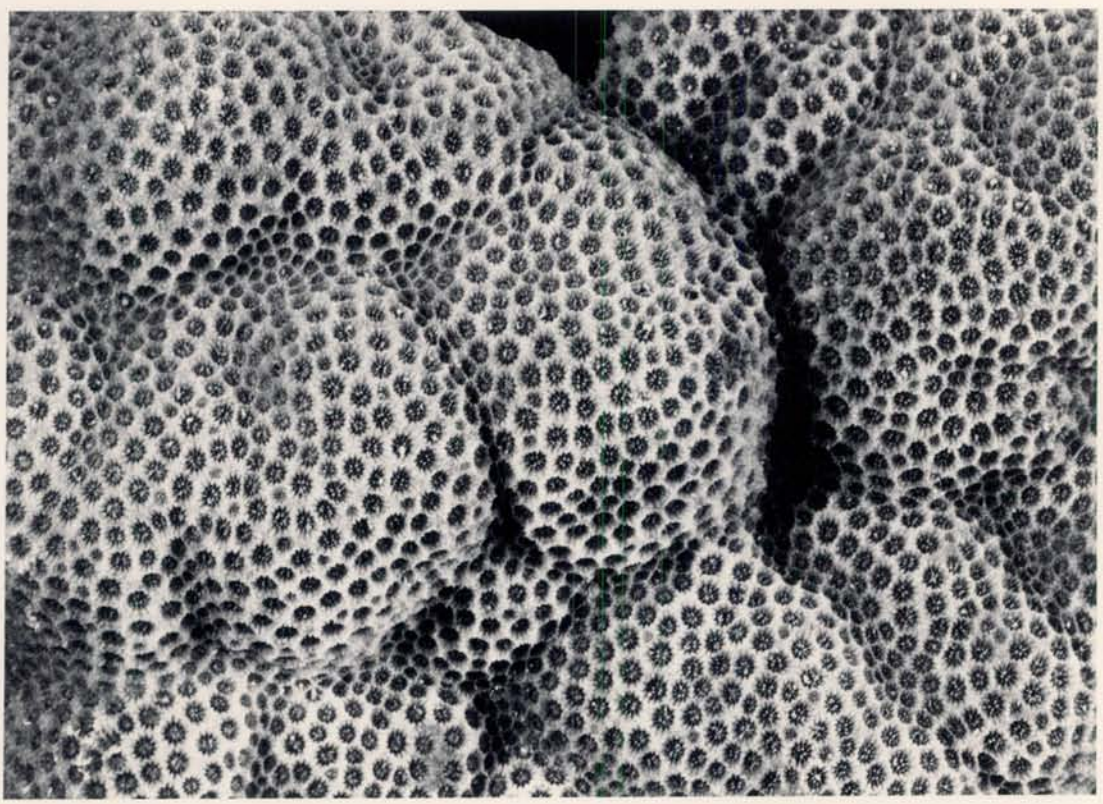

Plate 2.2. Enlarged section of Plate 1.1 displaying formation of calices on or towards the summit of bumps and compression of calices at or towards the bottom of valleys formed between bumps on a colony of *P. lobata*.

2.3.1. Appearance of calices at the growth surface of colonies.

The shape and size of calices were examined in both colonies and slices cut from colonies for X-radiography. Very small, but regular calices, less than 0.5 mm in diameter, were observed on the tops of walls between adjacent, fully developed calices (Plate 1.2 & 2.2). These calices represented the newly forming calices arising from extratentacular division of the tissue. These small calices were, almost always, found at the summit of bumps on the colony growth surface. New calices were seldom found forming on the sides of bumps.

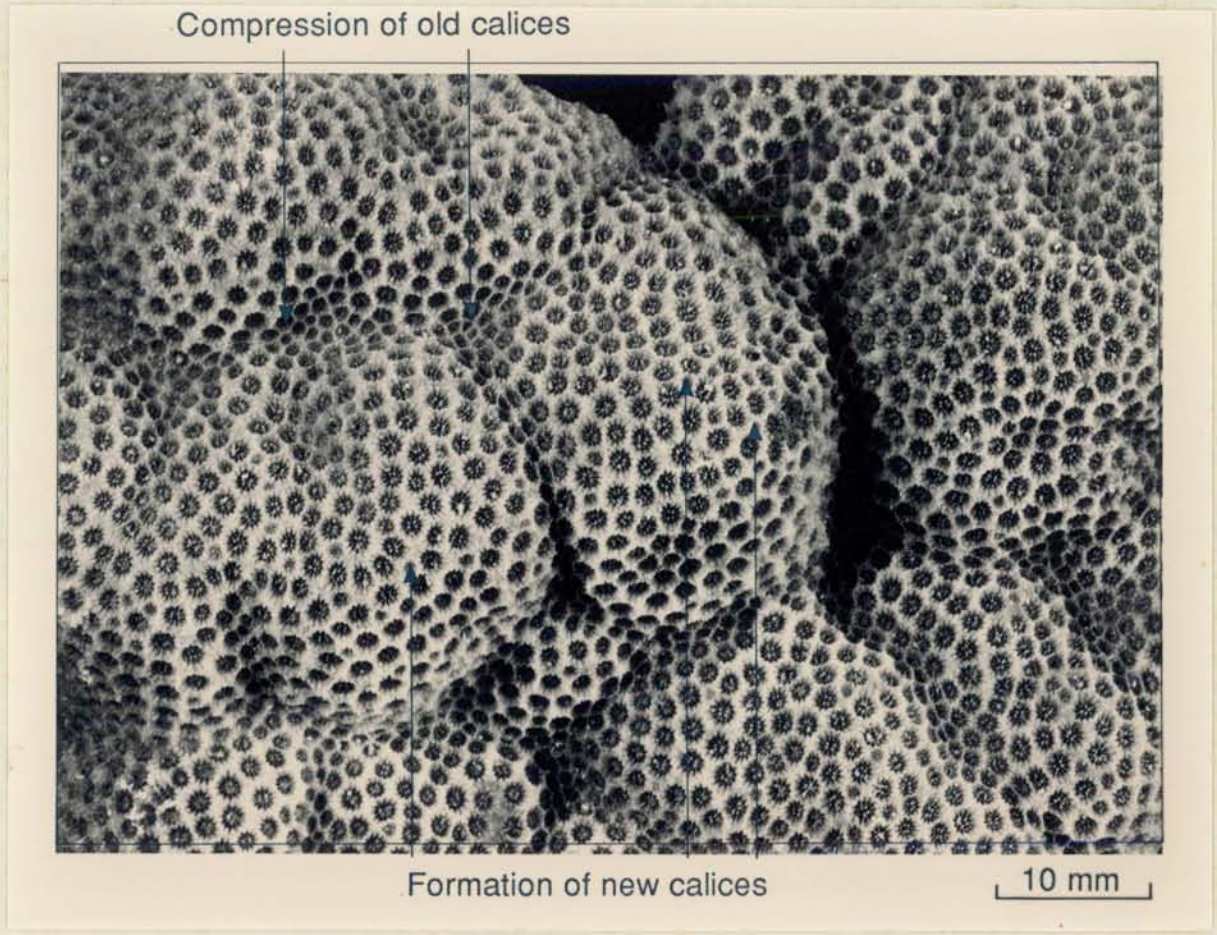

Plate 2.2. Enlarged section of Plate 1.1 displaying formation of calices on or towards the summit of bumps and compression of calices at or towards the bottom of valleys formed between bumps on a colony of *P. lobata*.

In valleys between adjacent bumps, calice walls were thinner and calices tended to be smaller and rhomboid or triangular in shape, in contrast to the hexagonal appearance of calices elsewhere (Plate 1.2. & 2.2). At the very bottom of valleys, calices appeared to be greatly compressed and were hardly distinguishable, one from another (Plate 1.2 & 2.2).

2.3.2. Annual skeletal extension rate.

For all 36 colonies, the mean length over which annual skeletal extension rate was determined was 204 ± 60 mm i.e., about 20 years of growth. Mean annual rates of skeletal extension for *P.lobata, P.lutea* and *P.solida* are presented in Table 2.3.

Table 2.3.

Mean annual skeletal extension rate (mm ± S.D.) for three species of *Porites* collected from the central G.B.R.

Species	Number of colonies	Skeletal extension mm yr^{-1} ± S.D.	Skeletal extension range
P. lobata	17	10.4 ± 2.9	7.6 - 18.6
P. lutea	9	9.1 ± 2.9	6.7 - 15.5
P. solida	7	8.7 ± 1.8	6.8 - 11.4

There was no significant difference in annual skeletal extension rate between the species presented in Table 2.3 (ANOVA; F value = 1.33 (F), Probability > 0.05 (*P*)).

The mean annual skeletal extension rate for all 36 colonies collected from the three reefs (i.e., including *P. mayeri*) was 9.8 ± 1.8 mm yr^{-1}. Annual skeletal extension rates between reefs are shown in Table 2.4.

Table 2.4.

Mean annual skeletal extension rate (mm ± S.D.) for 36 *Porites* collected from three reefs of the central G.B.R.

Species	Number of colonies	Skeletal extension mm yr^{-1} ± S.D.	Skeletal extension range
Pandora	12	10.3 ± 2.1	7.3 - 15.0
Rib	12	11.3 ± 3.1	7.8 - 18.6
Myrmidon	12	7.8 ± 0.8	6.7 - 9.5

There was a significant difference in annual skeletal extension rate between reefs, both for data excluding *P. mayeri* (ANOVA; $F = 7.22$, $P < 0.05$) and data including *P. mayeri* (ANOVA; $F = 8.14$, $P < 0.05$). About 33% of the variability in annual skeletal extension in the ANOVA test including *P. mayeri* could be accounted for by the reef effect.

2.3.3. Corallite longevity.

The average corallite life expectancy of 36 *Porites* colonies was 4.8 ± 0.88 years. Variations in corallite longevity for different *Porites* species are presented in Table 2.5.

Table 2.5.

Mean corallite longevity (years ± S.D.) for three species of *Porites* collected from the central G.B.R.

Species	Number of colonies	Corallite longevity years ± S.D.	Corallite longevity range
P. lobata	17	4.8 ± 0.9	3.6 - 7.8
P. lutea	9	5.1 ± 0.8	3.8 - 6.2
P. solida	7	4.9 ± 0.7	3.8 - 6.0

There were no significant differences in corallite longevity between these three species (ANOVA; $F = 0.264$, $P > 0.05$).

Mean differences in corallite longevity in massive *Porites* colonies collected from three reefs across the central G.B.R. are presented in Table 2.6. There was a significant difference in corallite longevity between *Porites* colonies collected from these three reefs as shown by the ANOVA tests excluding and including *P. mayeri* ($F = 3.88$, $P < 0.05$ and $F = 6.43$, $P < 0.05$ respectively). About 28% of the variability in corallite longevity in the ANOVA test which included *P. mayeri* data was associated with the reef effect. The simple correlation between annual skeletal extension rate and corallite longevity showed that skeletal extension and corallite longevity were not significantly related ($r = + 0.29$, the critical coefficients of significance at the 5% and 1% level are 0.33 and 0.42 respectively).

Table 2.6.

Mean corallite longevity ± (years ± S.D.) rate for 36 *Porites* collected from three reefs of the central G.B.R.

Species	Number of colonies	Corallite longevity years ± S.D.	Corallite longevity range
Pandora	12	4.2 ± 0.5	3.5 - 5.2
Rib	12	5.2 ± 1.1	3.6 - 7.8
Myrmidon	12	5.9 ± 0.6	3.8 - 6.0

2.3.4. Comparison of actual corallites with apparent corallites.

The number of calices counted along 100 mm sections marked on the four coral slices was slightly less than the number of corallites apparent in corresponding sections of the X-radiographs (Table 2.7).

Table 2.7.

Number of calices along 100 mm long sections on 4 skeletal slices of *Porites*, compared to the number of corallites apparent in the 4 corresponding 100 mm sections in X-radiographs. Percentage difference between calice number and corallite number = % dif.

Specimen number	Species species	Growth surface	Calices along coral slice	Corallites on X-radiograph	% dif
RIB-B35	*P. lobata*	Bumpy	94	101	7.4
RIB-B03	*P. lobata*	Smooth	90	94	4.4
RIB-B16	*P. lobata*	Smooth	84	87	3.6
RIB-B04	*P. lutea*	Bumpy	89	93	4.5

There were, on average, 89 ± 4 calices counted along the four 100 mm long sections marked on the skeletal slices, whereas there were, on average, 94 ± 6 corallites counted along the corresponding 100 mm section marked on the X-radiographs. Thus, there were, on average, 5 ± 2 more corallites per 100 mm long section along growth surfaces seen in X-radiographs than along the same surfaces on the actual skeletal slices. This difference was significant (Paired *t* test; $t = -5.20$, $P < 0.05$). There was 5% more corallites per unit length on the bumpy growth forms than on the smooth growth forms, regardless of species.

2.4. DISCUSSION.

2.4.1. The X-radiographic image of corallites.

Barnes *et al.*, (1989) point out that X-radiographic images of coral slices are often treated as if they are direct, photographic illustrations of skeletal density. They argue that such X-radiographs are images beyond normal experience and require

careful interpretation. These arguments relate to the appearance of apparent corallites in X-radiographs of *Porites*. Barnes *et al.*, (1989) pointed out that a slice of *Porites* skeleton 6-7 mm thick included at least 5 overlapping layers of corallites. Thus, the X-radiographs of *Porites* slices might be expected to display a confusion of corallites, Instead, such X-radiographs provide an image giving the impression of a single layer of corallites (e.g., Plate 2.1. 2.3). Barnes *et al.*, (1989) showed that the corallite walls displayed in X-radiographs of *Porites* are artifacts that are produced by the regular, approximately hexagonal, layering of corallites within skeletal slices (see Barnes *et al* 1989, page 52, Fig 3). Thus, the corallites seen in X-radiographs of *Porites* do not represent individual corallites. This raises questions about the use of X-radiographic images of corallites to make measurements and interpretations regarding real corallites.

Barnes *et al.* (1989) demonstrated that X-radiographs provide images resulting from the cumulative absorption of X-rays through the thickness of a skeletal slice. Thus, the X-radiographic image contains a record of the position of corallites averaged through the thickness of the slice. However, the pattern of corallite walls within the slice may repeat in such a way that corallites apparent in X-radiographs are narrower than the actual corallites. Perfect hexagonal packing of calices within skeletal slices would result in "corallites" in X-radiographs appearing one third to one half less in width than the actual corallites. Comparisons of actual corallites to corallites apparent in X-radiographs showed that the apparent corallites were approximately 5% less wide than the real corallites. It seems that irregularity in the packing of corallites within the skeletal slices kept the error in apparent corallite width quite small. This error was not considered sufficient to require corrections to be made on counts of corallites present in X-radiographs.

2.4.2 The arrangement of corallites in *Porites* skeletons.

In X-radiographs of skeletal slices cut from a growth axis of massive *Porites* colonies, apparent corallites radiate out from the origin of the colony to the growth surface whilst the growth surface remains fairly smooth. New corallites are inserted

uniformly over the growth surface between the initial corallites as the height of the colony increases. Observations of division of calices in small colonies support this interpretation.

Once small, rounded colonies of *Porites* grow to more than about 100 mm in diameter, the previously smooth growth surface begins to become irregular and uneven (see also Isdale, 1977). This process was first described by Barnes (1973; see also Chapter 1.1.1.). The process is easily seen in X-radiographs of coral skeletal slices because the density bands outline former positions and shapes of the growth surface (e.g., Plates 2.1, 5.1.). The surface becomes broken up into small, low, lenticular bumps. This change in the growth surface involves a change in the regular, radial disposition of corallites. Corallites become arranged into "fans", each of which is associated with a bump. Where one fan abuts with a neighbouring fan, there is a region in which the skeleton is of different, usually lower, density (e.g., Plates 2.1, 2.3). The arrangement of corallites into fans associated with bumps on the colony surface is a major feature of X-radiographs of *Porites*. Barnes and Devereux (1988) and Lough and Barnes (1990b) mention the density variations associated with corallite fans because they present sources of error in measurements of seasonal and annual density variations. They refer to density variations associated with corallite fans as macro-architectural variations. Apart from this, corallite fans appear to have aroused little interest in the literature.

Each corallite fan seen in X-radiographs is associated with a bump at the growth surface of the skeleton. The central axis of a fan terminates at the summit of a bump. New, apparent corallites first appear on, or close to, this central axis. On X-radiographs the corallites track upwards and outwards from the central axis to one side or the other. The corallites either terminate at the growth surface of the colony or they disappear when they run into corallites from adjacent fans (Plate 2.3).

This accords with observations on calice size and shape on the bumpy growth surface of colonies. The addition of new calices by extratentacular division, appears to be virtually restricted to the summit of bumps. In the valleys where adjacent

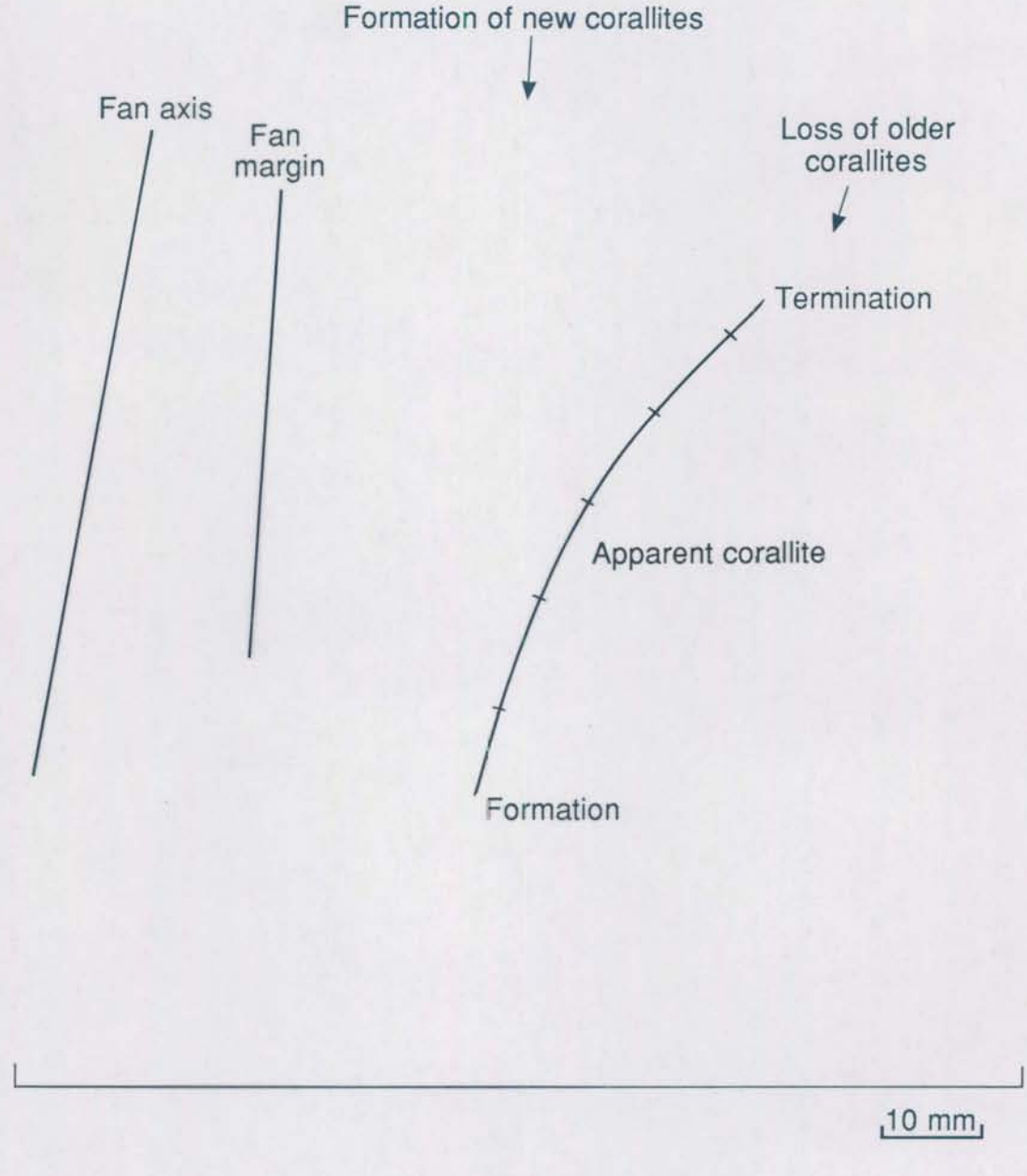
Formation of new corallites
Fan axis
Fan margin
Loss of older corallites
Termination
Apparent corallite
Formation
10 mm

bumps meet, the calices become compressed and distorted; they become squeezed, and progressively smaller towards the base of the valley where they eventually disappear and cease to exist on the growth surface (Plate 2.3.).

Plate 2.3. Enlarged section of Plate 2.1 displaying formation and termination of apparent corallites on an X-radiograph positive of *P. solida*.

bumps meet, the calices become compressed and distorted; they become squeezed, and progressively smaller towards the base of the valley where they eventually disappear and cease to exist on the growth surface (Plate 2.3.).

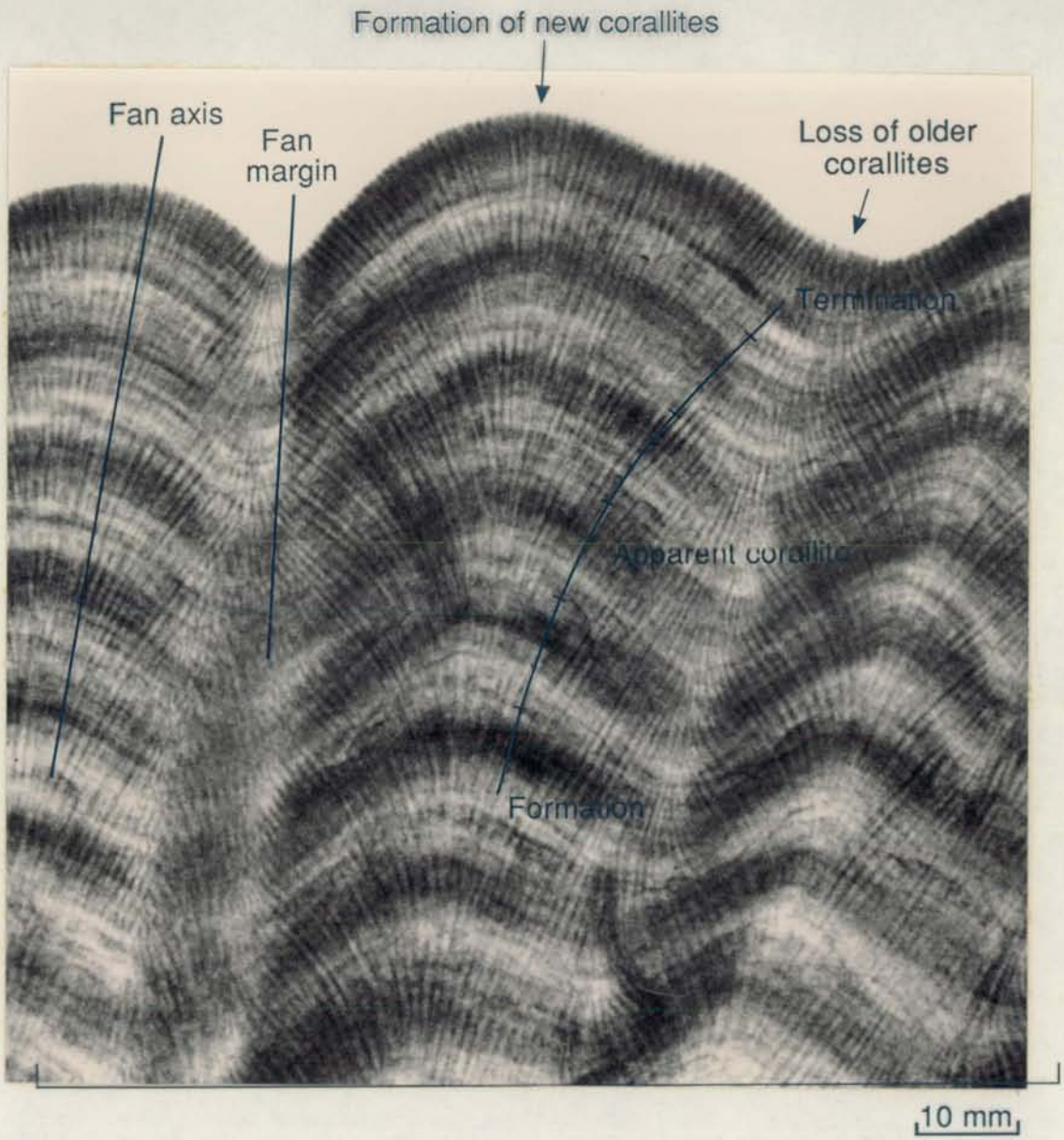

Plate 2.3. Enlarged section of Plate 2.1 displaying formation and termination of apparent corallites on an X-radiograph positive of *P. solida*.

2.4.3. The inevitable consequences arising from the formation of corallite fans.

Corallites remain more-or-less perpendicular to the growth surface, regardless of their orientation (Plates 2.1, 2.3.). It may be seen that the summit of a bump represents a place in which skeletal extension creates space between adjacent corallites (Fig. 2.1). Since corallites do not increase their diameter beyond a certain limit (around 1 mm in most species of *Porites*), new corallites can be inserted into the space which is generated at the summit of a bump by skeletal extension. On the sides of bumps, skeletal extension generates little or no space between existing corallites (Fig. 2.1). Thus, little division of calices is observed in this region. Corallites present at the convex surface in the valleys where adjacent bumps meet are actually growing towards each other. Barnes (1973) described the corallites in such regions as competing for space in which to grow. However, Barnes did not follow this idea through to its inevitable conclusion - that corallites and, hence, polyps are lost in the valleys between bumps. What then emerges is a picture in which new polyps are formed at the summit of bumps and are inevitably lost, some time later, in the valleys between bumps.

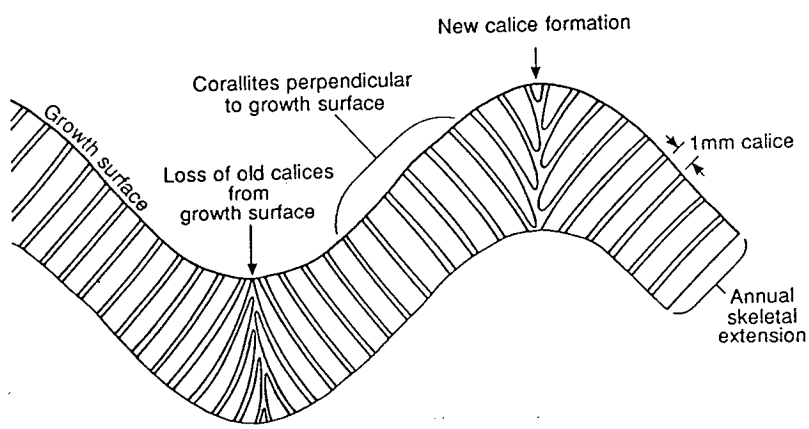

Fig. 2.1. Diagrammatic representation of the bumpy growth surface of a massive *Porites* colony displaying formation and loss of polyps from the growth surface as skeletal extension occurs.

2.4.4. The age of polyps on the growth surface of *Porites* colonies.

X-radiographs of skeletal slices of *Porites,* by virtue of the annual banding pattern, provide information about the time taken from formation of a new corallite at the summit of a bump to its loss at the margin formed between fans. In fact, no polyp on the surface of a bumpy *Porites* can be more than about 5 years old, although the colony may have been growing for several centuries.

Measurements made on the corallite fans seen in X-radiographs of the 36 colonies from Pandora, Rib and Myrmidon Reefs were designed to provide information about the longevity of polyps in colonies growing in different environments. The results presented in this chapter show that corallite longevity significantly increased with distance offshore. Corals from Pandora Reef had an average corallite longevity of 4.2 ± 0.5 years, whereas colonies from Myrmidon Reef had a corallite longevity of 5.9 ± 0.6 years. Because corallites can be equated with polyps, this means that polyps on colonies from the offshore reef survived longer than those on colonies from the inshore reef. Moreover, all polyps covering a colonies from Pandora Reef were likely to be completely turned over in around 4 years whereas the polyp turnover time for Myrmidon Reef approached 6 years.

2.4.5. Links between growth rates, growth form and environmental factors associated with *Porites*.

The results show that there was no significant relationship between skeletal growth rate and corallite longevity. Thus, the difference in corallite longevity between reefs was not likely to be associated with the decreased rate of skeletal growth at the offshore reef. It was apparent that the longevity of polyps was related to the angle at which corallites diverged from the central axis of their fan, and to the size and shape of the bump with which they were associated. It was also apparent that bumpiness bore some relationship to skeletal growth rate (see also Barnes, 1973;

Barnes and Lough, 1989). Thus, the results suggested that bumpiness was related to skeletal growth rate and that corallite longevity was related to bumpiness, but that there was no relationship between corallite longevity and skeletal growth rate.

Results described in this chapter confirm the many earlier findings that details of skeletal growth can be obtained from X-radiographs of slices cut from coral colonies. The results presented suggest that information about the absolute rate of polyp turnover within a colony can also be obtained from such X-radiographs. These two sets of information seemed to be linked in some way with the degree of bumpiness of a colony growth surface. It was, therefore, necessary to explore further the nature of bumpiness, and to devise procedures for quantifying and expressing bumpiness. This work is described in subsequent chapters.

2.5. CONCLUSIONS.

1. Calices on the growth surface of a massive *Porites* colony are initiated on the top of walls between older existing calices. It is therefore possible to record the age of each individual polyp on the growth surface of a massive *Porites* colony as the colony increases in size.

2. Once a massive *Porites* colony develops a characteristic bumpy growth surface, as it increases in size, new calices are formed on or around the summits of bumps. New calices are rarely seen forming on the sides or at the bottom of valleys formed between bumps. All calices at the bottom of valleys become compressed and ultimately become occluded from the growth surface as skeletal extension occurs.

3. X-radiographs of massive *Porites* colonies display apparent corallites arranged into corallite fans. These fans clearly show that new corallites appear at or

close to the central growth axis of a corallite fan, which passes though the summit of a bump. Each apparent corallite can be traced from its point of origin, at or close to the fan axis, to a fan margin where it ceases to continue to grow once it abuts another apparent corallite growing from an adjacent corallite fan. Thus, it is concluded that the location of a corallite, relative to the top of the bump, changes as the corallite grows older and skeletal extension occurs. Hence, younger polyps are located on top of bumps and older polyps are located at the bottom of valleys formed between bumps.

4. Growth of a new calice on top of a bump causes adjacent surrounding calices, positioned slightly lower, to become progressively displaced as skeletal extension occurs. It is therefore concluded that the rate at which the surface area of a new calice and therefore polyp increases, must be faster than the rate of increase in skeletal surface area of the growth surface created as skeletal extension occurs. Otherwise older corallites would not become displaced as new ones develop.

5. Displacement of older corallites resulting from growth of new corallites, is displayed by corallite fans in X-radiographs of massive *Porites* colonies. It is concluded that the amount of displacement of corallites displayed by a corallite fan is strongly related to the degree of bumpiness displayed on the growth surface. Thus well developed bumps are associated with well developed corallite fans displaying corallites that exhibit a large amount of displacement from the central fan axis.

6. It takes on average about 5 years from the formation of a calice on top of a bump to the point where the calice becomes compressed at the bottom of a valley formed between bumps where it ultimately becomes occluded from the growth surface. Thus all polyps on the growth surface of a bumpy massive *Porites* colony become replaced by younger polyps during roughly a 5 year period. It can therefore be concluded that the maximum age of any polyp on the growth surface of a massive *Porites* colony is about 5 years even though the genetic characteristics of the tissue and the skeleton may be centuries old.

CHAPTER 3

COMPUTER MODELS THAT SIMULATE GROWTH OF A MASSIVE *PORITES* COLONY

3.1. INTRODUCTION.

Computer graphic techniques are used to generate models which simulate growth of a massive *Porites* colony. Computer models require that principles of, and constraints on, colonial growth be identified. A model in which the simulation approaches reality requires that these principles and constraints have been incorporated in an appropriate manner. Once a reasonable model has been constructed, it can be used to test aspects of colonial growth which might otherwise involve years of field work. Here, models simulating growth of a massive *Porites* colony are used to investigate how the ratio of tissue growth to skeletal growth affects the growth form displayed by a *Porites* colony. Hence, the main reason for constructing the models was to generate hypotheses about massive coral growth, rather than to test any existing hypotheses.

3.1.1. The concept of modularity in colonial corals.

The nature of coloniality in corals has been the subject of considerable debate (Foster 1979). At one extreme, a coral colony can be considered as an organization in which individual polyps are more-or-less independent of each other. At the other extreme, the colony can be considered as a single organism with many mouths.

Neither of these extreme views will stand close examination. Polyps within a colony have their gastric cavities linked, and fluids circulate between them showing that there is a degree of integration between adjacent polyps (Gladfelter, 1983). However, that integration does not seem to be sufficient to consider a colony to be an individual. There is no indication of a central control mechanism, either nervous or chemical, which would suggest that a colony functions as an individual. Indeed, stimulation of a colony at one point may elicit no response in areas sufficiently remote from the stimulus.

Recently, Rosen (1986) proposed that coral colonies may be considered as modular organisms. He identified the fundamental module as a polyp, together with the skeleton secreted by that polyp. Thus, he envisaged growth as an iterative process involving the formation of new modules. This idea of modularity becomes somewhat tenuous if applied to colonies having well separated polyps and corallites. Where in the coenenchyme (tissue and skeleton separating polyps and corallites) does the division between modules occur? However, *Porites* species form cerioid colonies and the division between adjacent polyps and corallites is easily identified. Thus, Rosen's ideas are especially applicable to *Porites*. Rosen points out that polyps contribute to colony growth in two possible ways: laterally by budding new polyps, and longitudinally by continuously secreting skeleton beneath themselves, and thus elongating their corallites. Colonial growth form is then a product of the length and arrangement of corallites. Rosen further states, that although growth and form of corals has been extensively studied, most workers have dealt with the overall shape of corals (Roos, 1967; Macintyre and Smith, 1974; Graus and Macintyre, 1976; Brakel, 1983; Lewis, 1989), or variations in form between corallite structures (Wijsman-Best, 1974; Brakel, 1977; Foster, 1983), rather than with the spatial arrangements and life histories of the modular units in relation to the growth form displayed.

Work presented in Chapter 2 provides a description of growth in massive *Porites* colonies in terms of polyps and their associated corallites. This accords with Rosen's modular concept. In Chapter 2, initiation of polyps on a bumpy growth

surface was shown to occur, almost exclusively, at the summit of bumps. Older polyps were shown to become compressed at the bottom of valleys formed between bumps (section, 2.3.1). In these valleys, the size of polyps was shown to become increasingly reduced to a point at which they no longer existed. Thus, recycling of polyps was envisaged, with new ones forming on the top of bumps and older ones being lost and resorbed at the bottom of valleys formed between bumps.

An important point to arise from this work is that polyps cannot exist indefinitely on the surface of a bumpy *Porites* colony. Each polyp and its associated corallite has a longevity of around 5 years. The actual longevity appears to vary with the degree of bumpiness developed on the colonial growth surface, that is, with colonial growth form. These results strongly support Rosen's view that growth form is the resultant of the size and the arrangement of modular units.

3.1.2. Growth form variations within coral species.

Many corals characteristically display a range of growth forms within a species, that is, they have several different morphs. Some coral workers (e.g., Wijsman-Best, 1974; Dustan, 1975; Brakel, 1977; Veron, 1981; Willis, 1985; Willis and Ayre, 1985; Ayre and Willis, 1988) argue that morphological differences in certain species are caused by genetic variations between the various morphs. In contrast, other workers (e.g., Roos, 1967, Graus and Macintyre, 1976; Foster, 1979; Brakel, 1983; Willis, 1985; Titlyanov, 1981, 1987; Lewis, 1989) relate differences in colony morphology within species to environmental factors. Foster (1979) reviews this problematic area.

Corals that change their shape when exposed to different environmental conditions are considered to display phenotypic plasticity (Foster, 1979). Willis, (1985) found that *Turbinaria mesenterina* changed its growth form when transplanted to a different environment, and concluded that this coral displayed phenotypic plasticity. In contrast, she found that *Pavona cactus* did not change its shape when transplanted. She concluded that the different morphs of *P. cactus* were not

environmentally induced but were under genetic control. Ayre and Willis (1988) point out that, in general, phenotypic plasticity has been inferred when skeletal variability within a coral species is apparently correlated with some environmental variable, whereas a genetic basis for skeletal variations has been inferred when such variation is seemingly independent of environmental variation.

Variations in growth form displayed by massive *Porites* colonies have been related to differences in light intensity, depth and water turbulence (Roos, 1967; Brakel, 1983). Roos (1967) concluded that variations in growth form of *Porites asteroides*, from a hemispherical through to a flattened growth form, on a reef in the Caribbean, were depth related and resulted from a decrease in ambient light intensity. However, Brakel (1983), observed flattened growth forms of *P.asteroides*, in both deep and shallow water on reefs in the Caribbean, and concluded that the flattened growth forms developed in shallow water in response to high turbulence and in deep water in response to low light intensity. In contrast, Lewis (1989) found that the phenotypically plastic massive coral *Siderastrea radians* developed its more hemispherical growth form in high energy environments. Thus, relationships between environmental factors and growth form are not clear.

Graus and Macintyre (1976) constructed a computer model to simulate change in growth form of *Montastrea annularis* with increasing depth. They decreased skeletal extension as a response to decreasing light intensity with increasing depth. Although Barnes (1973) had pointed to the importance of the ratio of tissue growth to skeletal growth in controlling growth form, Graus and Macintyre did not include tissue growth in their model. They achieved a flattening of their colonies with increasing depth by introducing a "flattening factor" into their model. Indeed, apart from Barnes (1973), proposed mechanisms regarding the relationships between growth form and environmental variables have taken little account of tissue growth.

3.1.3. Genetic constraints on coral growth and growth form.

The size of polyps and the type of budding displayed by corals is, presumably,

controlled by the coral genotype. Both size of polyps and type of budding (see Wells, 1956; Hill, 1981) displayed by corals place limitations on the growth form produced. Colonies with larger polyps must modify their skeletons more than colonies with small polyps to accommodate new polyps. Consequently, it will take relatively longer for colonies with larger polyps to change their skeletons, and hence their growth form, as they increase in size. It will also take them longer to accommodate and adapt to changes in environmental conditions. Colonies which display a phaceloid arrangements of polyps must modify their skeletons more to accommodate new polyps than colonies with a linear-meandroid arrangements (Barnes, 1973). Thus, differentials between rates of tissue growth and rates of skeletal growth will be more difficult to accommodate in growth forms which display a phaceloid arrangement of polyps than in corals, such as *Porites,* which display a cerioid arrangement of polyps.

Massive *Porites* colonies therefore have the potential to exhibit considerable flexibility in their growth form because they have small polyps (around 1 mm in diameter) which are arranged in a cerioid pattern. Formation of new polyps on the growth surface of a massive *Porites* colony does not require much alteration to the skeletal architecture.

3.1.4. Geometric constraints on coral growth and growth form.

Galileo first pointed out, nearly 350 years ago, that organisms can not grow beyond certain sizes unless they change the relative proportions of the structures from which they are built (see Thompson, 1963). Thus, unless they change the materials from which they are built, they must change their shape as they grow bigger. As an organism increases in size, surface area increases as the square of the linear dimension and volume (and weight) increases as the cube. This phenomenon is known as the *Principle of Similitude.* Thompson (1963) and Huxley (1972) extensively applied the *Principle of Similitude*, and consequences arising from the principle, to explain an astounding range of phenomena associated with growth and growth form in the living world.

Barnes (1973) applied the *Principle of Similitude* to growth of massive hemispherical corals. He showed that, as rounded coral colonies having discrete polyps grow larger, they must extend their skeletons further for each doubling of the number of polyps. He proposed that breaking up a smooth growth surface into hummocks was one way in which this constraint on colonial growth could be overcome (section, 1.1.1.). Barnes' (1973) work set forth principles and constraints necessary to build a computer simulations of growth in coral colonies. It is disappointing that Graus and Macintyre (1976) did not incorporate some of these principles into their computer models. The importance of computer models to understanding plant growth has been well established (e.g., Harper, 1977; Harper and Bell, 1979; Bell, 1984) but its application to the growth form of corals has yet to be explored.

3.2. MATERIALS AND METHODS.

Growth of a massive *Porites* colony can be considered almost entirely in terms of: (i) polyp addition, which increases the lateral dimension of a colony, and (ii) skeletal extension which increases the longitudinal dimension of the colony. Rosen (1986) introduced the concept of modularity within colonial corals as a means of linking the polyp to its corallite such that the polyp and corallite together constituted a structure referred to as a modular unit. It was, therefore, appropriate to take the idea of modular units, which represent aspects of both tissue growth and skeletal growth, and use them as the basic building blocks for computer models to simulate *Porites* growth.

The modular unit chosen was an inverted trapezium (Fig. 3.1). Increase in length of the more vertical sides of the trapezium represented skeletal extension of a corallite. Increase in the width of the trapezium from its base to its upper surface (see Fig. 3.1) represented increase in the amount of tissue (as well as a certain amount of additional skeletal growth). Since *Porites* form cerioid colonies, that is,

adjacent corallites share the same walls, the form of the colony could be modelled by placing the trapezium modules side by side. The increase in width of the trapezium allowed for addition of new modules at the upper surface once the initial trapezium had become wide enough to include the base of two new trapeziums (Fig. 3.1). This represented growth and division of polyps with associated modification of the skeleton. An important aspect of this model was the ease with which "tissue growth" could be altered independently of "skeletal growth". Thus, a widely diverging trapezium represented high tissue:skeletal growth and a thin, narrow trapezium represented low tissue:skeletal growth.

Thus, the use of modular trapeziums allowed for the construction of an iterative computer model of colonial growth in which growth involved addition of modules one at a time and layer by layer. It was not possible for each trapezium present at a growth surface to develop into two new trapeziums, due to the lack of space available (see Chapter 1, Fig. 1.3). Some of the trapeziums were therefore prevented from continuing into the next layer. This feature of the models was considered to be similar polyp occlusion which is an important growth characteristic of massive *Porites* colonies (see page

3.2.1. Computer equipment used to build growth form models.

An IBM Cleveland XTSP personal computer equipped with an enhanced graphic adapter card (EGA card) was used to build and display two dimensional models simulating growth of a massive *Porites* coral. The program used to construct these models was written in Quick Basic Version 4.00b (see appendix, *Growth.bas*). A step by step account of the operation of this program is given below.

3.2.2. Design and operation of the computer models.

Programs simulating colonial growth in *Porites* were designated *Growth.bas*. *Growth.bas* required only two pieces of information: a length value (l) and a width value (w). The length value represented skeletal extension. The width value

represented tissue growth (see above). The length value set the length of the sides of the trapezium. The width value set the basal width side of each trapezium (see Fig. 3.1). The angle of divergence of the two sides of the trapezium was set by making the upper trapezium width (*dw*) twice that of the basal width (*w*) (Fig. 3.1).

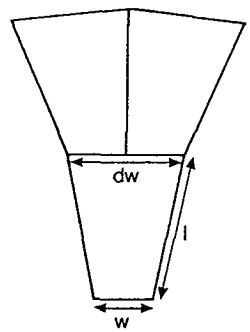

Fig. 3.1. Three modular units. A Modular unit represents a polyp and its associated corallite. The length value (*l*) represents skeletal extension and the increase in the width of the trapezium from the basal width (*w*) to the double width side (*dw*) represents the tissue growth.

Models were constructed using a range of different width (*w*) and length (*l*) values until growth forms were produced that appeared to resemble actual growth forms displayed by massive *Porites*. The width and length values used were, therefore, arbitrary rather than based on measurements on real colonies. The value of width/length (*w/l*) was called the *model growth rate ratio*.

Determination of the start point co-ordinate.

Computer calculations of the shape of a single trapezium were quite different to those for calculating the positions and shapes of two trapeziums side by side. Thus, to simplify the model, it began by drawing two trapeziums side by side. The paired trapezium was actually the iterative unit for the model since two trapeziums,

side by side, were added to the upper surface of an existing trapezium once it attained the appropriate width (*dw*) (Fig. 3.1.).

The centre point at the bottom of the computer screen was selected as the starting point co-ordinate, (x1,y1) for each model. The second co-ordinate, (x2,y2) was determined from the start point co-ordinate. x2 equalled x1 plus the double width value (*dw*). The y2 co-ordinate was given the same value as y1. A line between (x1,y1) and (x2,y2) represented the first double width line in each model (Fig. 3.2).

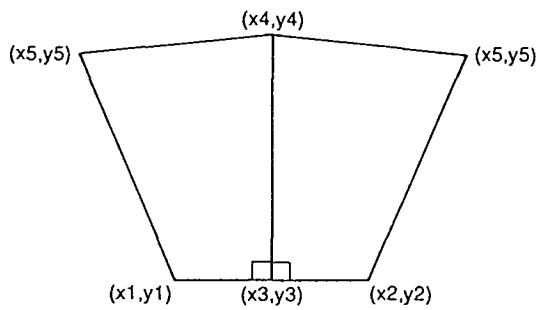

Fig. 3.2. Two modules displaying co-ordinates calculated to construct trapeziums: start point (x1,y1); baseline co-ordinate (x2,y2); *Mid Point* (x3,y3); *New Point* (x4,y4) and *End Point* (x5,y5).

Determination of the *Mid Point* co-ordinate on each double width line.

The *Mid Point* (x3,y3; see Fig. 3.2) on the double width line, (x1,y1) - (x2,y2), was calculated using the equation below.

$$x3 = INT((x1 + x2)/2) + 0.01)$$
$$y3 = INT((y1 + y2)/2) + 0.01)$$

X and y co-ordinates can only be plotted on a computer graphic screen if they are whole numbers since each co-ordinate corresponds to a pixel on the screen. The

integer command (INT) in Quick Basic, version 4.00b rounded values of 0.5 and less downwards i.e., INT(2.5) = 2.0. Because of this, the *Mid Point* was occasionally given a value that appeared below the (x1,y1) - (x2,y2) line. Therefore the values of x3 and y3 were increased by 0.01 before the integer was determined (see equations above) so that the (x3,y3) co-ordinate appeared on or directly above the double with line.

Determination of the *New Point* co-ordinate in each pair of modules.

The fourth co-ordinate (x4,y4; see Fig. 3.2) to be determined in each model was referred to as the *New Point* because the direction and extent of growth of a new module was determined by the position of this point (Fig. 3.2). The *New Point* (x4,y4) in each module was located a distance of (*l*) away from the *Mid Point* (x3,y3) and was positioned such that a line drawn from (x3,y3) to (x4,y4) was at right angles to the double width line (Fig. 3.2). This ensured that linear extension in the model was always at right angles to the growth surface. This procedure was important because the model would, otherwise, quickly develop lower extension rates away from the central growth axis of the colony. Annual growth banding seen in X-radiographs of skeletal slices from *Porites* showed that growth was fairly even over the whole surface (Plate 2.1 & 5.1).

The *New Point* (x4,y4) co-ordinate was determined from the three double width line co-ordinates, (x1,y1), (x2,y2) and (x3,y3) and the *equation of two circles*. The *equation of two circles* (see below) calculates two points of intersection of two overlapping circles. In the programme *Growth.bas*, two points of intersection of two circles whose centre points were (x1,y1) and (x2,y2) were calculated. The radius of the two circles (*m*) was calculated as the length of the hypotenuse of a right angle triangle whose adjacent sides had lengths (*l*) and (*w*). The *equation of two circles* calculated two points of intersection. These were designated;($x4_1$,$y4_1$) and ($x4_2$,$y4_2$). Only one of these represented the required *New Point* co-ordinate, (x4,y4). The two

points of intersection were obtained from the equations:

$$(x4_1 - x1)^2 + (y4_1 - y1)^2 = m^2$$
$$(x4_2 - x2)^2 + (y4_2 - y2)^2 = m^2$$

It was, then, necessary to choose between the two points of intersection because only one was appropriate to the model. The rules for selection of the appropriate point alter with the inclination of the base line. Thus, it was first necessary to determine the inclination of the base line i.e., to determine whether the line was more horizontally or vertically inclined. This inclination was determined from the co-ordinates of the ends of the base line. The rules for deciding upon the inclination of the line from the co-ordinates at its ends are shown in Figure 3.3.

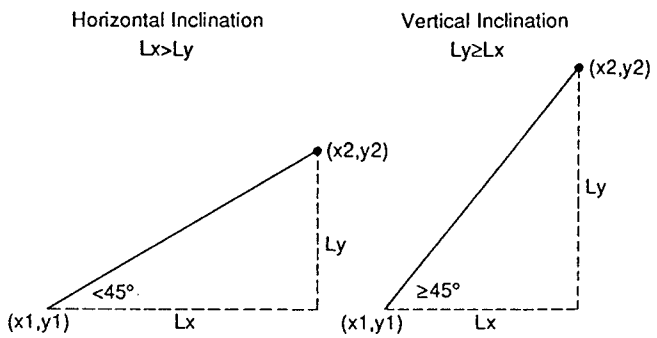

Fig. 3.3. Inclination of a line.

The rules for selecting the appropriate point of intersection, given the inclination of the base line, are shown in Figure 3.4.

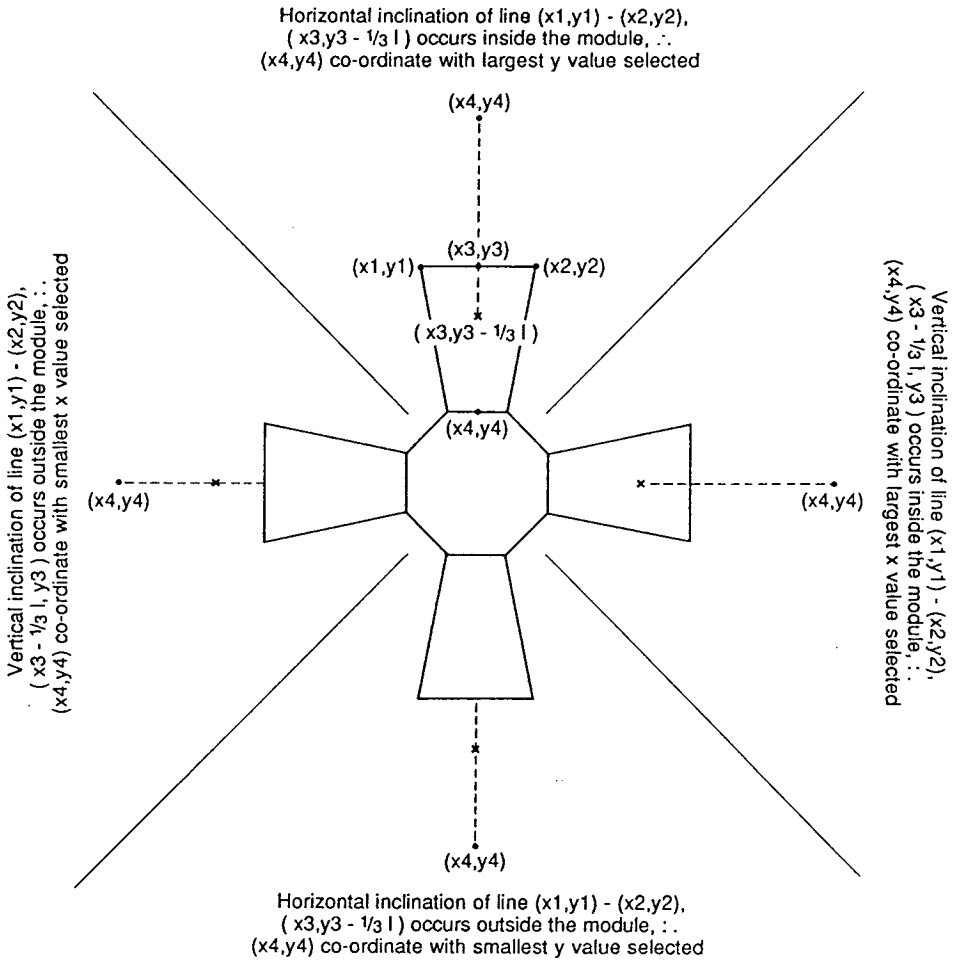

Fig.3.4. Rules governing the selection procedure of the appropriate *New Point* co-ordinate (x4,y4).

Determination of the *End Point* co-ordinate in each module.

To this point, the basal line had been established and a line could be drawn from the exact centre of the base line, "upwards" and at right angles to it. The length of the base line and the length of the "upright" line were defined by the initial settings for the model, (*w*) and (*l*). The next step was to determine the two points (x5, y5) on either side of the upper end of the "upright" line which would allow two complete, mirror-image "trapeziums" to be drawn (e.g., Fig. 3.2). These points were termed the *End Point* co-ordinate in both the left and right hand modules.

The *equation of two circles* was used to determine the positions for the *End Point* co-ordinates. The centre point for the two circles were (x4,y4) and either (x1,y1) or (x2,y2), depending on whether the *End Point* being determined was for the left or right hand module (Fig. 3.2). A radius of (*w*) was assigned to the circle centred at (x4,y4) and a radius of (*l*) was assigned to the circles centred at (x1,y1) and (x2,y2).

There were, again, two points of intersection for each pair of circles and it was necessary to select the appropriate one. The choice again depended upon the inclination (i.e., is it more horizontal than vertical) of the base line. This was established as before (see Fig. 3.3). It was also necessary to determine the orientation of the base line. This line was positioned somewhere amidst 8 possible orientations (see Fig. 3.5). The rules for establishing the orientation are given in Figure 3.5.

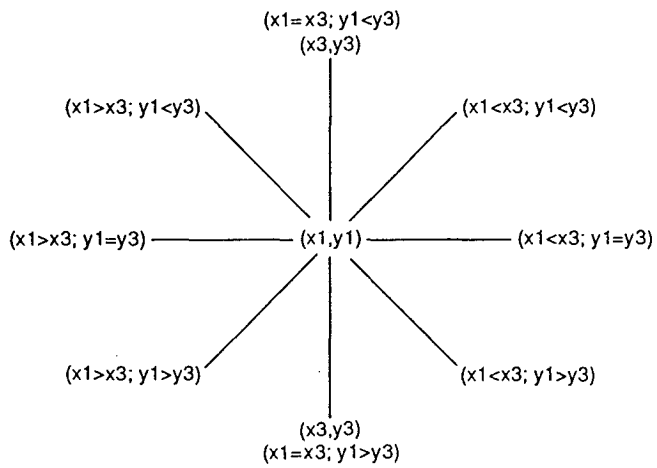

Fig. 3.5. Orientation of a line. If the orientation of the basal width line of the right hand module is being determined then (x1,y1) and (x3,y3) in this diagram become substituted by (x3,y3) and (x2,y2) respectively.

Having established both the inclination and the orientation of the base line, the appropriate *End Point* co-ordinate was selected using the rules set out in Figure 3.6.

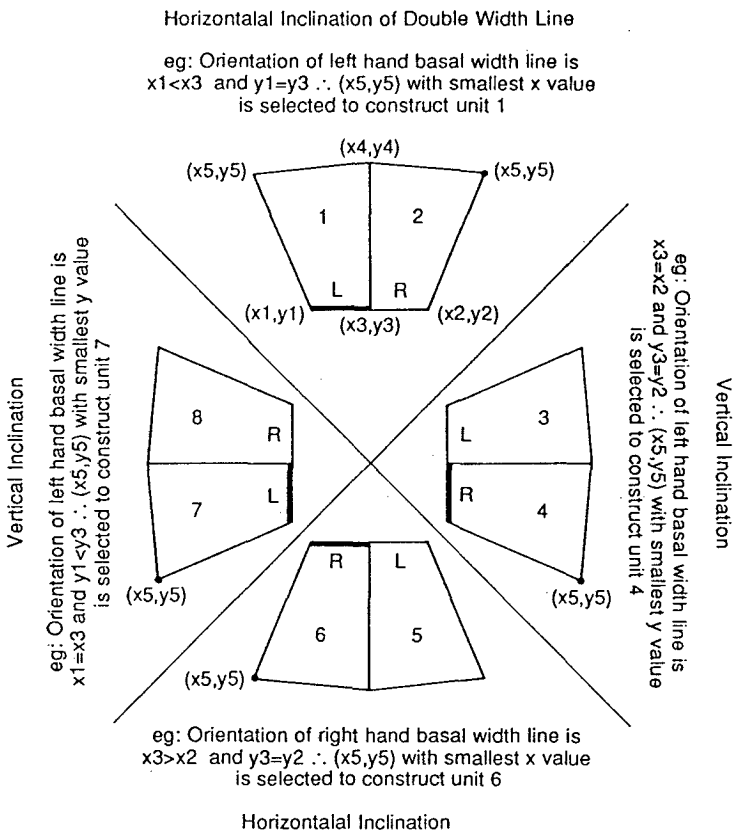

Fig. 3.6. Rules governing the selection procedure of the appropriate *End point* co-ordinate (x5,y5) in both the right hand (R) and left hand (L) modules.

Old file and *New file* co-ordinates.

The procedure described thus far could be used to draw a pair of trapeziums relative to a starting position at the bottom of a computer screen. The next step was to use the upper surface of each of these trapeziums as the base line from which a new pair of trapeziums could be constructed. This was done, quite simply, by declaring the top surface of each existing trapezium as the base line for another pair.

Each individual trapezium was defined by the co-ordinates of its 4 corners. Each of these co-ordinates was stored in computer memory as a single line of data. The 2 sets of co-ordinates designating the corner positions of the first pair of trapeziums were stored in a file, *Oldfile.dat* (see appendix). The pair of trapeziums were then drawn on the computer screen by joining up the appropriate corner points (Fig. 3.2). The computer then filled in, the pair of trapeziums, using the *PAINT* command. This indicated that space was occupied by a module. The upper surfaces of these trapeziums were delimited by (x4,x4) - (x5,x5); (see Fig. 3.3). The left hand and right hand upper surfaces, (x5,x5) - (x4,x4), were then considered to be the 2 new base lines, (x1,y1) - (x2,y2), for 2 new pairs of trapeziums. The co-ordinates of these 2 new base lines were stored in the computer file, *Newfile.dat* (see appendix). From these 2, new base lines, the positions for the corners of 4 new trapeziums were calculated. These data were then appended to the *Oldfile.dat.*

In this way, a model could be built up layer by layer. The *Oldfile.dat* contained information about the corner positions of each of the trapeziums making up the complete image. The *Newfile.dat* contained only the co-ordinates defining the positions of the upper surfaces of the most recent layer of trapeziums.

Problems with the models as they increase in size.

Different models were defined by the values for (l) and (w) initially set (see above). As each model increased in size it was not possible for all the basal width lines on each new growth layer to develop in to new modules. This occurred because the relative amount of new space made available for module growth following each linear extension of the model decreased as the model became bigger (see section, 1.1.1 for a more detailed explanation of this). It was not possible for a model to maintain a constant doubling of the length of its outer surface (by doubling of the number of modules) whilst the skeletal extension (l) remained constant. Therefore, in the model, some modules were prevented from continuing into the next layer.

The *Growth.bas* program was designed to scan along a set of co-ordinates for a potential module to test whether it could be constructed (drawn) without obscuring an existing module. If a potential module was found to conflict with an existing module, then the potential module was not drawn and its co-ordinate points were discarded. The mathematical procedures used for determining if such conflict existed were quite complex. These procedures are set out in the Appendix, program line 477 and 655.

Growth.bas version I and II.

Two versions of the *Growth.bas* program were developed to test whether the order of addition of new modules to the growth surface affected the growth form produced. In version I of the program, potential module co-ordinates were stored in sequential files. Therefore every time a model was constructed with the same width (w) and length (l) values, the same modules were developed and prevented from continuing to grow each time a model was grown. The appearance of the model produced was identical for a given set of width (w) and length (l) co-ordinates because the computer was following a set of sequential instructions which gave no latitude for variation. In version II of the *Growth.bas* program, co-ordinates were stored in random files and a random number generator was used to access sets of co-ordinates from which new modules co-ordinates were determined. Therefore, every time version II of the program was run, different models were constructed for identical width (w) and length (l) setting.

Models were constructed with width to length ratios (w/l) ranging from 0.2 through to 1. Models were constructed using the 2 different versions of *Growth.bas* program with the same width to length ratios but with different values for (w) and (l).

The ordering of co-ordinates in sequential file did not appear to have any effect on the overall growth forms displayed by models. The arrangements of modules developed by models constructed using *Growth.bas*, version I resembled more closely the arrangement of corallites in corallite fans displayed by X-radiographs of skeletal slices removed from massive *Porites* colonies than those displayed by models constructed suing version II of the program. Therefore measurements were made on models constructed using version I.

3.2.3. Measurements taken from computer models.

Twenty-six models were constructed to simulate growth of massive *Porites* colonies. The values for (*w*) and (*l*) ranged between 10-105 and between 30-140 respectively (Table 3.1). The growth rate ratios were in the range 0.2-1.0. A variety of architectural features common to all these models were measured on hard copies of models printed from the computer screen. These measurements were used to test for architectural differences between growth form models having the same growth rate ratio but different values for width (*w*) and length (*l*). This test was used to establish whether the way in which the computer graphically displays mathematically derived images affects the printed hard copy of a model (e.g. the affect of the aspect ratio of pixels). Measurements were also used to test for differences between growth form models with different growth rate ratios.

Measurements relating to architectural features of individual models were made on a particular sector common to each of the twenty-six growth form models. This sector, which included five module layers, was marked out on each of the models as close to the main vertical growth axis as possible (Fig. 3.7). The shape of this sector altered between models with the angle of divergence of modules from the central growth axis of the colony model and with the curvature of the growth surface. Usually, any contiguous set of modules persisted through at least 5 layers of growth before it was prevented from further division by interference from adjacent modules. Thus, the sector was defined to incorporate five layers of modules.

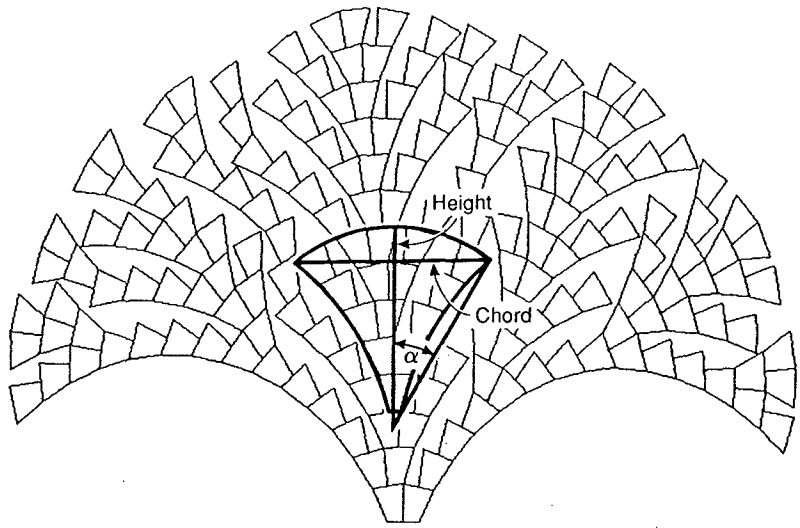

Fig. 3.7. Growth sector marked out on a computer model from which measurements were taken.

A line was drawn along the central axis in each sector (Fig. 3.7). This line defined the distance grown within the sector by addition of 5 layers of modules. It was used to calculate a theoretical annual rate of skeletal extension in each growth form model. For convenience, one layer of modules was considered to be added each year. This bore no relationship to real colonies but made more simple the task of describing and analyzing growth in the model, and comparing growth between models. Theoretical annual skeletal extension rate displayed by each model was determined by dividing the length of central line drawn for each sector by 5. The results were expressed in mm yr^{-1}.

The length of the curved, upper surface of each sector (Fig. 3.7) was measured by draping a fine chain along it. The linear length of chain required to follow the curved surface was then measured against a ruler. The measurements were made to the nearest millimetre. The length of this line was considered to represent the

amount of tissue generated within a sector during a five year period. The length of this line divided by five provided a theoretical annual rate of tissue growth. Tissue growth was also expressed as mm yr^{-1}. It was, then, possible to derive a dimensionless, theoretical tissue growth:skeletal extension ratio for each model.

A line was drawn from the initial point of the central growth axis to one end of the curved, upper surface of the sector (Fig. 3.7). The angle between this line and the central growth axis was then the angle of divergence of the sector. This angle was measured with a protractor.

The curvature of the growth surface of the sector was very similar to the degree of bumpiness at the outer surface of the model (e.g., Fig. 3.9). Thus, the amount of bumpiness in a model was determined from measurements on the growth sector. The horizontal distance was measured between the two end points of the curved, upper surface of the sector. This distance (i.e., the chord, Fig. 3.7) was the width of the sector. The distance between the midpoint on the chord and the curved, upper surface of the sector was taken to be the height of curvature (Fig. 3.7). The amount of bumpiness was expressed as the ratio between the height and half the width. This "bumpiness" ratio increased as the upper surface of the sector became more curved.

3.2.4. Statistical procedures.

A Macintosh SE personal computer, equipped with the *Statview* statistics package, was used to analyze the measurements taken from the computer models. Before growth form differences between computer models with different width to length ratios (w/l) were compared, preliminary tests were performed to investigate the variance in growth form features between models having the same width to length ratio (w/l) but with different values for width (w) and length (l). This was done to test if the ratio was controlling growth form, rather than the values assigned to width (w) and length (l).

Three sets of computer growth form models were developed with ratio values of 0.25, 0.5 and 0.75. Each set contained 6 models having different values for width (w) and length (l) (Table 3.1). The mean and standard deviation for the tissue:skeleton ratio, the angle of divergence and bumpiness ratio were determined for each set of models.

The value assigned to length (l) was considered to represent skeletal growth. The value assigned to width (w) was considered to represent tissue growth. Using values derived from all twenty-six models, the model growth rate ratio (w/l) was correlated with the three parameters derived from growth sectors; the sector tissue growth:skeletal growth ratio, the angle of divergence and the bumpiness ratio.

3.3. RESULTS.

3.3.1. General description of the growth form models produced.

The *Growth.bas* program (see appendix) was used to generate a range of computer growth forms designed to simulate growth and growth forms displayed by a massive *Porites* colony. Different growth forms were produced by changing the width to length ratio (w/l). Although there were differences in the appearance of models with different width to length ratios (w/l), all twenty-six models constructed displayed similar architectural features. Figure 3.8 shows a model constructed with a width to length ratio of 0.4.

About twenty layers of modules were grown in each model, with each layer considered to represent a years growth. Nearly all the models developed a roughly hemispherical growth form with a bumpy growth surface as they increased in size (Fig. 3.8). The layers of modules within each model were, therefore, arranged in a

roughly concentric pattern. Models with a higher width to length ratio (*w/l*) developed a more bumpy growth surfaces than models with a lower ratio (Fig. 3.9).

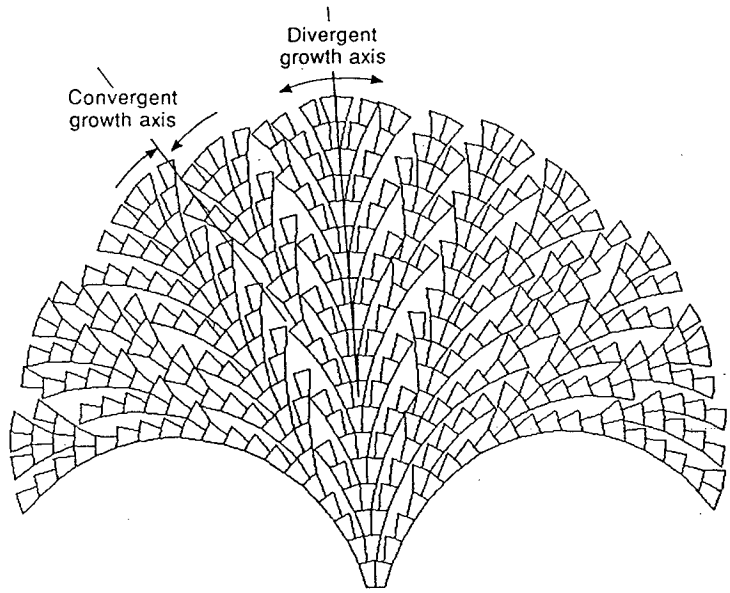

Fig. 3.8. Computer generated growth form model with a model width to length ratio (*w/l*) of 0.4.

Areas in the growth form models not occupied by modules were not considered to represent cavities in a real *Porites* skeleton. Instead, these areas marked regions where the model might have allowed modules to become compressed before they stopped growing. For the sake of simplicity, this attribute was not included in the model.

Bumps developed on the growth surface of models were associated with distinctive fan-like arrangements of modules. The major vertical axis passing through the centre of these fans is referred to as the divergent growth axis (Fig. 3.8). Modules tend to grow away from this axis and create the divergent modular growth pattern. An axis of divergent growth passes through the summit of its associated bump.

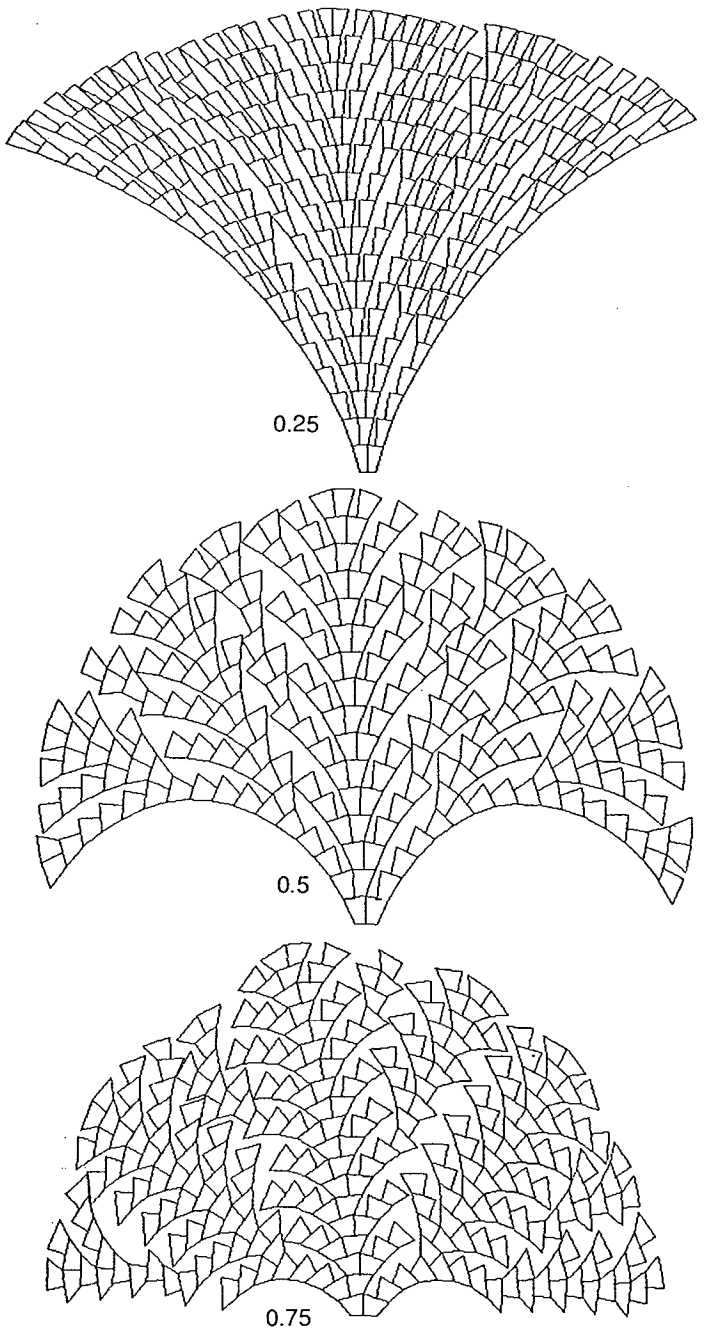

Fig. 3.9. Computer generated models designed to simulate growth forms of three massive *Porites* colonies with model width to length ratios (*w/l*) of 0.25, 0.5 and 0.75.

The axis marking the margin between adjacent fans passed through the bottom of the valley on the growth surface between the bumps associated with the fans. This axis is the convergent growth axis (Fig. 3.8). It marks a region where modules from adjacent bumps converge, interfere with each other and prevent continued growth.

3.3.2. Growth form models with the same width to length ratio (*w/l*).

Models with the same width to length ratios (*w/l*) showed virtually no differences in the three growth parameter measured from the growth sectors, despite differences in the absolute values assigned to (*w*) and (*l*) (Table 3.1). Thus, the growth form characteristics displayed by each model were controlled by the width to length ratio (*w/l*) and not by the values assigned to width (*w*) and length (*l*).

Table 3.1.

Mean and standard deviations (± S.D.) for growth and growth form features measured in 3 sets of models with different absolute width to length ratios.

	Model width to length ratio (*w/l*)		
	0.25	0.5	0.75
Number of models	6	6	6
Range of *w:l* values	10:40 - 35:140	15:30 - 40:80	30:40 - 105:140
Tissue:Skeleton mean ± SD	0.54 ± <0.01	1.02 ± <0.01	1.53 ± <0.01
Angle of divergence mean ± SD	13.45 ± 0.14	28.33 ± 0.07	47.67 ± 0.37
Bumpiness ratio mean ± SD	0.23 ± <0.01	0.43 ± <0.01	0.61 ± <0.01

3.3.3. Relationships between the width to length ratio and growth form displayed by a range of computer models.

The width to length ratio (*w/l*) associated with a model was strongly and positively correlated with the tissue growth rate to skeletal growth rate ratio measured in a sector ($r = 0.99$, $n = 26$; see Table 3.1 and Fig 3.9). Thus, higher tissue growth: skeletal growth ratios for models produced equivalent ratios in growth sectors. This indicates that measurements made on growth sectors reflect overall colony growth.

The angle of divergence of modules displayed by modular fan-like structures was shown to be strongly and positively correlated with the width to length ratio (*w/l*) associated with each model ($r = 0.99$, $n = 26$). Thus, fan-like arrangements of modules were better developed in models with higher width:length ratios (Table 3.1, Fig. 3.9).

The model bumpiness ratio was strongly and positively correlated with the width:length ratio (*w/l*) ($r = 0.97$, $n = 26$). Bumpiness increased with the width:length ratio (Table 3.1, Fig. 3.9).

3.4. DISCUSSION.

3.4.1. Similarities between architectural features displayed by computer models and those displayed by massive *Porites* colonies.

The computer-generated growth form models designed to simulate growth of massive *Porites*, displayed a range of growth forms that were highly comparable with those displayed by the 36 massive hemispherical *Porites* colonies presented in Chapter 2. X-radiographs of skeletal slices (Chapter 2) presented information about changes in shape and surface geometry that occurred over the life of a coral colony. Computer models described here presented similar information. As each computer

model increased in size, the initial fairly smooth growth surface became bumpy. Development of a bumpy growth surface with increasing colony size was a characteristic displayed by all massive *Porites* (Isdale, 1977; Chapter 2). Models with a width to length ratio (*w/l*) of 0.25 displayed fairly smooth growth surfaces which closely resembled some of the very smooth *Porites* colonies collected from the central G.B.R. transect (cf., Fig. 3.9, model 0.25 and Plate 5.1). The amount of bumpiness displayed on the growth surface of models with width to length ratios (*w/l*) between 0.4 and 0.6 resembled the bumpy growth surfaces displayed by the majority of the 36 massive *Porites* colonies (cf., Fig. 3.9. model 0.5 and Plate 2.1). Computer models with a width to length ratio (*w/l*) in excess of 0.75, displayed a growth form and surface architecture approaching that of the most bumpy of the corals collected from the central transect.

The internal, skeletal architectural features displayed by the computer models closely resembled skeletal patterns displayed in the X-radiographs of the 36 massive *Porites* colonies (Chapters 2, 5). The sequential layering of modules in each hemispherical growth form model produced a concentric pattern that resembled the concentric annual density banding pattern displayed by X-radiographs. Modular fans developed by the computer simulations closely resembled the corallite fans seen in X-radiographs (cf., Fig. 3.8. and Plate 2.3). The angle of divergence of modules associated with bumps in computer models was, therefore, equivalent to the angle of divergence of corallites in corallite fans (see below, Chapter 5). Similarly, the axes of divergent and convergent growth of modules on computer models equated with the central growth axis of corallite fans and the axis of fan margins, respectively.

In the same way that the bumpiness of real coral colonies was simulated by the degree of bumpiness developed in computer models, the angle of corallite divergence in actual coral slices was simulated by the angle of divergence of modules in a computer model sector. Moreover, models which approximated real corals had bumpiness and the angle of divergence combined in a way which approximated that in real colonies (Chapter 5).

3.4.2. Similarities between the growth process displayed by the computer models and that displayed in skeletal slices from colonies of massive *Porites*.

Some of the growth processes displayed by computer models as they increased in size followed closely growth processes revealed by X-radiographs of skeletal slices cut from massive *Porites* colonies (Chapter 2, section 2.4.2 & 2.4.3.). The addition of modules one layer at a time simulated, and thus represented, constant annual skeletal extension over the surface of a colony. Contiguous sets of modules displayed a radial pattern at the base of a "colony". As the "colony" increased in size, and developed a bumpy growth surface, modules became arranged into discrete fan-like structures. This change in the arrangement of modules with increasing size of the "colony" strongly resembled the change in arrangement of corallites seen in X-radiographs (cf., Fig. 3.8 and Plate 2.1).

Observations of calices on the top of bumps in real *Porites* colonies, and apparent corallites displayed in X-radiographs of skeletal slices, clearly revealed that the majority of new corallites, and hence polyps, were initiated on or towards the summit of bumps (Chapter 2). However, in the computer models, growth of new modules occurred over the entire growth surface and was not restricted to the tops of bumps (In fact, this inadequacy of the model led me to the more realistic description of the actual growth process displayed by massive *Porites* colonies). Modules located at the bottom of valleys formed between bumps were prevented from developing further once they met a module growing from the adjacent fan. It is obvious from observations on real colonies and X-radiographs that, in actuality, corallites become increasingly compressed and diminished towards the base of valleys between adjacent bumps, and eventually become occluded (Chapter 2). This aspect of growth was not simulated in computer models presented here. Hence, the "cavities" apparently present in the models (see above).

Contiguous sets of modules appeared to have an average "life" of around five layers. From the way the model was defined this equated to growth over five years.

The apparent longevity of corallites in real colonies was also around five years (Chapter 2). This similarity arose, essentially, from attempts to define the models in terms of growth processes and timing determined from actual colonies.

It may, then, be seen that architectural features and growth processes displayed by computer models clearly simulated equivalent features in real colonies. This equivalence suggests that the models may be used to examine features of growth and growth form in massive *Porites* which would, otherwise, take many years of difficult experimental work. Some aspects of such extrapolation from the models are described in sections 3.4.3 and 3.4.4.

3.4.3. The importance of the ratio of tissue growth:skeletal growth.

Models displaying a relatively faster rate of tissue growth compared with skeletal growth formed a well developed bumpy growth surface and the angle of divergence of modules associated with each bump was fairly large (about 47°). This contrasted with growth form models having relatively slower rates of tissue growth compared with skeletal growth. These models displayed a smoother growth surface and a smaller angle of divergence of modules (about 13°). It seems highly likely that the ratio of tissue growth to skeletal growth within a massive *Porites* colony profoundly affects the colonial shape and architecture which develops. These computer models strongly support the hypothesis (Barnes, 1973; Chapter 1) that the growth form of massive corals, including, and perhaps especially, *Porites*, is determined by the ratio of tissue growth to skeletal growth and not the absolute values for either parameter.

3.4.4. Tissue growth:skeletal growth ratio and colonial growth form.

Barnes (1973) suggested that certain types of massive coral colony, including *Porites*, must develop a bumpy surface as they grow bigger (see above; also 1.1.1.). Other observations support this view (Isdale, 1977; Chapter 2). In computer models presented here, colonies developed a bumpy growth surface in much the way

predicted by Barnes. However, the models go further than Barnes' predictions. They suggest that the degree of bumpiness displayed by a colonial growth surface will alter with the ratio of tissue growth:skeletal growth. For example, an especially bumpy growth surface is likely to develop where the ratio of tissue growth:skeletal growth is high. Thus, an especially bumpy surface suggests that tissue growth is being constrained by skeletal growth. The reverse is not necessarily true: a smooth growth surface does not necessarily suggest that skeletal growth is being constrained by tissue growth. Rather, it suggests that tissue growth is not being constrained by skeletal growth.

3.4.5. Bumpiness and the coral's environment.

Both nutrition and calcification in reef-building corals can be enhanced by light acting through the symbiotic algae present in the animal tissues (see Barnes and Chalker, 1990, for review). Barnes (1973) makes the point that there must also exist a degree of independence between tissue and skeletal growth; that both are not necessarily equally dependent upon light. This notion is supported by the fact that different colonies can display varying degrees of bumpiness. It follows from these ideas that the degree of bumpiness of the surface of a massive coral colony, such as *Porites*, may be used to provide information about the environmental conditions in which the colony grew. This is further explored in Chapter 5.

3.4.6. Tissue growth and change in the area of the colonial growth surface.

Implicit in what has been developed so far, and in other work regarding tissue growth in coral colonies (Marsh, 1970; Loya, 1976; McCloskey and Muscatine, 1984; Muscatine *et al.*, 1985; Meyer and Schultz, 1985), is the notion that the tissue biomass of a coral colony is proportional to its surface area. Also implicit in what has been developed so far, and in other work (Stephenson, 1931), is the notion that tissue biomass is proportional to the number of polyps. These notions do not appear to have been tested. Chapter 4 presents results of experiments designed to test these notions.

3.5. CONCLUSIONS.

1. Architectural features displayed by computer models designed to simulate growth of a massive *Porites* colony closely resembled patterns displayed in X-radiographs of skeletal slices cut from massive *Porites* colonies. The arrangement of modular units within the models was similar to the arrangement of corallites displayed in X-radiographs. Models which developed very bumpy growth surfaces tended to display high divergence of modular units. In an equivalent fashion, colonies of massive *Porites* with bumpy growth surfaces tended to display corallite fans having high angles of divergence.

2. All computer models developed a roughly hemispherical growth form. However, the degree of bumpiness developed on the growth surface altered with the ratio of tissue growth to skeletal growth.

3. The ratio of tissue growth:skeletal growth in *Porites* strongly influences, perhaps determines, colonial growth form and certain aspects of colonial architecture. The degree of bumpiness may provide information about the ratio of tissue growth:skeletal growth in a *Porites* colony.

4. Similarity between elements of the models, and the architecture and growth processes demonstrated for real colonies suggests that the models may be used to examine other features of growth in *Porites*.

CHAPTER 4

AN ANALYSIS OF THE AMOUNT OF PROTEIN AND CHLOROPHYLL PER UNIT SKELETAL SURFACE IN *PORITES*

4.1. INTRODUCTION.

In the computer generated growth form models presented in Chapter 3, tissue growth was equated with increase in surface area. These models were based on the assumption that tissue biomass is directly proportional to skeletal surface area. Work described in this chapter investigated the relationship between tissue biomass and skeletal surface area within massive *Porites* colonies.

4.1.1. The tissue biomass to skeletal surface area relationship.

Several workers have estimated tissue biomass, in various coral species, from measurements of the skeletal surface area covered by tissue. For example, Marsh (1970) covered a coral growth surface with aluminium foil and used the weight of the foil to estimate tissue biomass. Very similar procedures were used by Loya, 1976; Stearn *et al.*, 1977; McCloskey and Muscatine 1984; Muscatine *et al.*, 1985; see especially, Lewis, 1981. A variation of this technique was developed by Meyer and Schultz (1985). These workers coated corals in a special, liquid latex. After the latex had solidified, it was peeled away from the skeleton. The solidified latex was flattened between glass sheets and its surface area was determined with a digitizer.

All of these techniques assume that tissue biomass is proportional to skeletal surface area.

In the 36 slices of skeleton cut from hemispherical colonies from the transect in the central section of the G.B.R. (see Chapter 2), the tissue formed a fairly even layer, about 4-9 mm thick (see Chapter 5), around the outer, growth surface (see also, Plate 1.3). This, together with earlier work outlined above, made it reasonable to equate tissue biomass in massive *Porites* colonies with surface area to enable computer growth form models to be constructed. The assumption that tissue biomass is proportional to the calicinal surface area of a coral colony has not been tested. Work describe here was aimed at testing this assumption. The relationship of tissue protein to chlorophyll content was also examined to establish whether chlorophyll can be used instead of protein to estimate tissue biomass.

4.1.2. Polyp density on the growth surface of a *Porites* colony.

Observation of calices on the growth surface of the 36 massive *Porites* colonies presented in Chapter 2, revealed that the polyp density on a well developed, bumpy growth surface appeared to be very slightly higher than the polyp density on a smoother growth surface (Chapter 2, section 2.3.4.). Similarly, the localised polyp density over a bumpy growth surface appeared to vary (i.e. relatively fewer polyps per unit surface area on, or near, the summit of a bump compared with the number of polyps per unit surface area towards the bottom of valleys between bumps (Plates 1.2, 2.2). This difference is probably due to greater compaction of polyps towards the base of a valley. Moreover, the degree of surface bumpiness appeared to diminish from the summits of colonies towards their lower surfaces. Dustan (1979) noted that the polyp density displayed by colonies of *Montastrea annularis* decreased with increasing water depth.

There is, then, a slight suggestion that polyp density alters with the growth form of the colony, and, hence, with environmental factors, and with the profile of the colonial surface. This may affect the amount of tissue present at a colony

surface, regardless of whether the tissue layer maintained a more-or-less constant thickness. For example, fewer fatter polyps per unit surface area may contain more tissue biomass than fewer thinner polyps per unit surface area. Thus, the work described here examines the relationship between polyp density and tissue biomass.

4.1.3. The relationship of tissue protein and chlorophyll content.

Coral tissue is predominantly composed of protein and a smaller amount of lipid, about 14% in *Pocillopora capitata* (Patton *et al.*, 1977). Zooxanthellae contribute 5-15% of the total biomass (Patton *et al.*, 1977; Muscatine and Porter, 1977). Drew (1972) has suggested that the density of zooxanthellar cells per unit surface area is regulated by the animal host and does not alter with factors such as light intensity and water depth. Other workers have presented evidence that regulation of zooxanthellar density is one of several mechanisms by which corals adapt to differing light conditions, a phenomenon known as photoadaptation (Dustan, 1979, 1982; Titlyanov, 1981, 1987; Falkowski and Dubinsky, 1981; Chalker and Dunlap, 1983a, b). The evidence suggests that regulation of algal density is, perhaps, less important in photoadaptation than changes in the concentration of photosynthetic pigment and alterations in chloroplast structure, both of which increase the efficiency with which available light is trapped and used (see Jokiel, 1988 for recent review). For example, Porter *et al.* (1984) studied light-shade adaptation of *Stylophora pistillata* and found that shade-adapted corals had significantly more chlorophyll per individual zooxanthellar cell than light-adapted corals, but did not have a significantly different number of cells per unit surface area (see also Dubinsky *et al.*, 1974).

Porter *et al.* (1984) concluded that the mass of chlorophyll per unit surface area is greater for shade-adapted corals than for light-adapted corals. Thus, populations of zooxanthellae may be proportional to coral tissue biomass but tissue chlorophyll content may be more closely related to the ambient light intensity. The relationship of chlorophyll concentration to tissue biomass and light has not been investigated for *Porites*. The second part of this study was designed to test the relationship between tissue biomass and chlorophyll content in *Porites* to assess

whether chlorophyll content can be used to estimate tissue biomass so as to eliminate the need to perform a protein analyses to determine coral tissue biomass.

4.2. MATERIALS AND METHODS.

Protein and chlorophyll analyses were performed using 18 massive *Porites* colonies. These colonies were collected at Reef 21/141 in the southern G.B.R. and Yonge Reef in the northern section of the G.B.R. (refer to section 1.3, Fig. 1.6) These colonies represented 2 species of *Porites*; *P. lobata* and *P. lutea* (Veron and Pichon, 1982; Veron, 1986; see Table 4.1).

Table 4.1.

18 massive *Porites* colonies collected for protein and chlorophyll analyses. 30 samples were removed from each colony.

	Reef and Species Groups.			
	Group 1	Group 2	Group 3	Total
Reef	21/141	Yonge	Yonge	2
Species	*P. lutea*	*P. lutea*	*P. lobata*	2
No. of colonies	6	4	8	18
No. of tissue samples	180	120	240	540

The experimental design involved collecting 18 colonies from 2 reefs, with 12 colonies from one reef representing 2 species (6 x 2). Thus, protein and chlorophyll content could be compared between environments and species. Unfortunately, 2 of the colonies from Yonge Reef identified in the field as *P. lutea* were subsequently re-identified in the laboratory as *P. lobata*. Because of this, the

data set became unbalanced. Colonies were collected from 2 reefs located at opposite ends of the G.B.R. to maximize probable environmental differences (Maxwell, 1968).

4.2.1. Tissue samples collected.

At each reef locality divers wearing SCUBA used numbered floats to tag massive *Porites* colonies growing in < 5 m of water (relative to MLWS) in back reef areas. Colonies tagged were roughly hemispherical and between 350 - 550 mm in diameter. The size of colonies selected was a compromise between colonies small enough to be easily collected, manhandled and taken to the research vessel, and colonies large enough to provide a surface from which 30 core samples, approximately 20 mm in diameter, could be removed. Colonies were collected from shallow, back reef environments at Yonge Reef and Reef 21/141 to reduce possible environmental variability associated with reef and depth (see section 1.1.3).

A hand-sized piece of coral was chiselled off each colony after it was tagged. These sub-samples were taken to the research vessel for species identification using a binocular microscope. Identifications were according to Veron and Pichon, 1982 and Veron, 1986. Time restrictions and a paucity of specimens in shallow water in the back reef area at Reef 21/141 meant that some colonies had to be tagged in depths up to 8 m.

Once the colonies had been identified to species on the research vessel, appropriate tagged specimens were selected for collection. Each colony selected was placed in a strong nylon string bag and the bag was then hung beneath an inflatable boat. Colonies were taken to the research vessel in this position. They remained beneath the boat for up to 1½ h, until tissue samples could be removed. Care was taken to minimise damage to the tissue surface during the collecting procedures.

Colonies in their rope bags were lifted on to the after deck of the research vessel. They were sprayed, regularly, with salt water while exposed. An air drill with a 20 mm diameter core attachment was used to remove 30 cores at random over

the entire growth surface of each colony. Cores were removed where the local surface of the colony was reasonably smooth and flat so that the "living" surfaces of cores were reasonably similar. Thus, cores contained equivalent areas of tissue and subsequent measurements of protein, polyp density and chlorophyll were directly comparable. Cores removed were 17.5 mm in diameter. The surface area of each core was, therefore, 240.5 mm^{-2}. Each core was drilled to a depth of about 20 mm to ensure that the entire tissue layer was included in the sample. Before a core was removed the distance from the summit of the colony to the centre of each core was measured. It was, then, possible to investigate any differences associated with increasing distance down the colony.

Two additional, control cores were removed at random from each colony. These cores were used to test whether analyses detected significant amounts of tissue beneath the obvious tissue layer at the surface of cores. The control cores were cracked in half just beneath the observable tissue layer and protein and chlorophyll analyses were carried out on the lower region of skeleton. This was necessary because all the other cores were reduced to a length of 10 mm, to facilitate photography of cores. It was, thus, necessary to ensure that discarded regions of skeleton were unlikely to have contributed to the protein and chlorophyll analyses.

All cores were placed in separate, numbered bags and placed in a freezer at -20°C. Colonies were returned to the reef once tissue samples had been removed. Tissue samples were kept frozen and in the dark to minimize degradation of protein and chlorophyll. Back at the laboratory, intact cores were photographed. The photographs allowed the numbers of polyps on the core surfaces to be simply and easily counted without requiring the cores to be removed from the freezer for extended periods. Cores were subsequently broken into pieces to assist chlorophyll extraction and, finally, protein was extracted from the tissue samples.

4.2.2. Photographing and counting polyps on cores.

All cores, excluding the control cores, were reduced to 10 mm in length, using

a hammer and chisel, so that it was possible to photograph several cores side by side while maintaining calicinal surfaces clearly in focus. A plastic holder was made to accommodate 6 cores with their respective identification numbers. Cores were photographed with a Hasselblad camera, with a 120 mm macro lens and no.55 extension tube, on black and white technical pan 120 mm film rated at 100 I.S.O. Black and white film was used in preference to colour film to emphasise the contrast between light corallite walls and the darker polyps. Contact prints were made from the negatives and the numbers of polyps on each core were counted from these prints.

Polyps were counted under a binocular microscope. Polyps were counted in an area 10 mm by 10 mm (100 mm^2) in the central region of each core photograph. A stencil was placed over the photograph to delimit this area. A felt-tip pen was used to mark off each polyp with a dot as it was counted. A hand tally counter was used to record the number of polyps. Polyps on the surface of cores from 2 of the colonies, 1 from Yonge Reef and 1 from Reef 21/141, were not clearly distinguishable. Therefore, polyps densities could not be determined for 2 of the 18 colonies.

4.2.3. Extraction and quantification of chlorophyll pigments.

100% acetone is one of the most widely used solvents for extraction of chlorophyll pigments from coral zooxanthellae (see Chalker and Dunlap, 1981). The spectrophotometric equations used for determining chlorophyll a and c_2 in zooxanthellae, using 100% acetone are based on the extinction coefficients of Jeffrey and Humphrey (1975). The efficiency with which 100% acetone extracts chlorophyll from *Porites* had not previously been tested. Preliminary tests were performed on trial samples of *Porites* tissue to assess this efficiency. The results showed that after 5 extractions with 100% acetone, each of 24 h, chlorophyll was still present in the coral tissues. Crushing core samples with a pestle and mortar did not improve the extraction efficiency. Resulting suspension of the tissue in the solvent interfered with subsequent protein determinations. It was decided that 100% acetone was not appropriate for analyses described here. An alternative method was sought.

Chalker and Dunlap (1981) showed that 20% tetrahydrofuran (THF) and methanol was more efficient at extracting chlorophyll pigments from reef-building corals than either 90% aqueous acetone or 100% methanol. The spectrophotometric equations used for the quantification of chlorophyll-a and c_2 in 20% THF and methanol have been derived (Chalker and Dunlap, pers. comm.). Preliminary tests were carried out on *Porites* tissue using 20% THF and methanol for chlorophyll extraction. Extraction techniques were as before. No chlorophyll was detected by the fifth extract. Consequently, 20% THF and methanol was chosen for *Porites* chlorophyll extractions.

All 576 cores were broken, but not crushed, into about 6 - 10 pieces using a pestle and mortar. This facilitated solvent penetration into the tissue and thus aided chlorophyll extraction. Core pieces were placed into separate vials and covered with 2.5 ml of 20% THF and methanol. This volume was just sufficient to totally immerse all of the pieces. Vials were sealed to prevent evaporation of the solvent and placed in the dark at 6°C for 24 h in a shaking bath set at 1,000 oscillations per min. The extracts were then pipetted to new vials and stored in an ultra-freezer at -80°C. The extraction procedure was repeated on the core pieces 3 more times. The 4 extracts were combined. The core pieces were returned to the freezer to await protein determinations.

The total volume of each of the combined extracts was measured. This volume was sometimes slightly less than 10 ml (i.e., 4 x 2.5 ml) because solvent was retained in pore spaces in some samples. 5 ml of each extract were centrifuged at 5,000 rpm for 5 minutes at 0°C. This removed any particulate matter present which would, otherwise, interfere with subsequent spectrophotometry.

A Hitachi U-3200 scanning spectrophotometer was used to measure the optical density of each combined chlorophyll extract. 3 ml of each extract were placed in a spectrophotometer cuvette, whilst 3 ml of 20% THF and methanol were placed in the reference cuvette.

Chlorophyll was determined by the method of Chalker and Dunlap (1981) which is based on the absorption, in 20% THF and methanol, of chlorophyll a and chlorophyll c_2. Two samples from each colony i.e., one from the top and one from the base were scanned in the spectro-photometer in the visible light range from 350 nm to 750 nm. This checked that absorbtion in individual colonies peaked at the wave lengths (665 nm for chlorophyll-a and 635 nm for chlorophyll-c_2) predicted by Chalker and Dunlap (pers. comm.). All scans showed 2 major peaks at 665 nm and 636 nm. The optical densities of all 576 samples were recorded at wave lengths, 750 nm, 665 nm and 636 nm. The 750 nm wave length was used to check for turbidity in the extract. In all samples, the 750 nm reading was 0, and it was not necessary to compensate for turbidity.

The equations used to determine chlorophyll-a and chlorophyll-c_2 concentration in each core sample, derived by Chalker and Dunlap (pers. comm.), are presented below.

$$[\text{chlorophyll-a}] = \text{volume} \times (13.42\ E_{665} - 1.889\ E_{636})$$
$$[\text{chlorophyll-c}_2] = \text{volume} \times (36.65\ E_{636} - 8.527\ E_{665})$$

The "volume" was that for the combined extracts. Chlorophyll concentrations determined from the equations were adjusted by the surface area of the core and expressed as μg chlorophyll per 100 mm^2 (i.e., per square cm).

4.2.4. Protein extraction and determination.

Although it is appreciated that the protein extract from each tissue sample will include some protein derived from the zooxanthellae, the amount of algal protein will be so small that its affect on the over-all tissue biomass measurement per core will be insignificant. The pieces from each core sample were immersed in 2.5 ml of 1M NaOH and placed in a water bath for 30 minutes at 90°C. Evaporation was reduced by placing a marble over the opening of each vial. Protein extracts were then left to cool and centrifuged for 5 minutes at 3,000 rpm to remove any particulate matter that

would interfere with subsequent spectrophotometric readings. The centrifuged extract was poured into a clean vial and stored at 6°C.

The Bio-Rad protein assay was chosen for the protein determination in preference to the widely used method of Lowry *et al.* (1951). Major advantages of the Bio-Rad method over that of Lowry *et al.* are speed and simplicity, an important points with 576 samples to process. The Bio-Rad method is based on the colour change of a dye-albumin complex solution in response to various concentrations of protein. A standard curve based on a range of known protein concentrations is constructed and used to estimate the concentration of protein in tissue samples from their optical density readings.

Preparation of the standard curve.

Bio-Rad kits purchased for protein determination contained Bio-Rad dye reagent and a protein standard. The diluted dye concentrate was filtered through Whatman No.1 paper and stored in the refrigerator at 4°C to reduce the rate of deterioration of the dye which has a life span of 2 weeks. The Bio-Rad protein standard consisted of lyophilized bovine gamma globulin (BGG). This was reconstituted in 20.0 ml of distilled water and yielded a protein concentration of approximately 1.46 mg/ml. The protein standard was stored in the freezer at -6°C when not in use.

A set of 6 standard solutions were made-up using distilled water and the protein standard to have the following concentrations; 0.0, 29.2, 58.4, 87.6, 116.8 and 146.0 µg BBG/0.1 ml. Triplicate samples were prepared containing 0.1 ml of each standard solution. 5 ml of the diluted dye reagent was added to each of the 18 samples. Each solution was mixed gently with a motorized mixer to prevent a froth developing. Solutions were then left to stand for 15 min. Optical density of 3 ml sub-samples of each solution were measured, within 45 minutes, at 595 nm. The reference cuvette contained the diluted dye reagent (see Bio-Rad manual, Bio-Rad Corp., Richmond, California, U.S.A.).

The mean optical density for the three replicates for each standard solution was plotted against protein concentration for each standard solution. The equation of this line was determined by linear regression analysis performed on a Macintosh computer using the statistical package, *Statview*. The r^2 value generated by each linear regression analyses was used to test the accuracy of each standard curve. In all 12 linear regressions determined during the course of the protein analysis the r^2 value was ≥ 0.97. The values for the slope and intercept for each fitted line were used in conjunction with the optical density (OD) reading for each core sample to determine the protein concentration for each sample. The equation used is given below.

Protein mg/0.05 ml = (OD reading - intercept)/slope.

Protein determination for tissue samples.

Triplicate samples of 0.05 ml of the protein extract from each core sample were pipetted into separate test tubes. 0.05 ml of 1M hydrochloric acid (HCl) were added to each test tube to neutralise the NaOH. Otherwise, procedures used were as described above for analyses used in construction of the standard curve. The concentration of protein in each sample was adjusted for the total volume of the extract. Protein values were then adjusted for the surface area of the core samples and expressed as mg protein per 100 mm^2 (i.e., per square cm).

The dye solution rapidly deteriorates and a new standard curve was calculated every 3 hours. A new curve was also derived every time a new dye solution was prepared.

4.2.5. Statistical procedures.

Mean and standard deviations (± S.D.) of protein, chlorophyll-a and chlorophyll-c_2 values were calculated for 572 samples (4 samples were lost in

processing). The mean and standard error (± S.E.) for protein and chlorophyll-a values were determined for each of the 18 colonies (as is discussed below, chlorophyll-c_2 was found to have a constant relationship to chlorophyll-a and therefore it was not considered necessary to present the chlorophyll-c_2 results). The mean and standard error (± S.E.) for polyp density was also determined for 16 massive *Porites* colonies.

Statistical analysis were performed using the 4 continuous variables; protein, polyp density, chlorophyll-a and chlorophyll-c_2 and three nominal variables; distance, colony number and group (Table 4.2). The group variable assigned to each sample depended upon the reef and species from which the sample came (see Table 4.1. for three reef and species groups). Each colony was assigned a number from 1 - 18. Cores were assigned to positions at the upper, middle or lower regions of the colony according to colony size and the distance of the core from the summit of the colony.

Table 4.2.

Information associated with each tissue core sample. Nominal variables (n) and continuous variables (c).

1. Protein mg 100 mm^{-2}	(c)	e.g., 1.8 mg 100 mm^{-2}
2. Polyp density 100 mm^{-2}	(c)	e.g., 65 100 mm^{-2}
3. Chlorophyll-a ug 100 mm^{-2}	(c)	e.g., 22.1 ug 100 mm^{-2}
4. Chlorophyll-c_2 ug 100 mm^{-2}	(c)	e.g., 5.6 ug 100 mm^{-2}
5. Reef and species group	(n)	e.g., 1 range (1 - 3)
6. Colony number	(n)	e.g., 6 range (1 - 18)
7. Sample number	(n)	e.g., 22 range (1 - 576)
8. Distance category	(n)	e.g., 3 range (1 - 3)

Both within and between colony differences in the 4 continuous variables listed above were assessed by analysis of covariance and by analysis of variance tests performed using the SAS, Version 6, General Linear Model (GLM) procedure (Sas Institute Inc, SAS Circle, Box 8000, Cary, NC 275 12-8000). The SAS GLM

procedure was chosen for these analyses because it is specifically designed to handle unbalanced data sets. The protein and chlorophyll analyses represented an unbalanced data set. There were unequal numbers of colonies in the reef and the species group (see Table 4.1), and unequal numbers of cores in the three distance categories (see Fig. 4.2 4.4 and 4.7). The GLM uses least square analyses to fit straight lines to the data and estimates characteristics such as variance and covariance.

Missing values included values for polyp density for the 60 cores in which definition of calices was inadequate in the photographs (see 4.2.2). Other missing values included 4 protein, chlorophyll-a and chlorophyll-c_2 values for samples that were lost during processing. If a data set included a missing value that was required by the analysis then all data for that sample were omitted from that part of the analysis.

The term "model" is used in this study to describe all the statistical calculations performed each time the GLM procedure is run on a set of data. In the first model, protein was used as the dependent variable and polyp density, distance, colonies within groups and the groups themselves were used as independent variables. This model tested several things: whether there was a significant relationship between tissue protein and polyp density, whether tissue protein varied with distance from the summit of a colony, and whether there were significant differences in tissue protein between colonies belonging the same and different reef and species groups (see Table 4.1).

In a second model, polyp density was designated as the dependent variable and distance, colonies within groups and groups themselves were used as the independent variables. This model tested: whether polyp density varied significantly with distance from the summit of colonies, whether significant differences in polyp density occurred between colonies belonging to the same and different reef and species groups (see Table 4.1). A first run of this model showed that differences in polyp density were greater within groups (i.e., same species and same reef) than

between groups. The group variable was, therefore, omitted from the final version of this model as it contributed no additional information to the model. This modified version of the second model had polyp density as the dependent variable and distance and colony number as sources of variance.

The third and fourth models used chlorophyll-a and chlorophyll-c_2 as dependent variables respectively. Independent variables used in these models were protein, distance, polyp density, colonies within groups and groups themselves. The chlorophyll models were designed to investigate the relationship between tissue protein and chlorophyll content. These models also tested: whether distance from the summit of a colony significantly affected chlorophyll concentration, whether polyp density significantly affected chlorophyll content, and whether there were significant differences in chlorophyll content between colonies belonging to the same and different reef and species groups (see Table 4.1). As before, initial runs of the model showed that differences within groups were considerably greater than differences between groups. Moreover, polyp density was not significantly associated with chlorophyll content. Hence, group and polyp density were omitted from the final version of the model as they added no additional information.

Type III sums of squares (SS) were used in preference to type I SS for all tests of significance because type I SS are inappropriate for unbalanced designs. Type III SS give equal weighting to each source of variance in a linear model. Therefore, the hierarchy of listing of independent variables in each model had no affect on the results produced since each effect is adjusted for every other effect in the model. This feature of the type III SS is particularly useful in this style of analysis where it is not clear which of the independent variables was likely to be exerting the greatest influence on the dependent variable.

The effect of distance from the summit of a colony on the 4 continuous variables (protein, polyp density, chlorophyll-a and chlorophyll-c_2) were assessed using least-square means (LSM) with their standard errors. LSM's were also used

to assess the group effect on tissue protein. The LSM is used in preference to the arithmetic mean when the data set is unbalanced. The LSM provides an estimate of the mean that would be expected for a balanced design involving the dependent variable with all independent variables at their mean value. The LSM is, therefore, an adjusted mean and is considered to be more informative than the arithmetic mean in unbalanced data sets (SAS/STAT User's guide, Version 6, Fourth edition, Volume 2, pp. 908-909).

The relative importance of each independent variable to the dependent variable was assessed by determining the partial coefficient of determination for each independent variable (Zar, 1984). Partial coefficient of determination values are calculated from the type III SS in each of the four linear models and expressed as percentages. Therefore, these values were used to identify which independent variable was, either exerting the greatest influence on the dependent variable, or exhibiting the strongest relationship with the dependent variable in each model.

4.3. RESULTS.

Neither protein nor chlorophyll pigments were detected by the spectrophotometer in control cores removed from just below the observable tissue layer. It was, then, reasonable to assume that all of the tissue layer was included in the analyses when samples included all of the visible tissue.

4.3.1. Protein analyses.

The mean protein concentration per skeletal surface area for 18 massive *Porites* colonies representing 2 species, collected from 2 reefs, was 1.57 ± 0.59 mg 100 mm^{-2} (± S.D.). Mean protein values for all 18 colonies ranged from 0.52 mg 100

mm^{-2} to 2.21 mg 100 mm^{-2}. Mean protein concentrations for each colony are presented in Figure 4.1.

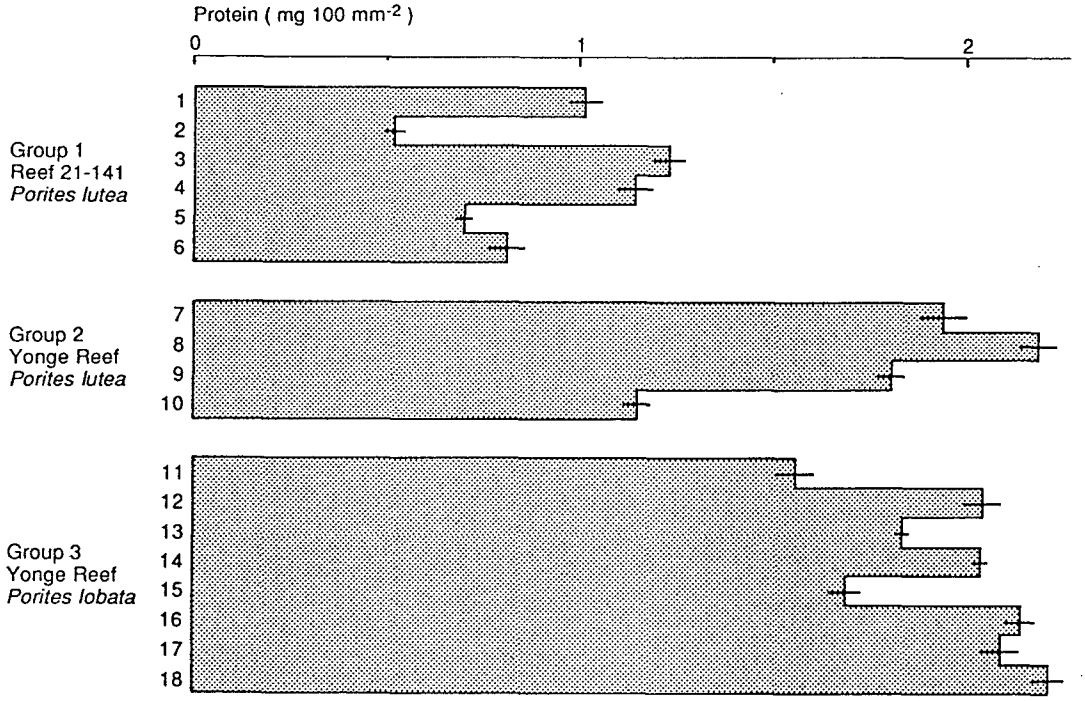

Fig. 4.1. Protein concentration (mg 100 mm^{-2}); mean ± S.E. for 18 massive *Porites* colonies representing 2 species collected from 2 reefs.

Results of the first GLM with protein as the dependent variable showed that the concentration of protein (mg 100 mm^{-2}) varied significantly between different distance categories i.e., upper, middle and lower colony ($P < 0.001$, Table 4.3).

Table 4.3.

Model 1. Analysis of covariance of protein mg 100 mm^{-2}. Number of observations (n = 478).

Source of variance	Degrees of freedom	Mean square	F value	Probability
Distance	2	1.62	36.80	< 0.001
Polyp density 100 mm^{-2}	1	0.22	5.11	< 0.05
Colonies (groups)	13	2.76	62.75	< 0.001
Groups	2	47.51	1080.26	< 0.001

The least-square mean values for protein concentration per skeletal surface area were shown to decrease towards the base of a massive *Porites* colony (Fig. 4.2). The decrease in protein was small but significant (1.6 to 1.4 mg 100 mm^{-2}).

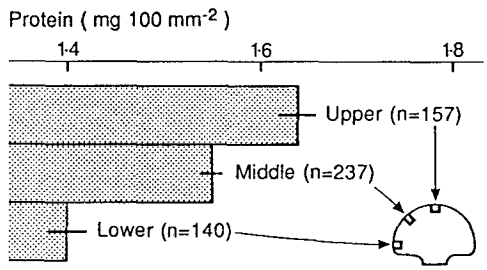

Fig. 4.2. Protein concentration (mg 100 mm^{-2}); least-square mean ± S.E., for the 3 distance categories in 18 massive *Porites* colonies.

The effect of distance on protein concentration displayed by the first model was shown to be very small by the partial co-efficient of determination (Table 4.4). 2.41% of the variability in protein concentration was attributed to the distance effect.

Table 4.4.

Partial coefficients of determination, expressed as percentages, determined from the protein analysis (Table 4.3).

Source of variance	Partial coefficient of determination (%)
Distance	2.41
Polyp density 100 mm^{-2}	0.17
Colonies (groups)	26.70
Groups	70.72

Similarly, although protein concentration was shown to be significantly related to polyp density (Table 4.3, $P < 0.005$), only 0.17% of the amount of variability in protein, expressed by the model, was attributed to the polyp density as indicated by the partial coefficient of determination value (Table 4.4).

Although mean protein concentration was shown to significantly vary between colonies belonging to the same reef and species groups ($P < 0.001$, Table 4.3), the variation in mean protein concentration (mg 100 mm^{-2}) between colonies belonging to different reef and species groups was highly significant ($P < 0.001$, Table 4.3). The partial coefficient of determination calculated for the groups effect, showed that 70% of the variability in protein concentration could be attributed to a reef and species effect. The least square mean test showed that the greatest amount of variability in protein concentration occurred between colonies from 2 different reefs. There was almost a 2 fold difference in protein concentration between reefs (Fig. 4.3). Differences in species contributed much less to this difference in tissue protein (Fig. 4.3).

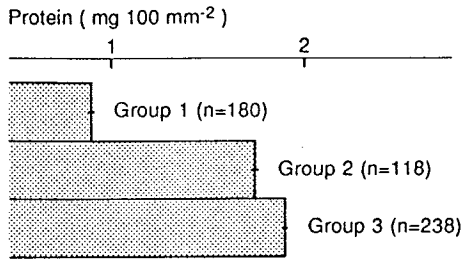

Fig. 4.3. Protein concentration (mg 100 mm^{-2}); least square mean protein ± S.E., for 3 reef and species groups (see Table 4.1).

4.3.2. Polyp density analyses.

Polyp density was shown to vary significantly between different distance categories i.e., upper, middle and lower colony ($P < 0.001$, Table 4.5).

Table 4.5.

Model 2. Analysis of variance of polyp density (number of polyps per 100 mm^2; n = 480).

Source of variance	Degrees of freedom	Mean square	F value	Probability
Distance	2	2475.77	1237.89	< 0.001
Colonies	15	32392.01	2159.47	< 0.001

Least-square means tests showed that polyp density decreased by about 10% towards the base of a colony (Fig. 4.4).

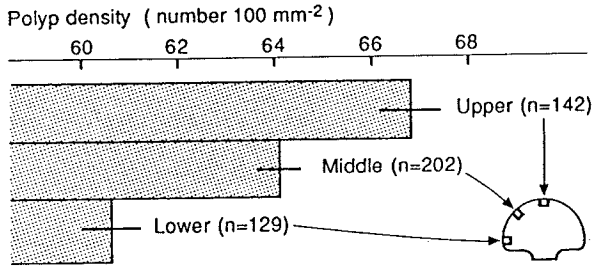

Fig. 4.4. Polyp density (number of polyps per 100 mm^2), least square mean ± S.E., for 3 distance categories in 16 massive *Porites* colonies.

Only 7.1% of the variability in polyp density expressed by the model could be attributed to the distance effect as shown by the partial coefficient of determination (see Table 4.6). The greatest amount of variability in polyp density occurred between *Porites* colonies, irrespective of which reef they came from or to which species they belonged.

Table 4.6.

Partial coefficients of determination, expressed as percentages, determined from the polyp density analysis (Table 4.5).

Source of variance	Partial coefficient of determination (%)
Distance	7.1
Colonies	92.9

Polyp density was shown by the model to be significantly related to the concentration of protein ($P < 0.05$, Table 4.3). However, the almost 2 fold difference in protein concentration between colonies from the 2 different reefs (Fig. 4.3.) was

not accompanied by a proportional difference in the number of polyps (cf., Fig. 4.1 and 4.5). There were no significant differences in polyp density between colonies from the 2 reefs and between different species.

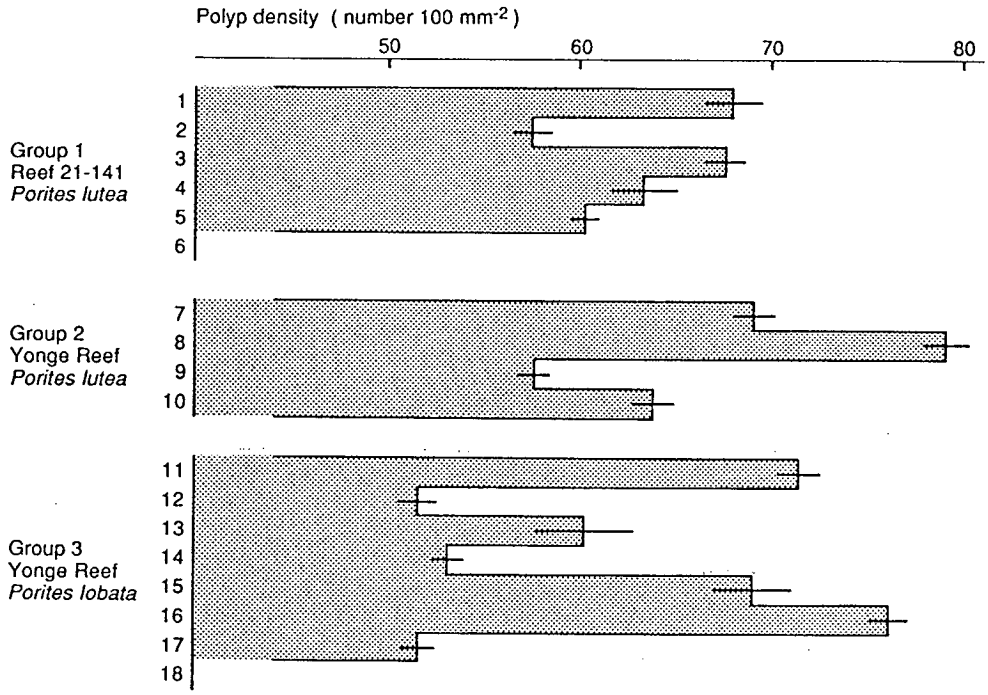

Fig. 4.5. Polyp density (number of polyps per 100 mm^2), mean ± S.E. for 16 massive *Porites* colonies.

4.3.3. Chlorophyll analyses.

Mean chlorophyll-a and chlorophyll-c_2 concentrations for 18 colonies of *Porites*, representing 2 species and collected from 2 reefs, were 25.19 ± 5.76 ug 100 mm^{-2} and 5.59 ± 1.7 ug 100 mm^{-2} (± S.D.) respectively. The mean chlorophyll-a and chlorophyll-c_2 values ranged from 18.35 ug 100 mm^{-2} to 34.11 ug 100 mm^{-2} and 4.16 ug 100 mm^{-2} to 7.75 ug 100 mm^{-2} respectively. Thus, the ratio of chlorophyll-a to chlorophyll-c_2 in zooxanthellae in these colonies of massive *Porites* was about 4.5 : 1. Small values for standard deviations associated with these data suggest that this

ratio is reasonably constant amongst the colonies sampled. It seemed probable that the values for chlorophyll-a and chlorophyll-c_2 were interchangeable. Models based on values for chlorophyll-c_2 were constructed, as well as models based on values for chlorophyll-a. Models based on chlorophyll-c_2 values gave results similar to models based on chlorophyll-a values. Thus, only results for models based on chlorophyll-a are presented and discussed. The mean chlorophyll-a concentration and associated standard error for each of the 18 colonies is displayed in Figure 4.6.

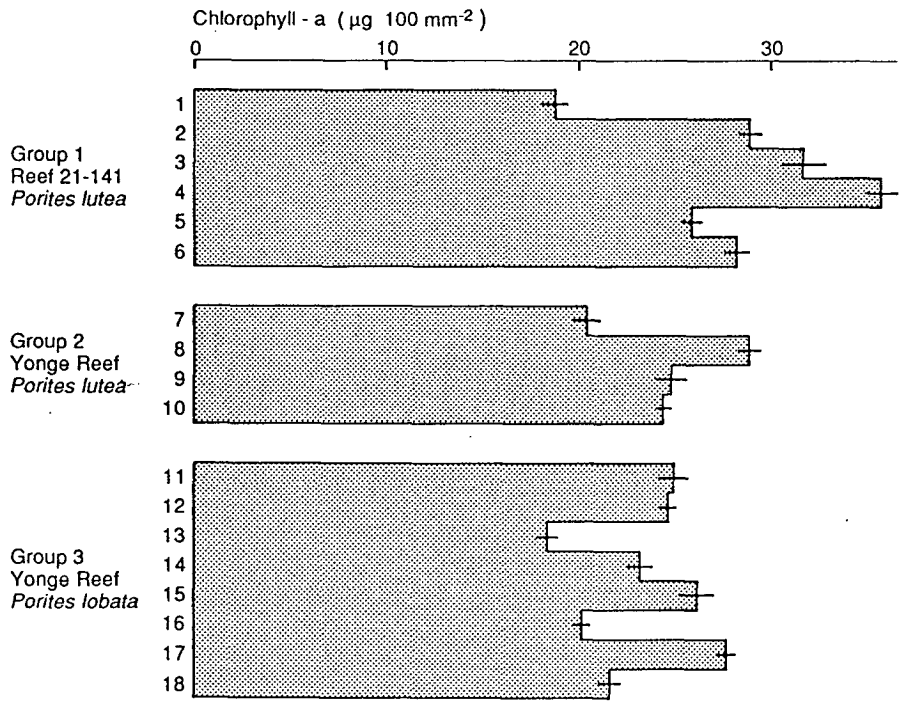

Fig. 4.6. Chlorophyll-a concentration (µg 100 mm^{-2}), mean ± S.E. of 18 massive *Porites* colonies representing 2 species collected from 2 reefs.

Results of the chlorophyll-a model showed that chlorophyll-a concentration in massive *Porites* colonies altered significantly between the upper, middle and lower sections of colonies ($P < 0.05$, Table 4.7).

Table 4.7.

Model 3. Analysis of covariance of chlorophyll-a μg 100 mm^{-2} (n = 534).

Source of variance	Degrees of freedom	Mean square	F value	Probability
Distance	2	56.37	4.99	< 0.05
Protein mg 100 mm^{-2}	1	1805.56	159.98	< 0.001
Colonies	17	664.86	58.91	< 0.001

In contrast to tissue protein values, the least square mean test showed that chlorophyll concentrations increased by about 5% from the summit to the base of colonies (Fig. 4.7). Over the same distance range, protein values decreased by 17% (see above; Fig. 4.2). As is also demonstrated, see below, protein and chlorophyll show differences in response to between-colony variables.

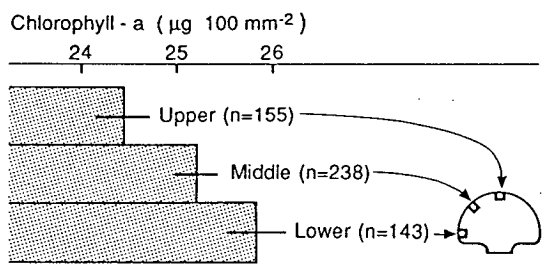

Fig. 4.7. Chlorophyll-a (μg 100 mm^{-2}), least square mean values for chlorophyll-a ± S.E. for 3 distance categories in 18 massive *Porites* colonies.

About 1% of the variability in chlorophyll-a concentration expressed by the chlorophyll-a model was shown, by the partial coefficient of determination, to be accounted for by the distance effect (Table 4.8).

Table 4.8.

Partial coefficients of determination, expressed as percentages, determined from the Chlorophyll-a analysis (Table 4.7).

Source of variance	Partial coefficient of determination (%)
Distance	0.85
Protein mg 100 mm^{-2}	13.66
Colonies	85.49

The concentration of chlorophyll-a was shown to be significantly associated with the concentration of protein ($P < 0.001$, Table 4.7). However, highly significant differences in mean protein concentration between colonies from different groups ($P < 0.001$, Table 4.3, Fig. 4.), particularly between colonies from the 2 different reefs, were not accompanied by variations in chlorophyll-a of the same proportions (cf., Fig. 4.1. and 4.6). Least-square mean values for protein (mg 100 mm^{-2}) for the 3 different reef and species groups (see Table 4.1) showed that there was almost a 2-fold difference in the mean protein concentration between colonies from the 2 different reefs (Figure 4.3.). The chlorophyll-a model showed that the greatest variations in chlorophyll occurred between individual colonies irrespective of the reef from which they came, or the species to which they belonged. Thus, although the chlorophyll concentration was significantly related to protein concentration, chlorophyll concentration did not always vary in the same way that protein concentration varied.

4.4. DISCUSSION.

4.4.1. Estimating tissue biomass from skeletal surface area within and between massive *Porites* colonies.

Protein concentration (mg 100 mm^{-2}) was shown to significantly decrease towards the base of massive *Porites* colonies. Therefore, tissue biomass is not directly proportional to skeletal surface area within these corals. The decrease in protein concentration (mg 100 mm^{-2}) from the summit to the base of massive *Porites* colonies was around 17%. It was considered that, for the purpose of building computer models (Chapter 3), this within colony difference was small enough to be disregarded.

Differences in protein concentration amongst colonies of the same species from the same reef were also small though significant. Again, these differences seemed small enough to disregard for the purposes of comparing growth form in real colonies with growth form displayed by the computer models.

The greatest differences in protein concentration occurred between *Porites* colonies from different reef and species groups (Table 4.3). Differences in mean protein between colonies from the same reef but belonging to different species were relatively small. In contrast there was almost a 2-fold difference in mean protein between colonies from different reefs, irrespective of species. These data suggest a latitudinal effect upon tissue protein. This latitudinal effect is presently being investigated (D.J. Barnes & J.M. Lough, pers. comm.). Comparative studies of tissue biomass between colonies from two different reefs on the G.B.R., based upon measurements of colonial surface area, are not recommended. Such comparative studies should be based upon more direct measurements of tissue biomass.

4.4.2. Factors affecting tissue protein per unit skeletal surface area.

There was a significant, direct relationship between tissue protein and polyp density. A 17% decrease in mean protein concentration from the summit to the base of massive *Porites* colonies was associated with a 10% decrease polyp density. It seems that greater tissue biomass is associated with higher polyp density.

The almost 2-fold difference in protein concentration between colonies from the northern and southern G.B.R. was not accompanied by an obvious difference in polyp density (cf., Figs. 4.1 and 4.5). Variations in polyp density between colonies from the northern and southern reefs were less than variations in polyp density between colonies from the same reefs. These results suggest that some other factor, or factors, may account for the highly significant difference in protein concentration between reefs.

Careful examination of tissue thickness in the skeletal slices from the 36 massive *Porites* (Chapter 2) showed that the thickness of the tissue layer decreased from the summit towards the base of most colonies. The significant decrease in tissue protein towards the base of colonies may be associated with this decrease in tissue thickness, as well as with the decrease in polyp density. Variation in tissue thickness is proposed as the most likely factor to account for the highly significant difference in tissue protein between the northern and southern reefs. Unfortunately, tissue thickness was not measured as part of this work. Recent work by D.J. Barnes and J.M. Lough has shown considerable differences in tissue thickness are associated colony size, distance off-shore, latitude and season (pers. comm.).

It is suggested that the 2-fold difference in the tissue biomass between the northern and southern reefs may reflect significant differences in the levels of nutrients associated with each reef locality. Although both Reef 21/141 and Yonge Reef are located on the outer G.B.R., Reef 21/141 is located 182 km off-shore in contrast to Yonge reef which is only located 50 km off-shore. Yonge Reef is

therefore considerably closer to the coastline and corals may benefit from higher nutrient levels associated with coastal river discharge. If differences in tissue thickness do exist between colonies located on different reefs then comparative studies in tissue thickness may provide insights into the nutritional status and, hence, the "health" of a reef.

4.4.3. Factors affecting polyp density.

Differences in polyp density within colonies were small in comparison to differences between colonies. Between-colony differences in polyp density may reflect differences in the ratio of tissue growth to skeletal growth, and thus be associated with the amount of bumpiness displayed by a colony. Polyp density appeared to vary slightly between smooth and bumpy colonies (see Table 2.7). Material presented in Chapters 2 & 3 makes it probable that a colony with a relatively higher rate of tissue growth compared with skeletal growth will exhibit a higher polyp density. This arises because, in essence, a colony with a high tissue to skeletal growth ratio will have the tissue, and hence the polyps, more "crowded" than a colony with a lower tissue to skeletal growth ratio. This idea was supported by results arising from computer models presented in Chapter 3. It then follows that variations in polyp density between *Porites* colonies may reflect variation in the ratio of the tissue growth to skeletal growth. If higher polyp density does reflect relatively higher rates of tissue growth to skeletal growth, then higher polyp density would indicate that the rate of creation of space on the growth surface, by skeletal extension, is insufficient to accommodate tissue growth. D.J. Barnes and J.M. Lough (per. comm.) propose that changes in thickness of the tissue layer is another mechanism by which *Porites* attempts to overcome this "space" constraint. Thus, in larger colonies, there should be a correlation between polyp density and tissue thickness.

4.4.4. Estimating tissue biomass from chlorophyll concentration.

Protein concentration was significantly related to chlorophyll content. However, there were large differences in protein concentration between colonies that were not matched by differences in chlorophyll concentration. This was particularly apparent in comparisons between reefs. These analyses indicate that chlorophyll concentrations were not directly linked with tissue protein, but with some other factor or factors not included in the analyses. Chlorophyll does not seem to present a suitable alternative to protein for estimating tissue biomass within a massive *Porites* colony.

4.4.5. Factors affecting chlorophyll concentration.

Almost all of the variability in chlorophyll expressed by the model occurred between colonies, irrespective of reef and species. Variations in localised light intensity may account for these significant differences in chlorophyll concentration. This notion is supported by the finding that chlorophyll concentrations increased towards the base of massive *Porites* colonies. This increase is likely to be a photo-adaptive response to differing illumination associated with more horizontal and more vertical colonial surfaces (Jokiel, 1988, Chalker *et al.* 1988).

4.5. CONCLUSIONS.

1. Absolute variations in tissue protein over the growth surface of a massive *Porites* colony are small enough to allow reasonably good estimates of tissue biomass to be made from skeletal surface area.

2. Measurements of skeletal surface area of *Porites* colonies from the same reef can be used to compare tissue biomass between colonies, irrespective of species.

3. Measurements of the skeletal surface area should not be used to make comparisons of tissue biomass between *Porites* colonies from two different reefs on the G.B.R.

4. Large differences in tissue protein between colonies from a northern and a southern reef on the G.B.R. could not be accounted for by differences in polyp density.

5. Chlorophyll concentration cannot be used as an alternative to protein to estimate tissue biomass in massive *Porites* colonies.

CHAPTER 5

LINKS BETWEEN GROWTH AND GROWTH FORM OF *PORITES* AND THE ENVIRONMENT

5.1. INTRODUCTION.

Many of the suggestions and hypotheses that have arisen during this research project on growth and growth form of the massive coral *Porites* are examined in this chapter. An investigation is carried out to determine to what extent the development of a bumpy growth surface increases the surface area available for accommodation of tissue growth. Growth forms of real colonies (Chapter 2) are examined in terms of growth forms created by computer simulations of *Porites* growth (Chapter 3). Growth, as revealed by X-radiographs, and growth form of actual colonies are examined in terms of likely environmental differences between the reefs at which they grew.

5.1.1. The characteristic bumpy growth surface displayed by massive Porites colonies.

Barnes (1973) pointed out that a hemispherical coral, having discrete polyps, encounters geometric problems as it increases in size. As it becomes larger, the

colony's rate of skeletal extension must increase, or its rate of tissue growth decrease, or it must alter its growth form (see 1.1.1., Figs. 1.2 & 1.3). Barnes proposed that such colonies alter their growth form. The smooth surface of the colony becomes bumpy, increasing the surface area available to accommodate tissue.

All massive *Porites* colonies develop a characteristic bumpy growth surface once they approach about 100 -150 mm in diameter, that is, when they are about 4 - 8 years old (see also Isdale, 1977). Development of a bumpy growth surface with increasing size is clearly displayed by the annual density banding pattern because the bands outline former positions of the growth surface of a colony. A technique was devised to estimate the surface area presented by a bumpy growth surface. This technique was used to evaluate the extent to which a bumpy surface provides a greater surface area than a smooth surface of a colony of equivalent radius.

5.1.2. Tissue growth, skeletal growth and growth form in *Porites*.

A major hypothesis presented here is that the ratio of tissue growth to skeletal growth considerably affects growth form in massive *Porites* colonies. Computer models presented in Chapter 3 supported this hypothesis. These models suggested that a *Porites* colony with a relatively higher tissue growth compared with skeletal growth would display well developed corallite fans, with high angles of corallite divergence. These fans would be associated with very prominent bumps on the growth surface. In contrast, models with a relatively smooth growth surface would develop if the rate of tissue growth was low compared with the rate of skeletal growth.

The controls of, and constraints on, colonial growth elucidated by computer simulated growth (Chapter 3) are tested against various growth-related variables measured in actual colonies.

5.1.3. Links between environmental factors and *Porites* growth.

Changes in a coral's environment are not likely to alter tissue growth and skeletal growth in exactly the same way (Barnes, 1973; section 1.1.3). Since, as is discussed above, coral growth probably alters in a predictable fashion with relative changes in tissue growth and skeletal growth, colonial growth form and growth morphology may provide considerable information about environmental conditions which obtained during growth. The major factors likely to affect rates of tissue growth and rates of skeletal growth are discussed in Chapter 1 (sections 1.1.3). Nutrient availability and light are the factors most likely to exert major influences on tissue growth. Light is the factor, universally agreed to exert the major influence on calcification.

Selection of reefs at different locations on the G.B.R. can provide systematic differences in environmental conditions. *Porites* colonies used in this study were collected from Pandora, Rib and Myrmidon Reefs (Fig. 1.6), which represent inner, mid and offshore reefs positioned across the width of the central G.B.R. Strong differences in physical environmental conditions observed along this cross-shelf transect (Wilkinson and Cheshire, 1988). There is a strong terrigenous influence at the inshore end of the transect and a strong oceanic influence at the offshore end (section 1.3). Large variations in light transmittance, turbidity, sedimentation, wave energy, nutrient concentration and salinity occur between these three reefs. Measurements were made of several growth features of massive *Porites* colonies collected from Pandora, Rib and Myrmidon Reefs. Tests were performed to see if there were systematic differences in the growth features between colonies which might be associated with systematic differences the environment.

5.2. MATERIALS AND METHODS.

The specimens used in this study were described in Chapter 2 (Table 2.1). These specimens comprised 36 massive *Porites* colonies collected from Pandora, Rib and Myrmidon Reefs (Fig. 1.6) representing four species, *P. lobata, P. lutea, P. solida* and *P. mayeri.* Details of the collection of colonies, cutting of skeletal slices and X-radiography of the slices are described in sections, 2.2.2, 2.2.3 & 2.2.3.

5.2.1. Estimation of surface area displayed by a bumpy *Porites* colony from X-radiographs.

X-radiographs of 2 massive *P. lobata* colonies collected from Rib Reef were selected for an examination of differences in surface area between the actual, bumpy growth surfaces presented by the 2 colonies and theoretical, smooth surfaced colonies of equivalent size. Both X-radiographs displayed about 20 annual band couplets, that is, both colonies were about 20 years old when collected. One of the colonies displayed an annual rate of skeletal extension of 9.3 mm yr^{-1} and was half the size of the second colony which exhibited an annual skeletal extension rate of 18.6 mm yr^{-1}. The colony which grew slowly had a very bumpy growth surface; the faster growing colony had a fairly smooth surface (Plates 5.1 & 5.2). These colonies represented the extremes in growth form and growth rate amongst the 36 colonies from the central G.B.R. Thus measurements taken on these 2 colonies should encompass results for all 36 colonies.

The tissue layer within the skeletons of massive *Porites* exists as a thin brown band at the outer edge of the colony (Plate 1.3). The bumpy colony and the smooth-surfaced colony had tissue thicknesses averaging 8.12 mm and 8.62 mm, respectively. Thus, differences between the 2 colonies in tissue biomass per unit surface area were probably small. Tissue biomass in the 2 colonies could reasonably be compared by comparing linear measurements and respective estimates of surface area.

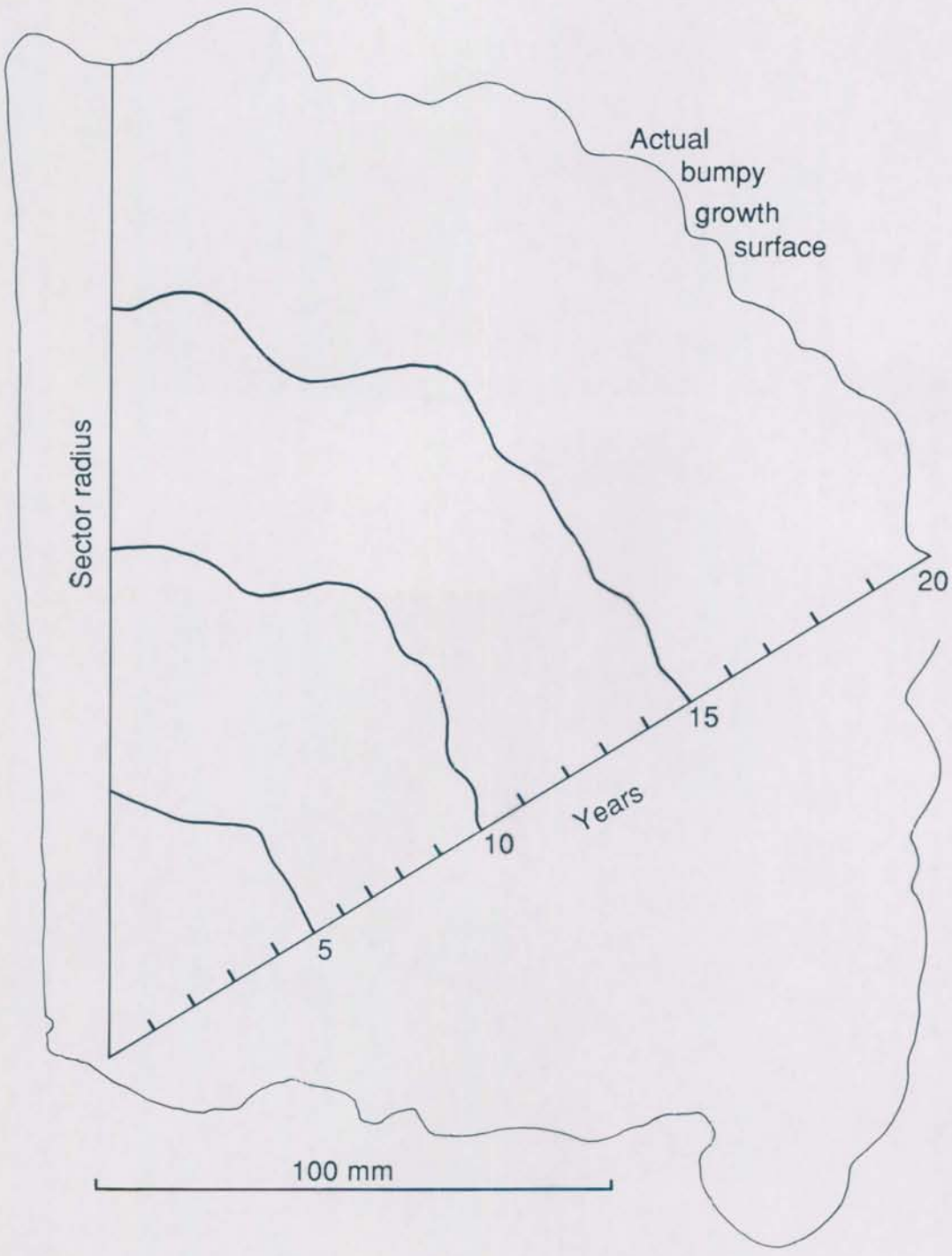

Plate 5.1. X-radiograph positive of a 7 mm thick skeletal slice cut from the vertical growth axis of a bumpy *P. lobata* colony collected from Rib Reef, central G.B.R. The annual rate of skeletal extension for this colony was 9.3 mm yr $^{-1}$. The linear dimension of the former growth surface was measured at yearly intervals as indicated.

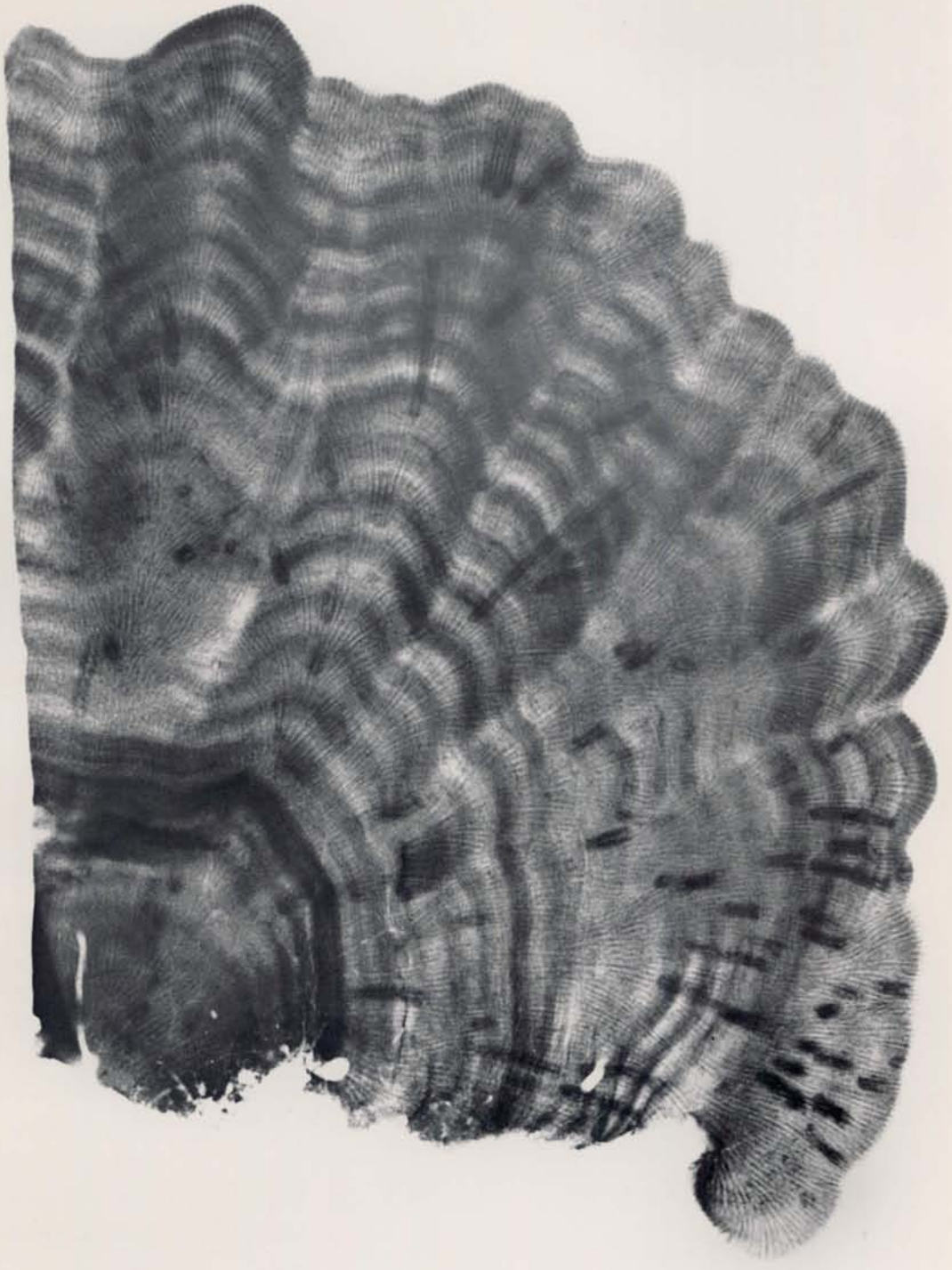

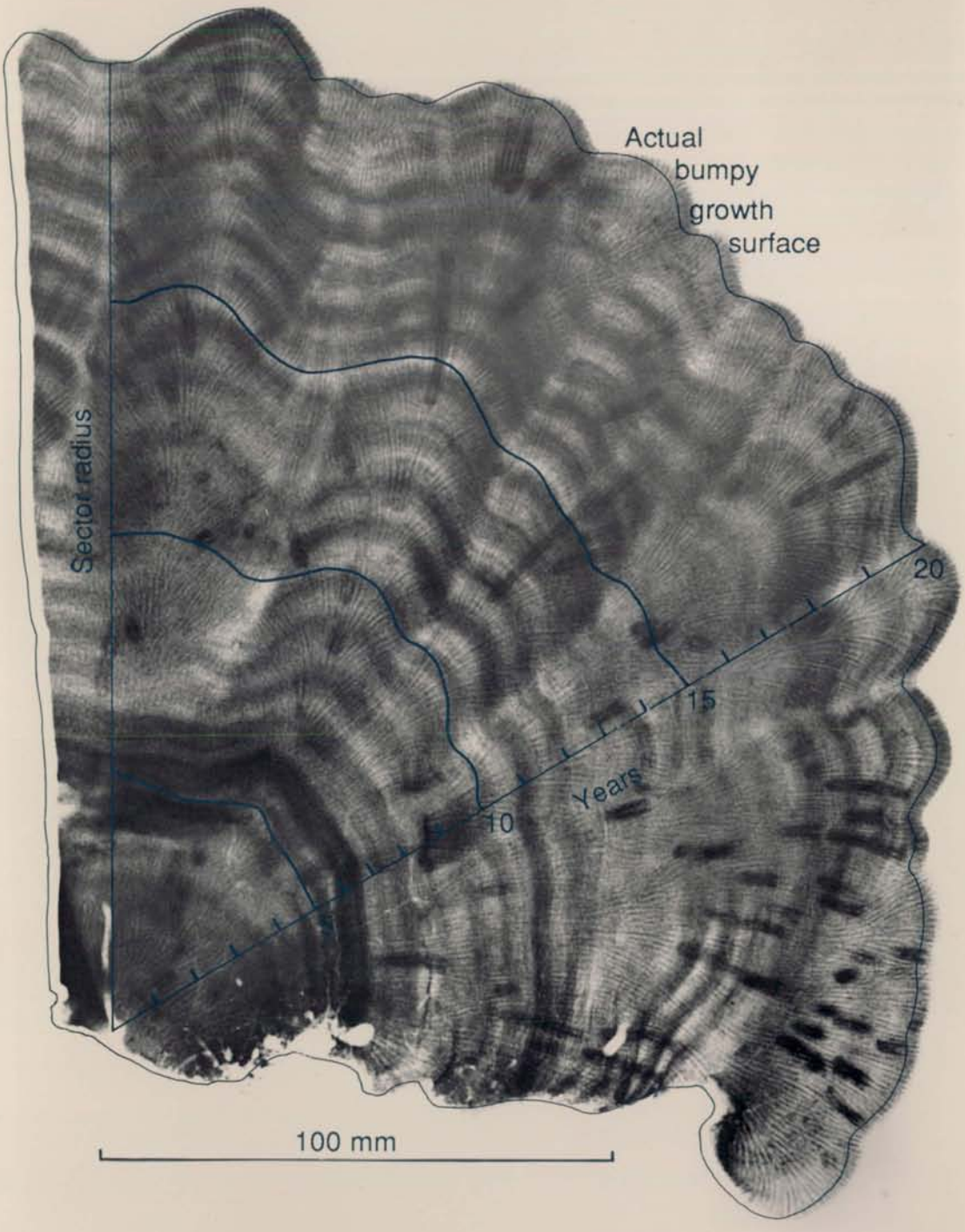

Plate 5.1. X-radiograph positive of a 7 mm thick skeletal slice cut from the vertical growth axis of a bumpy *P. lobata* colony collected from Rib Reef, central G.B.R. The annual rate of skeletal extension for this colony was 9.3 mm yr $^{-1}$. The linear dimension of the former growth surface was measured at yearly intervals as indicated.

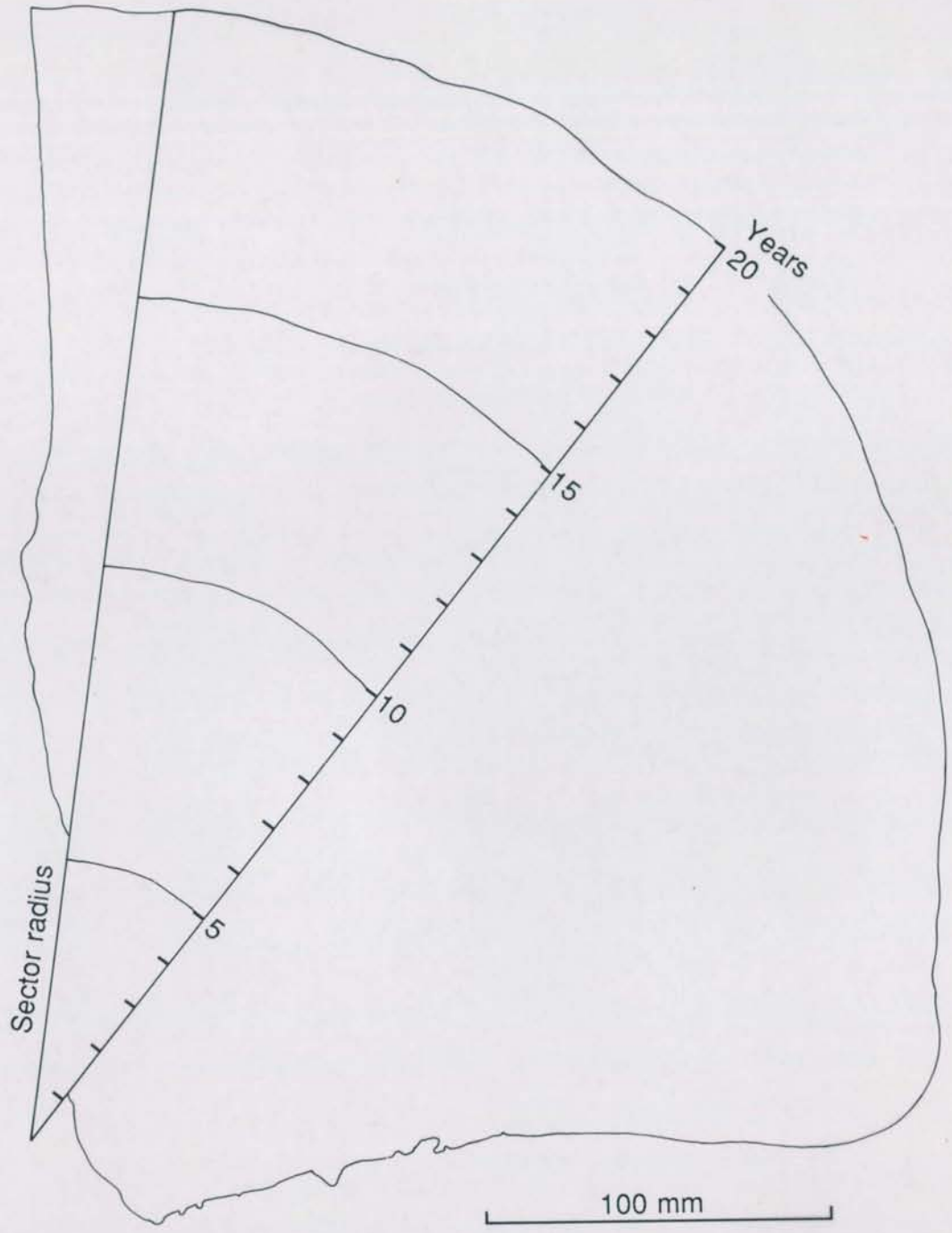

Plate 5.2. X-radiograph positive of a 6 mm thick skeletal slice cut from the vertical growth axis of a smooth *P. lobata* colony collected from Rib Reef, central G.B.R. The annual rate of skeletal extension for this colony was 18.6 mm yr^{-1}. The linear dimension of the former growth surface was measured at yearly intervals as indicated.

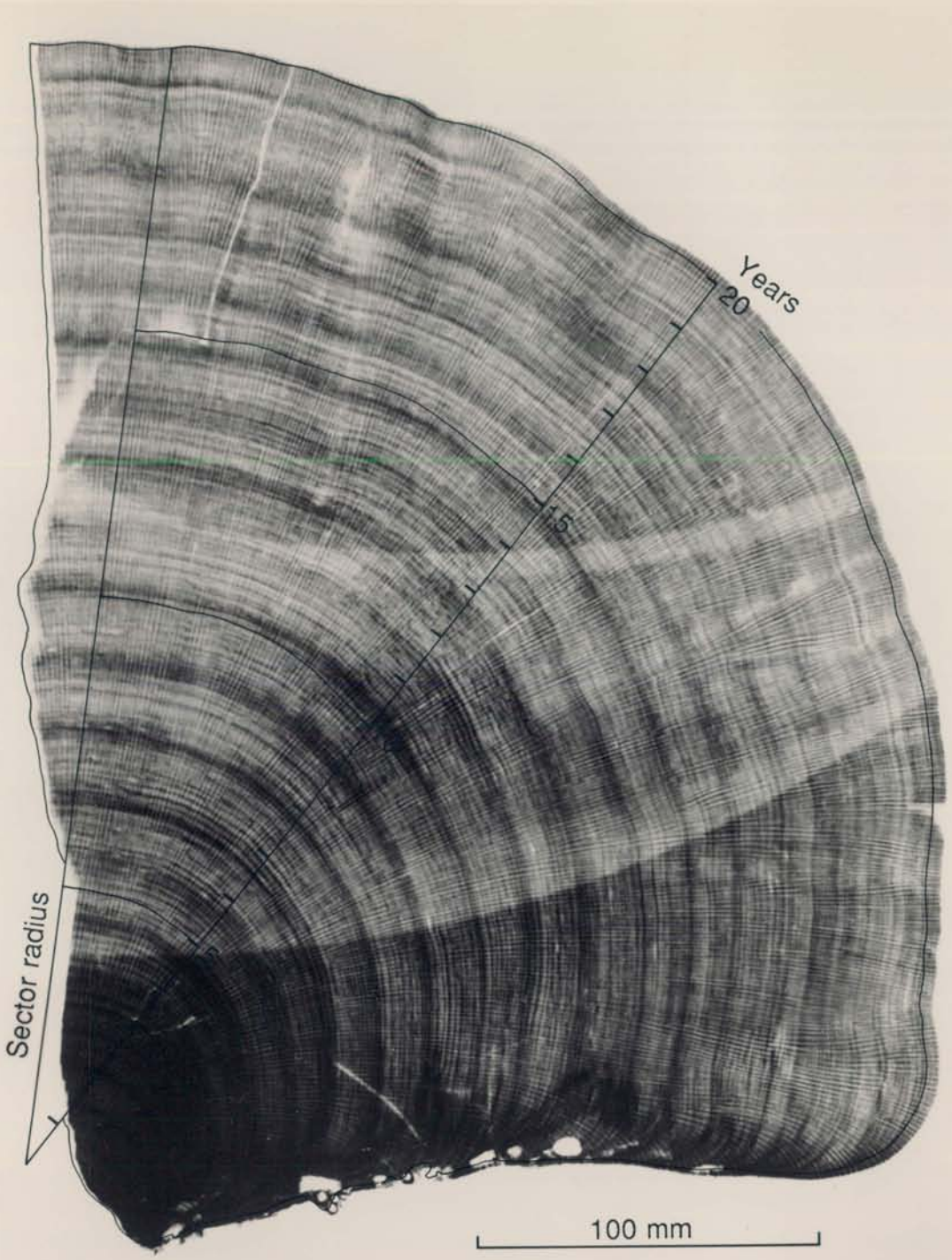

Plate 5.2. X-radiograph positive of a 6 mm thick skeletal slice cut from the vertical growth axis of a smooth *P. lobata* colony collected from Rib Reef, central G.B.R. The annual rate of skeletal extension for this colony was 18.6 mm yr^{-1}. The linear dimension of the former growth surface was measured at yearly intervals as indicated.

Transparent film was placed over each X-radiographic positive. It was, then, possible to mark out a sector for growth measurements without damaging the print. A line was drawn from the origin of each colony to a point close to its summit. This line marked the major growth axis (Plate 5.1. & Plate 5.2). It represented one sector radius. The annual band couplets clearly apparent along this line were marked. A radial line was drawn from the marked annual band couplet closest to the origin of the colony. This second radial line was kept to the same length as the first. It was drawn so that it ended at the outer surface of the colony displayed by the X-radiograph. In the bumpy-surfaced colony, this second radial line was drawn at 60° from the first line. In the smooth-surfaced colony, this line could be drawn only such that it was separated from the first line by 30° (Plates 5.1 & 5.2). This simply reflected the ratio of vertical to horizontal growth in the 2 colonies. The bumpy colony had grown more evenly than the smooth colony and was more hemispherical. The smooth colony was distinctly higher than it was wide (Plates 5.1 & 5.2).

The radial lines were marked, from their origins, at intervals corresponding to the average annual growth rate for that colony. The colony outline and former outlines, within the sector defined by the radial lines, were drawn at each marked interval along the outline defined by the annual density bands (Plates 5.1 & 5.2). A fine chain was used to measure the distance along each of the outlines drawn. These lengths were used to calculate the radius of a colony which would have subtended a "spherical" surface (i.e., a section with a circular outline) having the same length. This was considered to be the theoretical radius for the colony (Fig. 5.1);

$$\text{Theoretical radius } (r) = s \times 180/\pi \times \alpha,$$

where s was the length of each bumpy surface measured and α was the angle of the sector (i.e., 60° in the bumpy colony and 30° in the smooth colony).

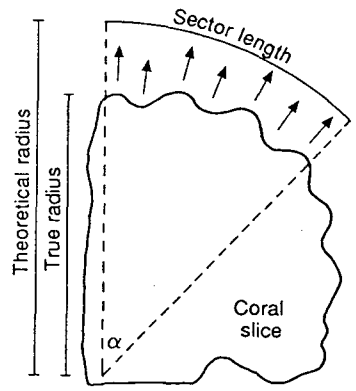

Fig. 5.1. Estimation of the theoretical radius for a colony from the angle of a sector and the length of colony surface falling within that sector.

The theoretical radius calculated for each annual growth layer in each colony was used to calculate the surface area of a theoretical, hemispherical colony having that radius;

$$\text{Surface area of a hemisphere} = 2\pi \times r^2$$

The surface area of this theoretical colony is, then, the same as the surface area of a hemispherical colony having the same degree of bumpiness all over as that measured from the X-radiograph for the sector (Fig. 5.1). This theoretical colony, then, provided a value for the surface area of the actual colony at each year of its life. This "actual" surface area could be compared with the surface area of a smooth, hemispherical colony of the same (i.e., true) radius (Fig.5.1).

Figure 5.2 shows how the surface areas of the "actual" and "smooth" colonies would have changed as the colonies increased in age and size. The difference between the two curves for the bumpy colony provides an indication of the increased surface area made available by the colony becoming bumpy. That is, this difference indicates the effectiveness with which a bumpy growth surface would accommodate

more tissue growth than a directly equivalent smooth growth surface. It was possible to make a similar comparison for a smooth surfaced colony (Fig. 5.2). In addition, it was possible to examine the way in which differing skeletal extension rates provided increased surface area and, hence, accommodated tissue growth. These comparisons were for colonies having a 2-fold difference in the annual rate of skeletal extension but for equivalent growth periods.

5.2.2. Characteristics of growth and growth form measured from X-radiographs of massive *Porites*.

Six relatively large, well developed corallite fans were selected in each of the 36 X-radiographs. Full details of the corallite fans selected are given in Chapter 2 (section 2.2.4). These fans were used for further measurements of *Porites* growth. A region of the fans clearly displaying apparent corallites was selected. Corallites were traced from a point of origin at or close to the central fan axis to the points at either side of the fan, at the fan margins, where they became occluded (Plate 5.3). The former outline of the colony was traced between the points at which the corallites became occluded. Straight lines were then drawn between the point of origin and the points of occlusion, between the points of occlusion, and along the central axis of the corallite fan (see Plate 5.3). This "kite" shaped design was known as a growth segment. Six such segments were constructed for each X-radiograph of all 36 colonies from Pandora, Rib and Myrmidon Reefs.

Measurements made using growth segment.

1. Colony Bumpiness. Once a bumpy surface was established, the size and shape of bumps appeared to remain fairly uniform over the upper to middle growth surface as a colony increased in size. The prominence of bumps decreased towards the base of some colonies. For this reason, corallite fans in the central to upper regions of

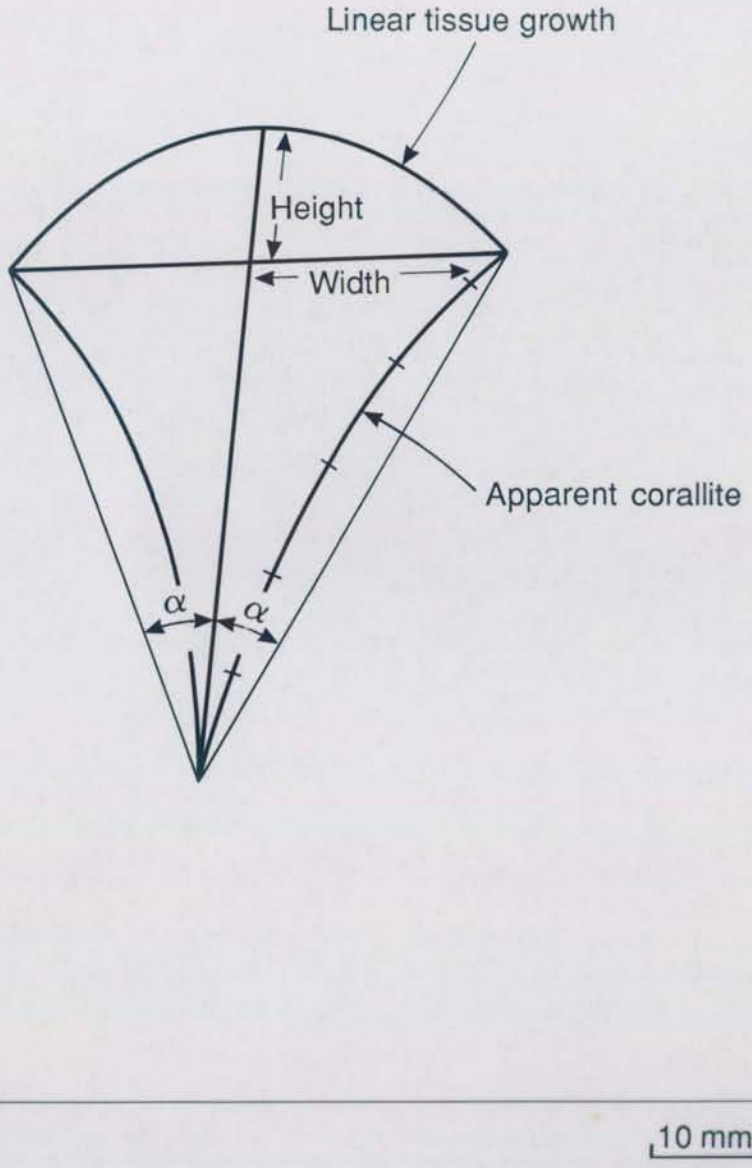
Linear tissue growth
Height
Width
Apparent corallite
α
α
10 mm

colonies were selected for these measurements. The size and shape of bumps displayed varied widely between colonies. A technique was devised to estimate the degree of bumpiness displayed in X-radiographs.

Plate 5.3. Enlarged section of Plate 2.1 displaying growth and growth form characteristics measured in X-radiographs of massive *Porites* colonies.

colonies were selected for these measurements. The size and shape of bumps displayed varied widely between colonies. A technique was devised to estimate the degree of bumpiness displayed in X-radiographs.

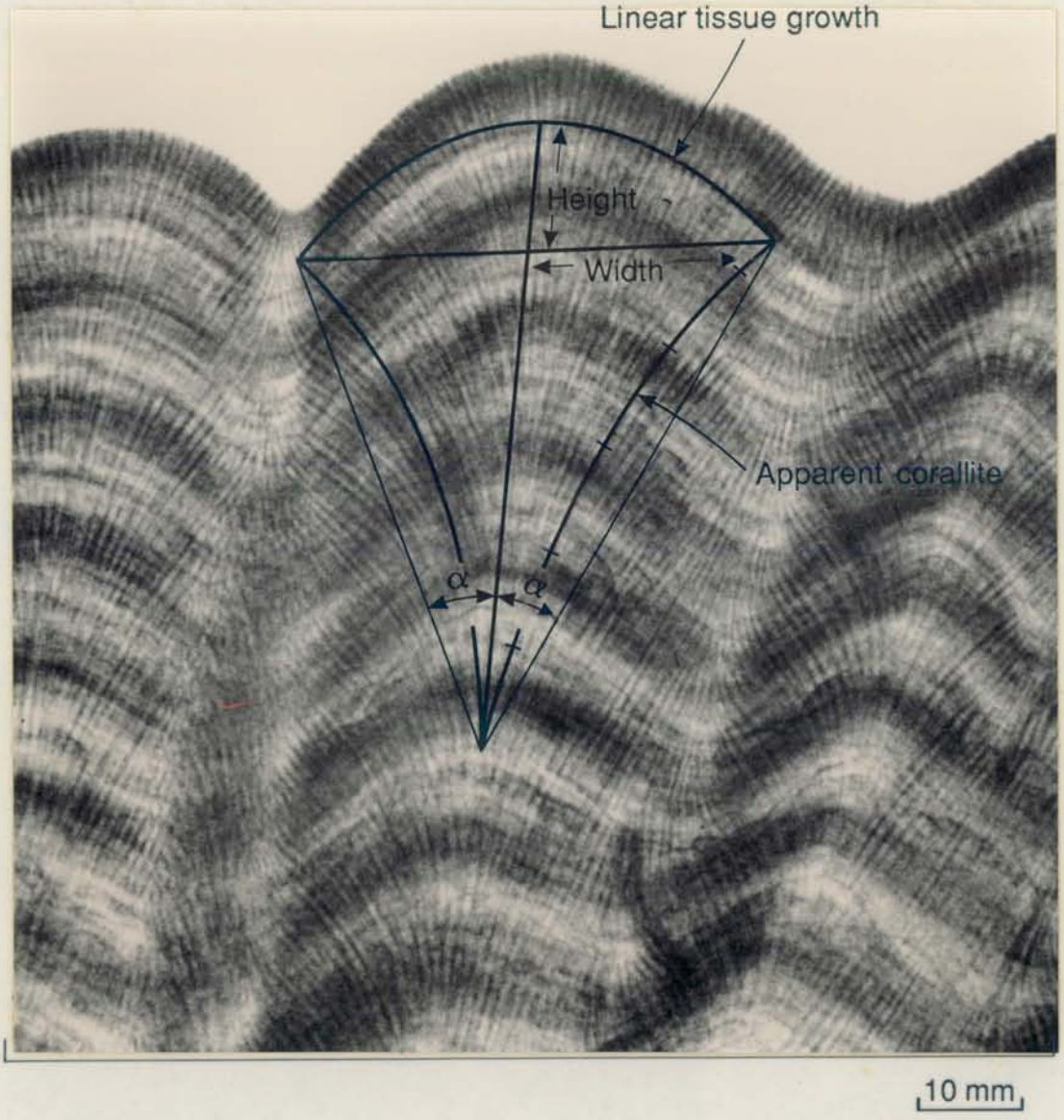

Plate 5.3. Enlarged section of Plate 2.1 displaying growth and growth form characteristics measured in X-radiographs of massive *Porites* colonies.

The 6 growth segments marked in each of the 36 X-radiographs were used to determine a mean bump ratio value for each colony. The straight line between the 2 points of corallite occlusion (Plate 5.3) represented the width of the bump associated with each the corallite fan. The height of the bump was the distance along the central axis of the fan from its interception with the "width" line to the former outline of the colony drawn between the ends of the "width" line (Plate 5.3). The bump ratio was determined by dividing the height by half the width. Well developed, more prominent bumps gave high bump ratios. The mean bump ratio was determined for each colony from the 6 growth segments marked on each X-radiograph.

2. Angle of divergence of corallites. This was the angle between the central growth axis and the line drawn from the point of origin of an apparent corallite to its point of occlusion (Plate 5.3). The angle of divergence was a measure of the displacement of a corallite, during its life time, from the central fan axis. The mean angle of corallite divergence for each colony was determined from 12 angles of divergence measured from the 6 segments.

3. Corallite longevity. Corallite longevity was determined from the number of annual bands crossed by an apparent corallite between its point of origin and its point of occlusion (see also 2.2.4). The mean corallite longevity for each colony was determined from 12 apparent corallites defining each of the 6 growth segments.

4. Annual skeletal extension rate. The annual rates of skeletal extension previously determined for each of the 36 X-radiographs were used here (see section 2.2.3. & Plate 2.1 for a detailed account of the method used to determine annual skeletal extension).

5. Measurements of tissue growth on a bump. The length of the outline of a bump, between the points of corallite occlusion (see Plate 5.3), was considered to represent a measure of the amount of tissue added over the period of growth of the segment (cf. similar measurements on growth sectors in computer models; 3.2.4, Fig. 3.7). The distance along this line was measured using a fine chain and divided by

the longevity of the apparent corallites forming the segment. This gave the annual rate of tissue growth for a bump. The mean annual rate of tissue growth for bumps was determined for each colony from measurements on the 6 segments.

6. Calculation of a tissue growth rate to skeletal growth rate ratio. The annual tissue growth rate for each bump (5. above) was divided by the annual skeletal extension rate (4. above) to give the ratio of tissue growth rate to skeletal growth rate for a bump. The mean ratio for a colony was determined from results for the 6 growth segments. A high ratio indicated that tissue growth was, relatively, faster compared with skeletal extension.

5.2.3. Measurements made on colonies rather than X-radiographs.

This section gives details of measurements made on the large pieces of skeleton remaining after slices had been removed for X-radiography. This allowed development of techniques which could be used in the field. It also allowed assessment of the results gained using such techniques against data about colonial growth over time available from X-radiographs and computer models.

Measurements of the bumpy growth surface.

The horizontal distance between the summit of two adjacent bumps was measured. The depth of the valley between these two bumps was measured from a line joining the summits. This depth was divided by half the horizontal distance between summits to provide a bumpiness ratio. A mean bumpiness ratio for a colony was determined from measurements made using 20 valleys on the middle to upper regions of the colonies.

Measurements of the tissue thickness.

Tissue thickness was, initially, measured from the large pieces of colonies remaining after the slices had been removed. It quickly became apparent that tissue

thickness could be measured from the actual slices more easily and more accurately.

Results presented in Chapter 4 showed that significant differences in tissue biomass per skeletal surface area existed between colonies from the same and different reefs. It was proposed that differences in tissue thickness may account for these variations in biomass. It appears that tissue thickness may, very likely, account for such differences in tissue biomass between colonies from different reefs. Tissue thickness seems to be an important, easily available and totally overlooked parameter associated with massive *Porites* and perhaps other massive corals (Barnes and Lough, pers. comm). Consequently, it seemed appropriate to examine differences in tissue thickness amongst the 36 corals that form the core of analyses presented here.

Remains of the tissue were clearly visible in all the skeletal slices as a brown stained layer at the outer edge of the skeleton. The mean tissue thickness was determined for each colony from 4 measurements. Two measurements were taken in each of the 2 skeletal slices removed from each colony. The tissue thickness was measured close to the vertical growth axis in each slice and also measured about 150 mm along the skeletal edge from the vertical growth axis. All measurements were taken with a ruler perpendicular to the growth surface of the skeleton.

5.2.4. Statistical procedures.

As before (3.2.5), a Macintosh SE personal computer equipped with the statistical package *Statview* was used to analyse the growth and growth form variables measured on the 36 X-radiographs and *Porites* colonies. Mean and standard deviation of all the growth and growth form variables were determined for each of the 3 reefs; Pandora, Rib and Myrmidon Reefs. Variables measured were: the bump ratio determined from both the X-radiographs and actual colonies, the tissue to

skeletal growth rate ratio, the annual tissue growth rate for bumps, the annual skeletal extension rate for colonies, corallite longevity, the angle of divergence of corallites, and tissue thickness.

Statview was used for correlations between the various growth and growth form variables which evaluated the strengths of association between them. Mean values for variables appropriate to each of the 36 colonies were used in the correlations. All correlations performed were 2 tailed since both positive and negative correlations were tested. Thus, the number of degrees of freedom was 34 (i.e., n-2). The critical correlation coefficient values for significance at the 5% and 1% level of significance were 0.44 and 0.33 respectively.

One-way analysis of variance (ANOVA) tests were performed on the mean growth and growth form variables. These tests investigated whether there was a significant reef effect on the growth and growth form variables.

5.3. RESULTS.

5.3.1. The effectiveness of bumpiness in accommodating tissue growth

Figure 5.2 shows that the annual increase in skeletal surface area of the fairly smooth colony was almost the same as the annual increase in skeletal surface area of a theoretical, hemispherical colony displaying the same annual linear extension rate. The outer surface area of the smooth colony, which corresponded to the eighteenth year of growth, was only 2% greater than the surface area of a theoretical colony after 18 linear extensions of 18.6 mm each.

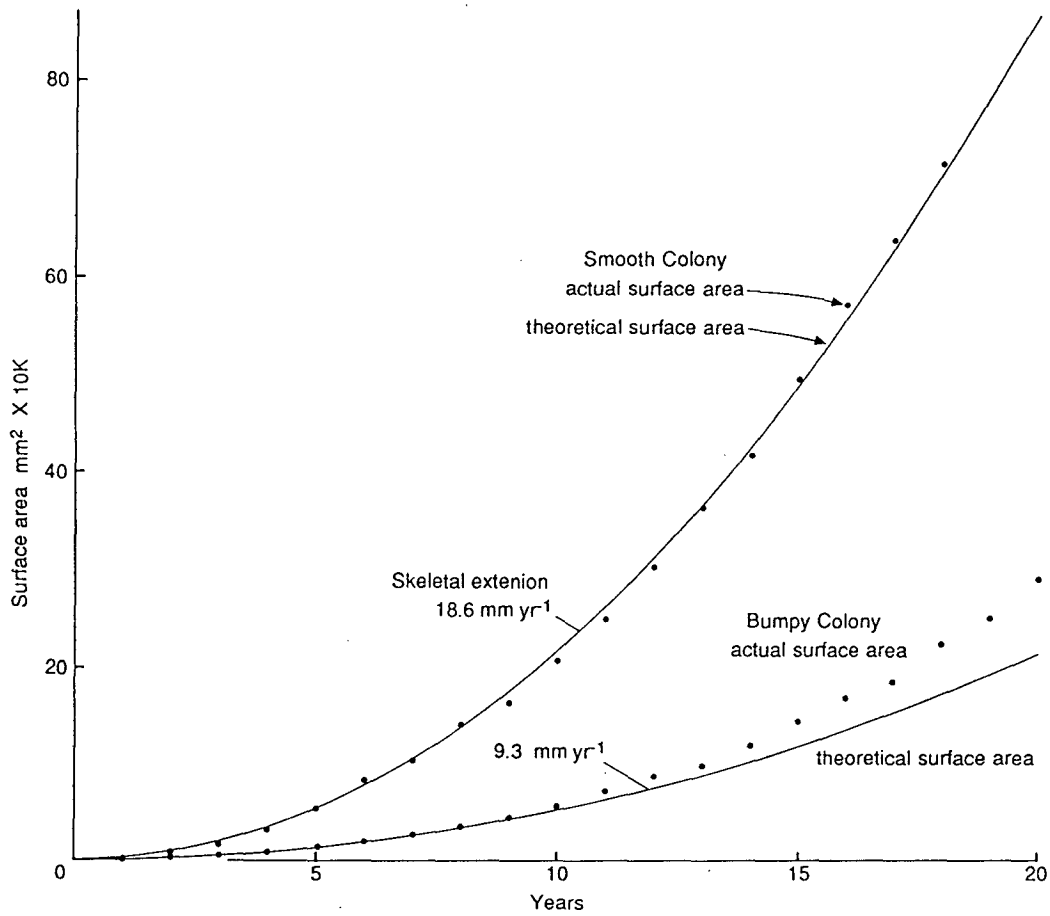

Fig. 5.2. Annual increase in surface area of a bumpy and smooth colony from Rib Reef compared with the theoretical annual increase in surface area 2 hemispheres with the same annual linear extension rates as the 2 colonies.

Former growth surfaces displayed in the X-radiograph of the bumpy colony from Rib Reef (Plate 5.1) showed that this colony had started to develop a bumpy growth surface by the time it was 55 mm high, or about 6 years old. The 10, 15 and 20 year old bumpy growth surfaces displayed in this X-radiograph had surface areas that were 5%, 17% and 20% greater, respectively, than the equivalent surfaces of a theoretical, smoothed, hemispherical colony having the same linear extension. The development of bumps increased the surface area of a colony. However, as Figure 5.2 clearly shows, this increase was small compared with the increase brought about by annual growth.

Annual skeletal extension rate profoundly affected the rate of increase in surface area and, hence, the rate of tissue growth of a colony. After 18 years of growth, the smoother colony had added almost 3 times as much tissue as the bumpy colony. Thus, after 18 years, a 2-fold difference in skeletal extension rate (18.6:9.3 mm yr^{-1}) resulted in a 3-fold difference in actual tissue growth. These results demonstrate that, although development of a highly bumpy growth surface does increase the surface area for accommodation of tissue growth, this increase is small in comparison to the increase in surface area that can be generated if the rate of skeletal extension is greater (Fig. 5.2).

5.3.2. Mean growth and growth form variables.

The mean and standard deviations (± S.D.) for all growth and growth form variables measured on the 36 massive *Porites* colonies collected from 3 reefs spanning the central G.B.R. are presented in Table 5.1.

Colonies collected from Pandora Reef, an inner shelf reef, had the highest tissue growth rate to skeletal growth rate ratio. They displayed growth forms with the most prominent bumps. Corallite fans in X-radiographs of *Porites* colonies collected from Pandora Reef had the greatest angles of corallite divergence (Table 5.1). Corallites on these corals had the shortest life expectancy; mean corallite longevity was 4.15 ± 0.46 years (Table 5.1).

In contrast, colonies collected from Rib Reef, a mid shelf reef, had the lowest tissue growth rate to skeletal growth rate ratio. These colonies displayed the smoothest growth surfaces. Corallite fans in these colonies had the smallest angles of corallite divergence (Table 5.1). The mean longevity of polyps was 5.17 ± 1.08 years (Table 5.1).

Table 5.1

Mean and standard deviations (± S.D.) for growth and growth form variables measured on 36 massive *Porites* colonies collected from the central G.B.R.

Growth and growth form Variables	Pandora Reef (Mean ± S.D.)	Rib Reef (Mean ± S.D.)	Myrmidon Reef (Mean ± S.D.)
Bump ratio (colony)	0.50 ± 0.11	0.35 ± 0.12	0.44 ± 0.09
Bump ratio (X-radiograph)	0.59 ± 0.13	0.42 ± 0.11	0.50 ± 0.08
Tissue : Skeleton	0.91 ± 0.18	0.71 ± 0.24	0.89 ± 0.14
Tissue growth (mm yr^{-1})	9.20 ± 1.66	7.42 ± 1.32	6.87 ± 0.77
Skeletal growth (mm yr^{-1})	10.33 ± 2.12	11.27 ± 3.06	7.77 ± 0.77
Corallite longevity (yr)	4.15 ± 0.46	5.17 ± 1.08	5.08 ± 0.63
Angle of divergence (°)	27.32 ± 5.00	20.69 ± 5.9	24.96 ± 0.63
Tissue thickness (mm)	6.59 ± 1.2	7.65 ± 0.75	5.21 ± 0.89

5.3.3. Correlations amongst growth and growth form variables.

Results of a series correlations amongst growth and growth form variables measured on the 36 massive *Porites* colonies collected from Pandora, Rib and Myrmidon Reefs are presented in Table 5.2.

Correlations of bump ratios with other growth and growth form variables.

Bumpiness ratios determined for X-radiographs were very strongly correlated with bumpiness ratios determined for actual colonies (r = 0.90, Table 5.2). Consequently, subsequent results only relate to bump ratios determined from X-radiographs. Although the relationship between these 2 methods for establishing the degree of bumpiness displayed on a *Porites* growth surface was highly significant,

absolute bump ratio values determined from X-radiographs were slightly higher than bump ratio values determined corresponding growth surfaces (Table 5.1).

Table 5.2.

Correlations amongst growth and growth form variables measured on 36 massive *Porites* colonies (n = 36 in all correlations). The critical coefficients of significance at the 5% and 1% level are 0.33 and 0.42 respectively (* and ** indicates significance at 5% and 1% respectively). The variables are indicated: bump ratio, colony, BRC; bump ratio, X-radiograph, BRX; tissue growth rate to skeletal growth rate ratio, T:S; annual tissue growth for a bump, TG; annual skeletal extension, SG; corallite longevity, CL; angle of divergence of corallites, AN, and tissue thickness, TT.

	Growth and growth form variables.						
	BRC	BRX	T:S	TG	SG	CL	AN
BRC	1.0						
BRX	0.90**	1.0					
T:S	0.77**	0.79**	1.0				
TG	0.63**	0.65**	-	1.0			
SG	-0.51**	-0.49**	-	0.01**	1.0		
CL	-0.55**	-0.62**	-0.60**	-0.72**	0.29	1.0	
AN	0.72**	0.71**	0.69**	0.60**	-0.43**	-0.55**	1.0
TT	-0.28	-0.25	-0.36*	0.09	0.51*	0.06	-0.38

Bump ratios for the growth surfaces of all 36 massive *Porites* colonies were highly and positively correlated with the ratio of tissue growth rate to skeletal growth rate (r = 0.79, Table 5.2). Thus colonies in which there was a higher ratio of tissue growth to skeletal growth displayed more prominent bumps.

Bump ratios were positively and significantly correlated with tissue growth ($r = 0.65$, Table 5.2). However, there was a stronger relationship between bumpiness and the ratio of tissue growth to skeletal growth than between bumpiness and tissue growth on its own. Similarly, the correlation between the bump ratio and annual skeletal extension, although significant ($r = -0.49$, Table 5.2), was less strong than the correlation between the bumpiness and the tissue growth to skeletal growth ratio. Since the bump ratio was negatively correlated with annual skeletal extension, colonies with slower rates of skeletal extension generally displayed more bumpy growth surfaces.

Correlations of the angle of divergence of corallites with other growth and growth rate variables.

The angle of divergence of corallites was positively and significantly correlated with the bump ratio value ($r = 0.72$, Table 5.2). Therefore, well developed corallite fans displaying greater angles of corallite divergence were shown to be strongly associated with prominent bumps. The correlation of the angle of divergence with the ratio of tissue growth rate to skeletal growth rate was highly significant ($r = 0.69$, Table 5.2). Although, the angle of divergence of corallites was significantly correlated with both tissue growth and skeletal growth ($r = 0.59$ and $r = -0.43$, respectively), the strengths of these correlations were less than the correlation of the angle of divergence with the tissue growth rate to skeletal growth rate ratio.

Correlation of corallite longevity with other growth and growth rate variables.

Corallite longevity was strongly and negatively correlated with tissue growth ($r = -0.60$; Table 5.2). Life expectancy of a corallite and, therefore, of a polyp was

generally shorter in colonies with relatively faster rates of tissue growth compared with skeletal growth. Corallite longevity was significantly and negatively correlated with the bump ratio value and the angle of divergence of corallites ($r = -0.62$ and $r = -0.56$) respectively. Corallite longevity was not significantly related to skeletal extension at either the 1% or 5% level of significance ($r = 0.29$; Table 5.2).

Correlations of tissue thickness with other growth and growth form variables.

Tissue thickness was not significantly correlated with any of the growth or growth form variables used in this analysis except for annual skeletal extension. Tissue thickness was positively and significantly correlated with the annual skeletal extension ($r = 0.51$, Table 5.2) and therefore colonies with thicker tissue layers were generally shown to have higher rates of annual skeletal extension. Table 2.2 shows that heights and ages of colonies were unlikely to have influenced this result.

5.3.4. One-way analysis of variance tests on growth and growth form variables.

One-way ANOVA tests, presented in Tables 5.3, showed that there were significant differences between reefs for all growth and growth form variables amongst the 36 massive *Porites* colonies ($P = <0.05$ or $P = <0.001$ in all ANOVA tests). These results strongly suggest that different environmental conditions associated with the reefs had a significant effect on rates of tissue growth, rates of skeletal growth and on growth form.

Table 5.3

One-way ANOVA tests for reef affects on growth and growth form variables measured on 36 massive *Porites* colonies collected from Pandora, Rib and Myrmidon Reefs.

Source of variance	Degrees of freedom	Mean squares	F value	Probability
Bump ratio (colony)				
Between reefs	2	0.073	6.54	< 0.05
Within reefs	33	0.011		
Bump ratio (X-radiograph)				
Between reefs	2	0.088	7.35	< 0.05
Within reefs	33	0.012		
Tissue:Skeleton ratio				
Between reefs	2	0.145	3.97	< 0.05
Within reefs	33	0.367		
Tissue growth (mm yr^{-1})				
Between reefs	2	17.900	10.57	< 0.001
Within reefs	33	1.694		
Skeletal growth (mm yr^{-1})				
Between reefs	2	39.364	8.14	< 0.05
Within reefs	33	4.846		
Corallite longevity (yr)				
Between reefs	2	3.779	6.43	< 0.05
Within reefs	33	0.588		
Angle of divergence				
Between reefs	2	136.867	5.95	< 0.05
Within reefs	33	23.007		
Tissue thickness (mm)				
Between reefs	2	17.976	20.44	< 0.001
Within reefs	33	0.879		

5.4. DISCUSSION.

5.4.1. The extent to which development of a bumpy growth surface assists with the accommodation of tissue growth.

Barnes (1973) suggested that development of a bumpy growth surface by massive coral colonies presented a solution to the geometric constraints on growth which develops as many types of such colonies increase in size. Data presented here for *Porites* show that this is not the case. Although development of a bumpy growth surface was shown to provide a larger surface area for tissue growth and new polyp formation, the absolute amount of increase in surface area generated, by even the most bumpy surfaces measured, was not considered to be very profound. X-radiographs show that it takes 2-4 years for a bumpy growth surface to become fully established. Even in very bumpy colonies, for instance that shown in Plate 5.2, bumpiness only provides a short-term solution to the geometric problem. Once a bumpy surface is established, continued growth provides no additional increase in surface area over a smooth surface. It is only during the change from a smooth to a bumpy surface that growth provides more surface area than would have been created if the surface had remained smooth.

5.4.2. Skeletal extension limitations imposed on tissue growth.

Computer models of *Porites* growth, and measurements of actual colonies, indicate that the degree of bumpiness displayed by a massive *Porites* growth surface partly reflects the extent to which tissue growth is being constrained by the rate of skeletal extension. Tissue growth is less severely constrained in colonies which display a smooth growth surface than in colonies with a bumpy surface. Colonies having a rapid skeletal extension rate seem more able to accommodate tissue growth, by more rapidly increasing their surface area. These colonies tend to display a smoother growth surface than colonies which extend more slowly (cf., Plates 5.1 and 5.2). However, faster growing colonies will ultimately encounter the same problems

as slower growing colonies, but not until they attain a greater absolute size.

Although bumpiness does assist with accommodation of tissue growth, skeletal extension rate has a far greater influence on such accommodation. Skeletal extension obviously exerts a very profound, perhaps the most profound, influence on tissue growth. A bumpy growth surface indicates that skeletal growth is constraining tissue growth; a smooth growth surface indicates that tissue growth is not being constrained by skeletal extension.

5.4.3. Controls and constraints on colonial growth in *Porites* indicated by computer simulations and actual colonies.

Computer simulations of colonial growth in *Porites* (Chapter 3) indicated that the amount of bumpiness displayed in each growth form model was strongly related to the ratio of tissue growth to skeletal growth. Measurements of growth and growth form features displayed by massive *Porites* colonies (this Chapter) provided evidence supporting this prediction. Indeed, measurements of growth and growth form features in actual colonies show that the ratio of tissue growth to skeletal growth is the factor most important in controlling growth form (see Table 5.2). The ratio of tissue growth to skeletal growth is more important in controlling growth form than the absolute rate of tissue growth or the absolute rate of skeletal growth.

The computer models indicated that there should be a strong relationship between the ratio of tissue growth to skeletal growth and the angle of corallite divergence. This prediction was also confirmed by measurements on actual colonies. Colonies with higher tissue growth to skeletal growth rate ratios had well developed corallite fans in which the angle of divergence of corallites was high. Such well developed corallite fans were associated with prominent bumps at the growth surface.

X-radiographs of skeletal slices of *Porites* showed that new polyps were being formed at the summit of bumps and older ones lost in the valleys between bumps (2.3.1 and 2.4.2). The rate of polyp loss and replacement, measured from corallite

longevity, was shown to be relatively faster in colonies with bumpy growth surfaces (5.3.2). Thus, as skeletal extension becomes less able to accommodate tissue growth, polyps tend to be occluded sooner. This presents a mechanism, not previously described, by which the geometric constraint on colonial growth in *Porites*, and perhaps other species, is partially alleviated.

5.4.4. Environmental factors affecting *Porites* growth and growth form.

Pandora, Rib and Myrmidon Reefs lie along a major environmental gradient between inshore conditions and oceanic conditions (Wilkinson and Cheshire 1988). Differences in growth and growth form of *Porites* appear to reflect these environmental differences. While the gradient in environmental conditions lies between Pandora and Myrmidon Reefs, the gradient in *Porites* growth response does not simply follow this environmental gradient. The ratio of tissue growth to skeletal growth was highest in colonies from Pandora Reef and lowest in colonies from Rib Reef (Table 5.1). Colonies from Myrmidon Reef, while showing the lowest absolute values for both tissue growth and skeletal growth, had a ratio which was intermediate between colonies from Pandora Reef and colonies from Rib Reef. The growth form of colonies reflected this gradient in ratios. The bumpiest colonies were found at Pandora Reef and the smoothest colonies at Rib Reef. Colonies from Myrmidon Reef were intermediate in bumpiness.

Colony extension rates were highest at Rib Reef, very slightly lower at Pandora Reef and significantly lower at Myrmidon Reef (Table 5.1). However, colonies at Rib Reef had relatively smooth surfaces compared with colonies at Pandora Reef. This suggests that tissue growth rate at Rib Reef is not so severely constrained by skeletal growth as at Pandora Reef. Since skeletal growth rates were much the same at the 2 reefs, it appears that tissue growth was much less at Rib Reef than at Pandora Reef. Calcification and skeletal growth in a hermatypic coral, such as *Porites*, is firmly linked to ambient light levels (see Barnes and Chalker, 1990, for recent review). Since skeletal extension rates are similar at Pandora and Rib Reefs,

and since calcification rates of *Porites* are similar at the 2 reefs (Lough and Barnes, per. comm.), light is probably acting upon corals at the 2 sites in much the same way. Thus, the difference in tissue growth must relate to the nutritional status of the corals, and hence the "food" available from the waters around the 2 reefs. It seems likely that corals at Rib Reef are less well fed than corals at Pandora Reef.

Figure 5.3 presents a summary of the ways in which environmental factors may affect growth and growth form in *Porites*. The point which this figure is intended to stress is that the relationship between environmental factors and *Porites* growth form depends upon the ratio between tissue growth and skeletal growth. Differences in growth forms of *Porites* between reefs very clearly demonstrates that there is a degree of independence between tissue growth and skeletal growth. Thus, photosynthesis of symbiotic algae in *Porites* cannot be supplying equally nutritional and skeletal growth requirements.

This now throws up a new and potentially very important insight into coral calcification. Corals at Myrmidon Reef have low tissue growth rates and skeletal growth rates. Although *Porites* colonies at Myrmidon Reef have higher density skeletons than *Porites* colonies at the other 2 reefs, their calcification rate is much lower (Lough and Barnes, per comm; in fact, colonies from Pandora Reef show the highest calcification rates). Thus, calcification and skeletal growth is lowest in colonies of *Porites* from Myrmidon Reef. Light is always presented as the factor which exerts the greatest influence on calcification rate in hermatypic corals. Since photo-inhibition does not seem to occur in hermatypic corals (see Barnes and Chalker, 1990), high light intensities, perhaps associated with the clear waters at Myrmidon Reef, are not likely to be reducing calcification rates. Some factor other than light must be exerting a major control on calcification and skeletal growth in *Porites* colonies growing along the inshore-offshore transect between Pandora and Myrmidon Reefs.

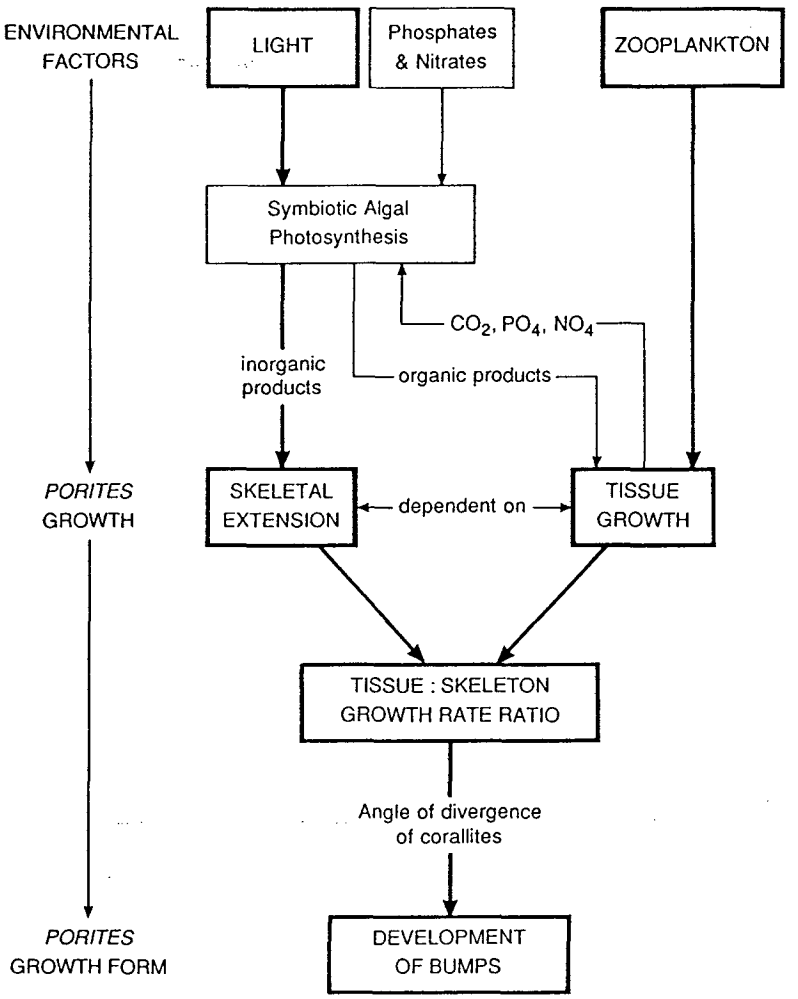

Fig. 5.3. Summary diagram showing the links between the environment and *Porites* growth and growth form.

It may be that tissue growth can exert a controlling influence on skeletal growth and calcification rate. The ratio of tissue growth to skeletal growth was lowest at Rib Reef, but the absolute rate of tissue growth was lowest at Myrmidon Reef. There is evidence that skeletal extension in corals consumes tissue (Barnes, 1971, 1972; but see discussion in Meek, 1982, p. 116). Thus, while a low ratio of tissue growth to skeletal growth may affect growth form, as at Rib Reef, a low absolute rate of tissue growth may affect skeletal growth rate and calcification.

For the moment, this remains a topic for speculation. Proper extension of these ideas awaits accumulation of further evidence. Nevertheless, data presented here suggests that factors other than light (and temperature) may play an important role in constraining, if not controlling, coral calcification.

5.4.5. Information to be gained from measurements of bumpiness in *Porites*.

Bumpiness of *Porites* colonies was measured from both X-radiographs of skeletal slices and actual colonies. The results provided by these 2 procedures were slightly different. This difference was due to actual bumps being used on X-radiographs and valleys being used on colony growth surfaces for determination of the bumpiness ratio of a colony.

The bump ratio does not, on its own, provide clear information about other growth characteristics of a colony. A colony which has grown to more than 100 mm in height and has maintained a smooth growth surface is likely to have had a high skeletal extension rate or a lower tissue growth rate. The converse is not true; a bumpy growth surface does not necessarily indicate a low skeletal extension rate. A bumpy surface merely indicates that the tissue growth is relatively faster than skeletal growth.

Growth and bumpiness together can indicate the nutritional status of a colony. For example, *Porites* corals growing at Pandora Reef exhibited a relatively faster rate of skeletal extension and well developed bumps on the growth surface indicating that these corals were well nourished and probably calcifying at a fairly rapid rate. In contrast, *Porites* colonies from Myrmidon Reef, although moderately bumpy, displayed relatively slower skeletal extension rates suggesting that these corals were poorly nourished and probably calcifying at a slower rate than colonies from Pandora Reef. The smooth, fast growing *Porites* colonies from Rib Reef indicated that although the rate of calcification of these corals was probably similar to that at Pandora Reef, the corals were less well nourished. It seems highly likely that the differences in growth form together with growth rates between colonies reflect

differences in the availability of nutrients for coral growth at the 3 reefs rather than differences in the efficiency of zooxanthellae between corals at the 3 sites.

Thus, measurements of bumpiness in *Porites* colonies together with measurements of growth rate can provide essential information about the reef environment. Growth rate could be determined from short cores of small diameter drilled from the colonies. Cores 50-100 mm long and 20-30 mm in diameter would be adequate for such measurements. Careful and conservative removal of such cores, together with subsequent sealing of the drill hole, would ensure that subsequent growth of the colony was little affected.

Similar information about reef environment might also be obtained from massive *Porites* present in fossil reefs. Many fossil corals appear to retain the density banding pattern and this, together with the actual surface profile or the surface profile indicated by X-radiographs, could provide comparative data about the environments surrounding the reefs on which the *Porites* grew.

The continual "turnover" of polyps associated with bumpiness raises possibilities for further studies. Large *Porites* colonies have grown over several centuries but, yet, no polyp on the growth surface is likely to be older than 4-7 years (Chapter 2). The demographic and genetic implications of this finding have yet to be explored. Further, polyps in smooth-surfaced corals are longer lived. Thus, there might be differences in the fecundity of corals from different sites depending upon the age at which polyps develop gonads. These reproductive implications have yet to be explored.

5.5. CONCLUSIONS.

1. A bumpy growth surface in *Porites* colonies indicates that the tissue growth is being constrained by the skeletal extension. The more bumpy the coral, the greater this constraint.

2. Development of a bumpy growth surface does not overcome the constraint that skeletal growth exerts on tissue growth, it merely offers very temporary relief.

3. Tissue growth in *Porites* approximates the increase in colony surface area. The rate of tissue growth in massive colonies decreases as the colony grows.

4. The rate of skeletal extension probably exerts a major control on the rate of tissue growth.

5. The ratio of tissue growth to skeletal growth in massive *Porites* controls the degree of bumpiness displayed by the growth surface: a colony with a relatively faster tissue growth compared with skeletal growth displays a well developed bumpy growth surface.

6. Significant differences in the degree of bumpiness displayed by massive *Porites* colonies indicate that there must exist a degree of independence between tissue growth rate and skeletal growth rate.

7. The ratio of tissue growth to skeletal growth also controls the angle of divergence of corallites at the colony surface. Hence it controls the internal macro-architecture (*sensu* Barnes and Devereux, 1988) of the colonial skeleton. Colonies with relatively faster tissue growth compared with skeletal growth display the greatest angles of corallite divergence.

8. The ratio of tissue growth to skeletal growth also controls the longevity of polyps at the colonial surface. The longevity of corallites is shortest in colonies with relatively higher rates of tissue growth compared with skeletal growth.

9. Alteration of the ratio of tissue growth to skeletal growth is the principal way in which the environment affects growth form in massive colonies of *Porites*.

10. Skeletal extension and, perhaps, calcification in *Porites* may be modified, or even controlled, by some other factor in addition to light. This factor may well be related to tissue growth.

11. Surface bumpiness and growth rate of *Porites* may be used to provide information about the environment in which the coral grew.

CHAPTER 6

CONCLUSIONS AND FUTURE RESEARCH

6.1 CONCLUSIONS.

1. All massive *Porites* colonies develop a bumpy growth surface as they increase in size.

2. Development of a bumpy growth surface indicates that tissue growth is becoming constrained by skeletal growth. The more bumpy the coral the greater this constraint.

3. A massive *Porites* colony becomes bumpy at a size determined by the ratio of its tissue growth to skeletal growth. A bumpy growth surface, is generally established by the time a colony reaches 80 mm in height, or about 8 years old.

4. The transition from an initial smooth hemispherical growth surface to a fully developed bumpy growth surface occurs over 2-4 years. Development of a bumpy growth surface increases the surface area of skeleton available to accommodate tissue growth.

5. The benefit of increase in surface area derived from development of a bumpy growth surface provides only a temporary solution to the geometric constraint on tissue growth brought about by increase in size.

6. The rate of skeletal extension exerts a profound effect on tissue growth in contrast to bumpiness which provides very limited increase in skeletal surface area.

7. Skeletal surface area in massive *Porites* colonies is a useful indicator of tissue biomass.

8. Chlorophyll should not be used, as an alternative to protein, for estimates of tissue biomass in massive *Porites*.

9. The degree of bumpiness of massive *Porites* colonies is controlled by the ratio of its tissue growth to skeletal growth. A colony displaying a highly bumpy growth surface exhibits a relatively faster tissue growth compared with skeletal growth.

10. The angle of divergence of corallites displayed in X-radiographs of skeletal slices of massive *Porites* is controlled by the ratio of tissue growth to skeletal growth of the colony. Colonies with relatively faster rates of tissue growth compared with skeletal growth exhibit corallite fans with greater angles of divergence.

11. Once a massive *Porites* colony develops a bumpy growth surface all new polyps are initiated at, or towards the summit of bumps.

12. Growth of a new polyp on a bump causes older adjacent polyps to become displaced. Displacement of polyps is indicated by the angle of divergence of corallite fans displayed in X-radiographs of skeletal slices of massive *Porites*.

13. The location of a polyp on the growth surface relative to the summit of a bump changes as skeletal extension occurs. Relatively younger polyps are located on and around the summit of bumps, whilst relatively older polyps are located at or towards the bottom of a valley formed between bumps.

14. Corallites located at or towards the bottom of valleys formed between bumps become compressed and occluded from the growth surface. Hence, polyps located in this region also become lost from the growth surface.

15. X-radiographs of skeletal slices cut from the growth axis of massive *Porites* colonies show that it takes 4-7 years from the formation of a corallite on the summit of a bump to its occlusion at the bottom of a valley formed between bumps.

16. Polyps are continually being lost and replaced from the growth surface of a massive *Porites* colony during a 4-7 year period. Hence, the tissue covering the growth surface can be no older than about 5 years even though the skeleton may have grown for centuries.

17. Differences in environmental conditions associated with different reefs exert a significant effect on the ratio of tissue growth to skeletal growth of a massive *Porites* colony.

18. Significant differences in the ratio of tissue growth to skeletal growth between colonies of massive *Porites* are reflected by significant differences in growth form between colonies from different reefal environments.

19. Thus growth form and growth rate of a massive *Porites* colony may provide information of the environment in which the colony grew.

20. Some factor, other than light, not yet recognised may be exerting a major controlling influence on skeletal extension of massive *Porites* under certain environmental conditions. This factor may be related to tissue growth.

6.2. FUTURE RESEARCH.

1. Histological, histochemical and biochemical studies on tissue covering a bumpy massive *Porites* colony could be used to examine polyp resorption and the subsequent translocation of resorbed products. This study would question whether resorbed products derived from the occlusion of older polyps are transported to regions of active tissue growth, that is on or towards the summit of bumps.

2. A study of polyps with fecundity and age over a bumpy growth surface of a massive *Porites* colony would establish whether the increase in age of polyps from the summit of a bump to its base is accompanied by a significant gradation in the fecundity of polyps.

3. The 2 dimensional models presented in this work could be developed further to explore the constraints on growth, and factors necessary, to evolve a wider range of growth forms to include columnar, plate-like, turreted and possibly branching forms.

4. An investigation should be undertaken to assess the effect on tissue biomass of massive *Porites* with different tissue thickness. Variation in tissue thickness displayed by massive *Porites* of different age and size on the G.B.R. is presently being investigated (Barnes and Lough, per. comm).

5. Results showed that growth form and growth rate of massive *Porites* colonies may provide information on the nutritional status of a reef. This results seems worthy of further investigation.

APPENDIX

GROWTH.BAS VERSION 1

This program is designed to produce 2 dimensional models that simulate growth of a massive *Porites* colony. Different growth form models are produced by changing the tissue growth:skeletal growth ratio assigned to each model. Tissue growth and skeletal growth are represented by the values *w* and *l* respectively. The dimensions of modules used to construct a model are designated values of *l*, *w* and *dw*. A modular unit, shaped like a trapezium, represents a polyp and its associated corallite. The two length sides of a trapezium are assigned the *l* value and the increase in width of a trapezium from its base to its upper surface is represented by an increase in width from *w* to *dw*. The growth of a model is depicted in modular units which are added in an iterative fashion one at a time and layer by layer. The order of addition of potential modules at each layer is determined by the sequential organisation of module co-ordinates in a sequential file in *Growth.bas* version I. In this program the same modules are developed and prevented from developing each time the program is run using the same *w* and *l* values. In *Growth.bas* version II a random file is used to store module co-ordinates at each layer and a random number generator is used to access module co-ordinates. Each time *Growth.bas* version II is run using the same *w* and *l* values "chance" determines which modules will develop and which ones will be prevented from continuing into the next layer. The co-ordinate information held in the most recent layer determines the growth pattern of modules in the subsequent layer in both versions of *Growth.bas*.

Input data

```
LOCATE  2,24: PRINT "CORAL GROWTH.BAS INPUT PARAMETERS"
LOCATE  5, 5: PRINT "Enter SCREEN 9 for EGA card "
LOCATE  7, 5: PRINT "Enter bottom left WINDOW co-or (0,0)= "
LOCATE  8, 5: PRINT "Enter upper right WINDOW co-or (639,349)= "
LOCATE 10, 5: PRINT "Enter start point co-or (x=320,y=0) = "
LOCATE 12, 5: PRINT "Enter Vertical Extension ie.Skeletal growth (l=50) ="
LOCATE 13, 5: PRINT "Enter Horizontal Extension ie.Tissue growth  (w=20) ="
LOCATE 15, 5: PRINT "Enter colour of coral (1-15)  (cc=9) = "
LOCATE 16, 5: PRINT "Enter colour of border (1-15) (bc=15) = "
dw = w + w          dw = double width
l2 = l * l
w2 = w * w
dw2 = dw * dw
m = SQR(w2 + l2)    m = hypotenuse of triangle l,w,m
m2 = m * m
```

```
xdw = INT((x + dw) + .01)
SCREEN s
WINDOW (wx1, wy1)-(wx2, wy2)
```

Open files

```
OPEN "Newfile.dat" FOR OUTPUT AS #1
    WRITE #1, x, y, xdw, y
CLOSE #1
```

Mid Point Routine

The *Mid Point* routine determines the midpoint (x3,y3) between two co-ordinates (x1,y1) and (x2,y2).

```
start:
    OPEN "Newfile.dat" FOR INPUT AS #1
    OPEN "Oldfile.dat" FOR OUTPUT AS #2

        DO WHILE NOT EOF(1)
            INPUT #1, x1, y1, x2, y2
                      x3 = INT(((x1 + x2) / 2) + .01)
                      y3 = INT(((y1 + y2) / 2) + .01)
            WRITE #2, x1, y1, x2, y2, x3, y3
        LOOP
    CLOSE #1
    CLOSE #2
```

New Point Routine

The *New Point* routine determines two points of intersection between two circles of radius *m* drawn from two co-ordinates (x1,y1) and (x2,y2).

```
    OPEN "Oldfile.dat" FOR INPUT AS #2
    OPEN "Intfile.dat" FOR OUTPUT AS #3

        DO WHILE NOT EOF(2)
            INPUT #2, x1, y1, x2, y2, x3, y3
                      yy = 0
                      xx = 0
                      x12 = x1 * x1
                      y12 = y1 * y1
                      x22 = x2 * x2
                      y22 = y2 * y2
                      e = x1 - x2
                      f = y1 - y2
                      e2 = e * e
                      f2 = f * f
```

```
                        d = x12 + y12 + m2 - x22 - y22 - m2
                        d2 = d * d
   IF x1 = x2 THEN
      GOTO 435
         ELSE
            GOTO 425
   END IF
```

Method 1 can be used if y1 = y2 but not if x1 = x2

```
425     a = (f2 / e2) + 1
        b = -2 * (((d * f) / (2 * e2)) - x1 * (f / e) + y1)
        c = ((d / (2 * e) - x1) ^ 2) - m2 + y12
        b2 = b * b
        x41 = (d + (f / a) * (b + SQR(b2 - (4 * a * c)))) / (2 * e)
        y41 = (-b - SQR(b2 - (4 * a * c))) / (2 * a)
        x42 = (d + (f / a) * (b - SQR(b2 - (4 * a * c)))) / (2 * e)
        y42 = (-b + SQR(b2 - (4 * a * c))) / (2 * a)
        GOTO 450
```

Method 2 can be used if x1 = x2 but not if y1 = y2

```
435     a = (e2 / f2) + 1
        b = -2 * (((d * e) / (2 * f2)) - y1 * (e / f) + x1)
        c = ((d / (2 * f) - y1) ^ 2) - m2 + x12
        b2 = b * b
        x41 = (-b - SQR(b2 - (4 * a * c))) / (2 * a)
        y41 = (d - (2 * e * x41)) / (2 * f)
        x42 = (-b + SQR(b2 - (4 * a * c))) / (2 * a)
        y42 = (d - (2 * e * x42)) / (2 * f)

450     lx = ABS(x1 - x2)
        ly = ABS(y1 - y2)

        IF lx >= ly THEN
           GOTO 455
              ELSE
                 GOTO 460
        END IF

455     IF y41 < y42 THEN
          GOSUB small.1a
             ELSE
                GOSUB large.1a
        END IF

        IF x1 = x AND y1 = y THEN
           GOTO 465
```

```
            ELSE
               GOTO 458
        END IF

458     IF POINT(x3, (y3 - INT(w * pw))) >= 1 THEN
          GOTO 465
             ELSE
               GOTO 470
        END IF

460     IF x41 < x42 THEN
          GOSUB small.1a
             ELSE
               GOSUB large.1a
        END IF

        IF POINT((x3 - INT(w * pw)), y3) >= 1 THEN
          GOTO 465
             ELSE
               GOTO 470
        END IF

small.1a:
            x4s = x41
            y4s = y41
            x4g = x42
            y4g = y42
RETURN
large.1a:
            x4g = x41
            y4g = y41
            x4s = x42
            y4s = y42
RETURN
465         x4 = x4g
            y4 = y4g
            GOTO 475
470         x4 = x4s
            y4 = y4s
            GOTO 475
475                     x1 = INT((x1) + .01)
                        y1 = INT((y1) + .01)
                        x2 = INT((x2) + .01)
                        y2 = INT((y2) + .01)
                        x4 = INT((x4) + .01)
                        y4 = INT((y4) + .01)
                        x34 = INT(((x3 + x4) / 2) + .01)
                        y34 = INT(((y3 + y4) / 2) + .01)
```

```
   IF y4 >= wy2 THEN
      GOTO 900
   END IF
```

477 Test to see if the line (x3,y3)-(x4,y4) is already occupied:-

```
   IF POINT(x4, y4) >= 1 THEN
      GOTO 520
   END IF
         IF POINT(x34, y34) >= 1 THEN
            GOTO 520
         END IF

   IF x3 = x4 THEN
      GOSUB ttxline1
         ELSE
            GOTO 480
   END IF
   GOTO 518

480 IF y4 = y3 THEN
       GOSUB ttyline1
          ELSE
             GOTO 485
   END IF
   GOTO 518

ttxline1:
       IF y3 < y4 THEN
            FOR ty = (y3 + INT(1 * pl)) TO y4
                     IF POINT(x3, ty) >= 1 THEN
                        GOTO 520
                     END IF
478           NEXT ty
      ELSE
            FOR ty = (y3 - INT(1 * pl)) TO y4 STEP -1
                     IF POINT(x3, ty) >= 1 THEN
                        GOTO 520
                     END IF
479           NEXT ty
      END IF
RETURN
ttyline1:
       IF x3 < x4 THEN
            FOR tx = (x3 + INT(1 * pl)) TO x4
                     IF POINT(tx, y3) >= 1 THEN
                        GOTO 520
                     END IF
```

```
483             NEXT tx
        ELSE
                FOR tx = (x3 - INT(l * pl)) TO x4 STEP -1
                        IF POINT(tx, y3) >= 1 THEN
                           GOTO 520
                        END IF
484             NEXT tx
        END IF
RETURN
485 lx1 = ABS(x3 - x4)
    ly1 = ABS(y3 - y4)
    tana = lx1 / ly1

    IF ly1 >= lx1 THEN
       GOTO 490
          ELSE
             GOTO 502
    END IF
490 IF y3 < y4 THEN
       GOTO 495
          ELSE
             GOTO 500
    END IF
495 FOR ty = y3 TO y4
       yy = yy + 1
       xx = tana * yy
          IF ty <= (y3 + INT(l * pl)) THEN
             GOTO 496
          END IF
                IF x3 < x4 THEN
                   tx = INT(x3 + xx)
                      ELSE
                         tx = INT(x3 - xx)
                END IF
                      IF POINT(tx, ty) >= 1 THEN
                         GOTO 520
                      END IF
496 NEXT ty
    GOTO 518

500 FOR ty = y3 TO y4 STEP -1
       yy = yy + 1
       xx = tana * yy
             IF ty >= (y3 - INT(l * pl)) THEN
                   GOTO 501
             END IF
                   IF x3 < x4 THEN
                      tx = INT(x3 + xx)
```

```
                    ELSE
                        tx = INT(x3 - xx)
                END IF
                    IF POINT(tx, ty) >= 1 THEN
                        GOTO 520
                    END IF
501 NEXT ty
   GOTO 518

502  IF x3 < x4 THEN
        GOTO 505
           ELSE
              GOTO 510
    END IF

505 FOR tx = x3 TO x4
      xx = xx + 1
      yy = xx / tana
           IF tx <= (x3 + INT(l * pl)) THEN
                GOTO 506
           END IF
                IF y3 < y4 THEN
                   ty = INT(y3 + yy)
                      ELSE
                         ty = INT(y3 - yy)
                END IF
                    IF POINT(tx, ty) >= 1 THEN
                       GOTO 520
                    END IF
506 NEXT tx
   GOTO 518

510 FOR tx = x3 TO x4 STEP -1
      xx = xx + 1
      yy = xx / tana
          IF tx >= (x3 - INT(l * pl)) THEN
              GOTO 511
          END IF

              IF y3 < y4 THEN
                 ty = INT(y3 + yy)
                    ELSE
                       ty = INT(y3 - yy)
              END IF
                    IF POINT(tx, ty) >= 1 THEN
                       GOTO 520
                    END IF
511 NEXT tx
```

```
   GOTO 518
518          WRITE #3, x1, y1, x4, y4, x3, y3
            WRITE #3, x2, y2, x4, y4, x3, y3
520   LOOP
      CLOSE #2
      CLOSE #3
```

End Point Routine

The *End Point* rountine determines two points of intersection of two circles of radius *l* and *w* drawn from two co-ordinates (x1,y1) and (x4,y4) respectively (i.e., for the left hand module) and also two points of intersection of two circles of radius *l* and *w* drawn from (x2,y2) and (x4,y4) respectively (i.e., for the right hand module).

```
   OPEN "Newfile.dat" FOR OUTPUT AS #1
   OPEN "Intfile.dat" FOR INPUT AS #3

        DO WHILE NOT EOF(3)
            INPUT #3, x2, y2, x1, y1, x3, y3
                        yy = 0
                        xx = 0
                        x12 = x1 * x1
                        y12 = y1 * y1
                        x22 = x2 * x2
                        y22 = y2 * y2
                        e = x2 - x1
                        f = y2 - y1
                        e2 = e * e
                        f2 = f * f
                        d = x22 + y22 + dw2 - x12 - y12 - l2
                        d2 = d * d
      IF x1 = x2 THEN
         GOTO 550
            ELSE
               GOTO 525
      END IF
```

Method 1 can be used if y1 = y2 but not if x1 = x2

```
525     a = (f2 / e2) + 1
        b = -2 * (((d * f) / (2 * e2)) - x1 * (f / e) + y1)
        c = ((d / (2 * e) - x1) ^ 2) - dw2 + y12
        b2 = b * b
        x51 = (d + (f / a) * (b + SQR(b2 - (4 * a * c)))) / (2 * e)
        y51 = (-b - SQR(b2 - (4 * a * c))) / (2 * a)
        x52 = (d + (f / a) * (b - SQR(b2 - (4 * a * c)))) / (2 * e)
        y52 = (-b + SQR(b2 - (4 * a * c))) / (2 * a)
```

```
        GOTO 575
```

Method 2 can be used if x1 = x2 but not if y1 = y2

```
550     a = (e2 / f2) + 1
        b = -2 * (((d * e) / (2 * f2)) - y1 * (e / f) + x1)
        c = ((d / (2 * f) - y1) ^ 2) - dw2 + x12
        b2 = b * b
        x51 = (-b - SQR(b2 - (4 * a * c))) / (2 * a)
        y51 = (d - (2 * e * x51)) / (2 * f)
        x52 = (-b + SQR(b2 - (4 * a * c))) / (2 * a)
        y52 = (d - (2 * e * x52)) / (2 * f)

575     lx2 = ABS(x2 - x3)
        ly2 = ABS(y2 - y3)
        IF lx2 >= ly2 THEN
           GOTO 600
              ELSE
                 GOTO 620
        END IF

600     IF x51 < x52 THEN
          GOSUB small.1b
             ELSE
                GOSUB large.1b
        END IF

        IF x2 <= x3 THEN
           GOTO 640
              ELSE
                 GOTO 645
        END IF

620     IF y51 < y52 THEN
          GOSUB small.1b
            ELSE
                GOSUB large.1b
        END IF

        IF y2 < y3 THEN
           GOTO 640
              ELSE
                 GOTO 645
        END IF
```

```
small.1b:
        x5s = x51
        y5s = y51
        x5g = x52
        y5g = y52
RETURN
large.1b:
        x5g = x51
        y5g = y51
        x5s = x52
        y5s = y52
RETURN
640                    x5 = INT((x5s) + .01)
                      y5 = INT((y5s) + .01)
                      GOTO 650
645                    x5 = INT((x5g) + .01)
                      y5 = INT((y5g) + .01)
                      GOTO 650
650                    x25 = INT((x2 + x5) / 2)
                      y25 = INT((y2 + y5) / 2)
                      x6 = INT((x1 + x2) / 2)
                      y6 = INT((y1 + y2) / 2)
```

655 Test to see if the line (x2,y2)-(x5,y5) is already occupied:-

```
IF y5 <= y THEN
  GOTO 720
END IF

IF POINT(x6, y6) >= 1 THEN
   GOTO 720
END IF

   IF POINT(x5, y5) >= 1 THEN
      GOTO 720
   END IF

      IF POINT(x25, y25) >= 1 THEN
         GOTO 720
      END IF

IF x2 = x5 THEN
   GOSUB ttxline2:
      ELSE
         GOTO 680
END IF
GOTO 718
```

```
680 IF y2 = y5 THEN
      GOSUB ttyline2:
         ELSE
            GOTO 685
   END IF
   GOTO 718

ttxline2:
       IF y2 < y5 THEN
            FOR ty = (y2 + INT(1 * pl)) TO y5
                  IF POINT(x2, ty) >= 1 THEN
                        GOTO 720
                  END IF
            NEXT ty
      ELSE
            FOR ty = (y2 - INT(1 * pl)) TO y5 STEP -1
                  IF POINT(x2, ty) >= 1 THEN
                        GOTO 720
                  END IF
            NEXT ty
      END IF
RETURN

ttyline2:
       IF x2 < x5 THEN
            FOR tx = (x2 + INT(1 * pl)) TO x5
                  IF POINT(tx, y2) >= 1 THEN
                     GOTO 720
                  END IF
            NEXT tx
      ELSE
            FOR tx = (x2 - INT(1 * pl)) TO x5 STEP -1
                  IF POINT(tx, y2) >= 1 THEN
                     GOTO 720
                  END IF
            NEXT tx
      END IF
RETURN
685 lx3 = ABS(x5 - x2)
   ly3 = ABS(y5 - y2)
   tanb = lx3 / ly3

   IF ly3 >= lx3 THEN
      GOTO 690
         ELSE
            GOTO 702
   END IF
```

```
690 IF y2 < y5 THEN
      GOTO 695
         ELSE
            GOTO 700
   END IF

695 FOR ty = y2 TO y5
      yy = yy + 1
      xx = tanb * yy
         IF ty <= (y2 + INT(l * pl)) THEN
            GOTO 696
         END IF
               IF x2 < x5 THEN
                  tx = INT(x2 + xx)
                     ELSE
                        tx = INT(x2 - xx)
               END IF
                        IF POINT(tx, ty) >= 1 THEN
                              GOTO 720
                        END IF
696 NEXT ty
   GOTO 718

700 FOR ty = y2 TO y5 STEP -1
      yy = yy + 1
      xx = tanb * yy

            IF ty >= (y2 - INT(l * pl)) THEN
                  GOTO 702
            END IF

                  IF x2 < x5 THEN
                     tx = INT(x2 + xx)
                        ELSE
                           tx = INT(x2 - xx)
                  END IF

                        IF POINT(tx, ty) >= 1 THEN
                              GOTO 720
                        END IF
   NEXT ty
   GOTO 718

702  IF x2 < x5 THEN
        GOTO 705
           ELSE
              GOTO 710
    END IF
```

```
705 FOR tx = x2 TO x5
      xx = xx + 1
      yy = xx / tanb
           IF tx <= (x2 + INT(l * pl)) THEN
                GOTO 706
           END IF
                IF y2 < y5 THEN
                   ty = INT(y2 + yy)
                      ELSE
                         ty = INT(y2 - yy)
                END IF
                      IF POINT(tx, ty) >= 1 THEN
                            GOTO 720
                      END IF
706 NEXT tx
   GOTO 718
710 FOR tx = x2 TO x5 STEP -1
      xx = xx + 1
      yy = xx / tanb
            IF tx >= (x2 - INT(l * pl)) THEN
                  GOTO 711
            END IF
                  IF y2 < y5 THEN
                     ty = INT(y2 + yy)
                        ELSE
                           ty = INT(y2 - yy)
                  END IF
                        IF POINT(tx, ty) >= 1 THEN
                              GOTO 720
                        END IF
711  NEXT tx
    GOTO 718
718                LINE (x3, y3)-(x1, y1), bc
                  LINE (x2, y2)-(x5, y5), bc
                  LINE (x1, y1)-(x5, y5), bc

                  PAINT (x6, y6), cc, bc

             WRITE #1, x1, y1, x5, y5
             WRITE #4, x3, y3, x2, y2, x1, y1, x5, y5, x6, y6
720 LOOP
     CLOSE #1
     CLOSE #3
     GOTO start
  CLOSE #4

END
```

REFERENCES

Ayre, D.J. & Willis, B.L. 1988. Population structure in the coral *Pavona cactus*:clonal genotypes show little phenotypic plasticity. *Mar. Biol.* **99**:495-505.

Barnes, D.J. 1971. A study of growth, structure and form in modern coral skeletons. PhD dissertation, University of Newcastle upon Tyne, pp. 180.

Barnes, D.J. 1972. The structure and formation of growth-ridges in scleractinian coral skeletons. *Proc. R. Soc. Lond.* **182**:331-350.

Barnes, D.J. 1973. Growth in colonial scleractinians. *Bull. mar. Sci.* **23** (2):280-298.

Barnes, D.J. 1982. Light response curve for calcification in the staghorn coral *Acropora acuminata*. *Comp. Bioch. Physiol.* **73A**, 41-45.

Barnes, D.J. & Crossland, C.J. 1977. Coral calcification : sources of error in radioisotope techniques. *Mar. Biol.* **42**:119-129.

Barnes, D.J. & Crossland, C.J. 1982. Variability in the calcification rate of *Acropora acuminata* measured with radioisotopes. *Coral Reefs* **1**:53-57.

Barnes, D.J. & Devereux, M.J. 1988. Variations in skeletal architecture associated with density banding in the hard coral *Porites*. *J. exp. mar. Biol. Ecol.* **121**, 37-54.

Barnes, D.J. & Lough, J.M. 1989. The nature of skeletal density banding in scleractinian corals: fine banding and seasonal patterns. *J. exp. mar. Biol. Ecol.* **126**, 119-134.

Barnes, D.J. & Lough, J.M. 1990. Computer simulations showing the likely effects of calix architecture and other factors on retrieval of density information from coral skeletons. *J. exp. mar. Biol. Ecol.* **137**, 141-164.

Barnes, D.J. & Chalker, B.E. 1990. Calcification and photosynthesis in reef building corals and algae. In, *Ecosystems of the world: Coral reef.* **25**: 109-131. (ed. Dubinsky, Z.), Elsevier, Amsterdam.

Barnes, D.J., Lough, J.M. & Tobin, B.J. 1989. Density measurements and the interpretation of X-radiographic images of slices of skeleton from the colonial hard coral *Porites*. *J. exp. mar. Biol. Ecol.* **131**, 45-60.

Bell, A.D. 1984. Dynamic morphology:a contribution to plant population ecology. In, *Perspectives on plant population ecology*. (Ed. Dirzo, R. & Sarukhan, J.). 45-65. Sunderland, Massachusetts: Sinauer Associates Inc.

Benniger, L.K. & Dodge, R.E. 1986. Fallout plutonium and natural radionuclides in annual bands of the coral *Montastrea annularis*, St. Croix, U.S. Virgin Islands. *Geochemica et cosimochimica acta,* **50**:2785-2797.

Boto, K. & Isdale, P.J. 1985. Fluorescent bands in massive corals result from terrestrial fulvic acid inputs to nearshore zone. *Nature, Lond.* **315,** 396-397.

Brakel, W.H. 1976. The ecology of coral shape: microhabitat variation in the colony form and corallite structure of *Porites* on a Jamaican reef. PhD. Dissertation. University of Yale.

Brakel. W.H. 1977. Corallite variation in *Porites* and the species problem in corals. *Proc. 3rd Int. Coral Reef Symp., Miami.* **2**:547-462.

Brakel, W.H. 1983. Depth-related changes in the colony form of the reef coral *Porites asteroides. Symposia series for undersea research. NOAA'S Undersea research program.* **1**(1):21-27.

Brown, B.E., Sya'rani, L. & Le Tissier, M. 1985. Skeletal form and growth in *Acropora aspera* (Dana) from the Palau Seribu, Indonesia. *J. exp. mar. Biol. Ecol.* **86**:139-150.

Brown, B.E., Le Tissier, M., Howard, L.S., Charuchinda, M. & Jackson, J.A. 1986. Asynchronous deposition of dense skeletal bands in *Porites lutea. Mar. Biol.* **93**:83-89.

Buddemeier, R.W. 1974. Environmental controls over annual and lunar monthly cycles in hermatypic coral calcification. *Proc. 2nd Int. Coral Reef Symp., Brisbane.* 259-267.

Buddemeier, R.W. & Kinzie, R.A. 1975. The chronometric reliability of contemporary corals. In *Growth rhythms and the history of the earth's rotation* (ed. Rosenberg, G.D. & Runcorn, S.K.), 135-146. John Wiley.

Buddemeier, R.W. & Kinzie, R.A. III 1976. Coral growth. *Oceanog. Mar. Biol. Ann. Rev.* **14**:183-225.

Buddemeier, B.W., Maragos, J.E. & Knutson, D.W. 1974. Radiographic studies of reef coral exoskeletons:rates and patterns of coral growth. *J. exp. mar. Biol. Ecol.* 14:179-200.

Carriquiry, J.D., Risk, M.J. & Schwarcz, H.P. 1988. Timing and temperature record from stable isotopes of the 1982-83 El Nino warming event in eastern Pacific corals. *Palaios*. **3**, 359-364.

Chalker, B.E. 1981. Simulating light-saturation curves for photosynthesis and calcification by reef building corals. *Mar. Biol.* **63**:135-141.

Chalker, B.E. & Dunlap, W.C. 1981. Extraction and quantification of endosymbiotic algal pigments from reef-building corals. *Proc. 4th Int. Coral Reef Symp., Manila* **2**:45-50.

Chalker, B.E. & Dunlap, W.C. 1983. Primary production and photoadaptation by corals on the Great Barrier Reef. *Proc.Inaug. Great Barrier Reef Conference,* (ed. Baker, J.T., Sammarco, P.W. and Stark, K.P.),Townsville : James Cook University Press, 293-298.

Chalker, B.E., Dunlap, W.C. & Oliver J.K. 1983. Bathymetric adaptations of reef-building corals at Davies Reef, Great Barrier reef, Australia. II.Light saturation curves for photosynthesis and respiration. *J. exp. mar. Biol. Ecol.* **73**:37-56.

Chalker, B.E., Barnes, D.J., Dunlap, W.C. & Jokiel, P.L. 1988. Light and reef building corals. *Interdisciplinary Sci. Rev.* **13**(3):222-237.

Charuchinda, M. & Chansang, H. 1985. Skeletal extension and banding formation of *Porites lutea* of fringing reefs along the south and west coasts of Phuket Island. *Proc. 5th Int. Coral Reef Cong., Tahiti.* **6**:83-87.

Chivas, A.R., Aharon, P., Chappell, J., Vlastuin, C. & Kiss, E. 1983. Trace-elements and stable-isotopic ratios of annual growth bands as environmental indicators. *Proc. Great Barrier Reef conf.* (ed. Baker, T.J., Carter, R.M., Sammarco, P.W. & Stark, K.P.), James Cook University Press, Townsville. 77-80.

Clausen, C.D. & Roth, A.A. 1975. Estimation of coral growth-rates from laboratory ^{45}Ca-incorporation rates. *Mar. Biol.* **33**:85-91.

Coles, S.L. & Jokiel, P.L. 1977. Effects of temperature on photosynthesis and respiration in hermatypic corals. *Mar. Biol.* **43**:209-216.

Coles, S.L. & Jokiel, P.L. 1978. Synergistic effects on temperature, salinity and light on the Hermatypic coral *Montipora verrucosa. Mar. Biol.* **49**:187-195.

D'Elia, C.F. 1977. The dissolved nitrogen flux of reef corals. *Proc. 3rd Int. Coral Reef Symp., Miami* **1**:325-330.

Davies, P.S. 1984. The role of zooxanthellae in the nutritional energy requirements of *Pocillopora eydouxi. Coral Reefs* **2**:181-186.

Davies, P.S. 1989. Short-term growth measurements of corals using an accurate bouyant weighing technique. *Mar. Biol.* **101**:389-395.

Dennison, W.C. & Barnes, D.J. 1988. Effect of water motion on coral photosynthesis and calcification. *J. exp. mar. Biol. Ecol.* **115**:67-77.

Dodge, R.E. 1978. The natural growth records of reef building corals. PhD dissertation. Dept. Geography and Geophysics, Yale University, New Haven, Connecticut, 237pp.

Dodge, R.E. 1981. Growth characteristics of reef building corals within and external to a naval ordinance range: Vieques, Puerto Rico. *Proc. 4th Int. Coral Reef Symp., Manila.* **2**:241-248.

Dodge, R.E. & Thomson, J. 1974. The natural radiochemical and growth records in contemporary hermatypic corals from the Atlantic and the Caribbean. *Earth and Planetary Sci. Lett.* **23**:313-322.

Dodge, R.E. & Vaisnys, J.R. 1975. Hermatypic coral growth banding as environmental recorder *Nature Lond.***258**:706-708.

Dodge, R.E. & Vaisnys, J.R. 1977. Coral populations and growth patterns: responses to sedimentation and turbidity associated with dredging *J. Mar. Research* **35**:715-730.

Dodge, R.E. & Vaisnys, J.R. 1980. Skeletal growth chronologies of recent and fossil corals. In,*Skeletal growth of aquatic organisms.*(Ed. Rhoads, D.C. & Lutz, R.A.), Plenum Press 493-517.

Dodge, R.E. & Lang, J.C. 1983. Environmental correlates of hermatypic coral (*Montastrea annularis*) growth on the east Flower Gardens Bank, northwest Gulf of Mexico. *Limnol. Oceanogr.* **28**:228-240.

Dodge, R. E. & Gilbert, T.R. 1984. Chronology of lead pollution contained in banding coral skeletons. *Mar.Biol.* **82**:9-13.

Dodge, R.E., Aller, R.C. & Thomson, J. 1974. Coral growth related to resuspension of bottom sediments. *Nature, Lond.* **247**:574-577.

Dodge, R.E., Jickells, T.D., Knap, A.H., Boyd, S. & Bak, R.M. 1984. Reef-building coral skeletons as chemical pollution (phosphorous) indicators. *Mar. Pollut., Bull.,* **15**:178-187.

Drew, E.A. 1972. The biology and physiology of alga-invertebrate symbioses. II. The density of symbiotic algal cells in a number of hermatypic hard corals and alcyonarians from various depths. *J. exp. mar. Biol. Ecol.* **9**:71-75.

Druffel, E.M. 1985. Detection of El Nino and decade time scale variations of sea surface temperature from banded coral records: implications for the carbon dioxide cycle. In, *The Carbon Cycle and Atmospheric CO_2: Natural Variations Archean to Present. Geophysical Monograph* **32**:111-122.

Druffel, E.M. 1987. Bomb radiocarbon in the Pacific:annual and seasonal timescale variations. *J. Mar. Research* **45**:667-698.

Dubinsky, Z., Falkowski, P.G., Porter, J.W. & Muscatine, L. 1974. Absorption and utilization of radiant energy by light- and shade-adaptive colonies of the hermatypic coral *Stylophora pistillata. Proc. Roy. Soc. Lond.* B. **222**:203-214.

Dunbar, R.B. & Wellington, G.M. 1981. Stable isotopes in a branching coral monitor seasonal temperature variation. *Nature Lond.* **293**:453-455.

Dustan, P. 1975. Growth and form in the reef building coral *Montastrea annularis. Mar. Biol.* **33**:101-107.

Dustan, P. 1979. Distribution of zooxanthellae and photosynthetic chloroplast pigments of the reef-building coral *Montastrea annularis* Ellis and Solander in relation to depth on a West Indian coral reef. *Bull. mar. Sci.* **29**(1):79-95.

Dustan, P. 1982. Depth-related photoadaptation by zooxanthellae of the reef coral *Montastrea annularis. Mar. Biol.* **68**:253-264.

Emiliani, C., Hudson, J.H., Shinn, E.A. & George, R.Y. 1978. Oxygen and carbon isotopic growth record in a reef coral from the Florida Keys and in a deep-sea coral from Blake Plateau.*Science* **202**:627-629.

Fairbanks, R.G & Dodge, R.E. 1979. Annual periodicity of the $^{18}O/^{16}O$ and $^{13}C/^{12}C$ ratios in the coral *Montastrea annularis*. Geochim. Cosmochim. Acta. **43**:1009-1020.

Falkowski, P.G. & Dubinsky, Z. 1981. Light-shade adaption of *Stylophora pistillata*, a hermatypic coral from the Gulf of Eilat. *Nature Lond.* **289**:172-174.

Foster, A.B. 1979. Phenotypic plasticity in the reef corals *Montastrea annularis* (Ellis and Solander) and *Siderastrea siderea* (Ellis and solander). *J. exp. mar. Biol. Ecol.* **19**:25-54.

Foster, A.B. 1980. Environmental variables in skeletal morphology within the Caribbean reef corals *Montastrea annularis* and *Siderastrea siderea. Bull. mar. Sci.* **30**(3):678-709.

Foster, A.B. 1983. The relationship between corallite morphology and colony shape in some massive reef-corals. *Coral Reefs* **2**:19-25.

Gladfelter,E.H. 1983. Circulation of fluids in the gastrovascular system of the reef coral *Acropora cervicornis. Biol. Bull.* **165**:619-636.

Gladfelter, E.H. 1984. Skeletal development in *Acropora cervicornis*. III.A comparison of monthly rates of linear extension and calcium carbonate accretion measured over a year. *Coral Reefs* **3**:51-57.

Glynn, P.W. & Wellington, G.M. 1983. Coral growth. In, *Corals and coral reefs of the Galapogos Islands*. University of California press. 330pp.

Goreau, T.F. 1959. The physiology of skeleton formation in corals.1.A method for measuring the rate of calcium deposition by corals under different conditions. *Biol. Bull.* **116**:59-75.

Goreau, T.F. 1961. Recent investigations on the growth of coral reefs in Jamaica. *Bull. scient. Res. Coun., Jamaica,* **2**:41-44.

Goreau, T.F. 1963. Calcium carbonate deposition by coralline algae and corals in relation to their roles as reef-builders. *Ann. N.Y. Acad. Sci.,* **109**:127-167.

Goreau, T.J. 1977. Coral skeletal chemistry : physiological and environmental regulation of stable isotopes and trace metals in *Montastrea annularis. Proc. Roy. Soc. Lond.* B. **196**:291-315.

Goreau, T.F. & Goreau, N.I. 1959. The physiology of skeleton formation in corals. II. Calcium deposition by hermatypic corals under different conditions in the reef. *Biol. Bull. mar. biol. Lab. Woods Hole,* **117**:239-250.

Goreau, T.F. & Goreau, N.I. 1960. The physiology of skeleton formation in corals. III. Calcification rate as a function of colony weight and total nitrogen content in the reef coral *Manicina areolata* (Linnaeus). *Biol. Bull.* **118**:419-429.

Graus, R.R. & Macintyre, I.M. 1976. Light control on growth form in colonial reef corals:Computer simulation. *Science* **193**:895-897.

Guzman, H.M. & Cortes, J. 1989. Coral reef community structure at Cano Island, Pacific, Costa Rica. *Mar. Ecol.* **10**(1):23-41

Harper, J.L. 1977. *Population biology of plants*. London: Academic Press.

Harper, J.L. & Bell, A.D. 1979. Population dynamics of growth form in organisms with modular construction. In, *Population dynamics. 20th Symp. Br. ecol. Soc.* (Ed. Anderson, R.M., Turner, B.D. & Taylor, L.R.). 29-52. Oxford:Blackwell.

Highsmith, R.C. 1979. Coral growth rates and environmental control of density banding, *J. exp. mar. Biol. Ecol.* **37**:105-125.

Hill, D. 1981. *Treatise on invertebrate paleontology Part F. Coelenterata. supplement 1. Rugosa and Tabulata.* (Ed. Teichert, C.), 2 vols. Kansas. The geological society of America and the University of Kansas.

Hopley, D. 1983. Morphological classification of shelf reefs: a critique with special reference to the Great Barrier Reef. In, *Perspectives on coral reefs.* (Ed. Barnes, D.J.), for the Australian Institute of Marine Science, Clouston publishers.

Houck J.E. 1978. The potential utilization of scleractinian corals in the study of marine environments. Ph.D. University of Miami. 245-231.

Hudson, J.H. 1981a. Response of *Montastrea annularis* to environmental change in Florida Keys. *Proc. 4th Int. Coral Reef Symp. Manila* **2**:233-240.

Hudson, J.H. 1981b. Growth rates in *Montastrea annularis* : a record of environmental change in Key Largo Coral Reef Marine Sanctuary, Florida. *Bull. mar. Sci.* **31**:444-459.

Hudson, J.H. 1985. Long tern growth rates of *Porites lutea* before and after nuclear testing: Eniwetak Atoll (Marshall Islands). *Proc. 5th Int. Coral Reef Cong. Tahiti* **6**:179-185.

Hudson, J.H., Shinn, E.A., Halley, R.B. & Lidze, B. 1976. Sclerochronology: a tool for interpreting past environments. *Geology* **4**:361-364.

Huston, M. 1985. Variations in coral growth rates with depth at Discovery Bay, Jamaica. *Bull. mar. Sci.* **37**:928-935.

Huxley, J. 1972. Problems of relative growth. Dover publications, inc. New York.

Isdale, P.J. 1977. Variation in growth rate of hermatypic corals in a uniform environment. *Proc. 3rd Int. Coral Reef Symp. Miami* **2**:403-408.

Isdale, P.J. 1984. Fluorescent bands in massive corals record centuries of coastal rainfall. *Nature Lond.* **310**:578-579.

Jeffrey, S.W. & Humphrey, G.F. 1975. New spectrophotometric equations for determining chlorophylls *a, b,* c_1 and c_2 in higher plants, algae and natural phytoplankton. *Biochem. Physiol. Pflanzen (BPP), Bd.* **167**:191-194.

Johnston, I.S. 1980. The ultrastructure of skeletogenesis in hermatypic corals. *Int. Rev. Cytology* **67**:171-214.

Jokiel, P.L. 1978. Effects of water motion on reef corals. *J. exp. mar. Biol. Ecol.* **35**:87-97.

Jokiel, P.L. 1988. Is the photoadaptation a critical process in the development, function and maintenance of reef communities? *Proc. 6th Int. Coral Reef Symp., Townsville* **1**:187-192.

Jokiel, P.L. & Coles, S.L. 1977. Effects of temperature on the mortality and growth of Hawaiian reef corals. *Mar. Biol.* **43**:201-208.

Jokiel, P.L., Maragos, J.E. & Franzisket, L. 1978. Coral growth:bouyant weight technique. In, *Coral reefs:research methods. Monogr. Oceanogr. Methodol. (UNESCO)* **5**:529-541.

Kawaguti, S. & Sakumoto, D. 1948. The effect of light on the calcium deposition of corals. *Bull. Oceanogr. Inst. Taiwan.* **4**:65-70.

Kendall, J.J., Powell, E.N., Connor, S.J., Bright, T.J., Zastrow, C.E. 1985. Effects of turbidity in calcification rate, protein concentration and free amino acid pool of the coral *Acropora cervicornis*. *Mar. Biol.* **87**:33-46.

Klein, R., Loya, Y., Gvirtzman, G., Isdale, P.J. & Susic, M. 1990. Seasonal rainfall in the Sinai desert during the late Quaternary inferred from fluorescent bands in fossil corals. *Nature Lond.* **345**:145-147.

Knutson, D.W., Buddemeier, R.W. & Smith, S.V. 1972. Coral Chronometers: seasonal bands in reef corals. *Science* **177**:270-272.

Knutson, R.A. & Buddemeier, R.W. 1973. Distribution of radionuclides in reef corals : opportunity for data retrieval and study of effects. *Int. Atomic Energy Agency, IAEA-SM*-158/49: 736-746.

Lamberts, A.E. 1978. Coral growth:alizarin method. In, *Coral reefs: research methods. Monogr. Oceanogr. Methodol. (UNESCO)* **5**:523-527.

Lewis, J.B. 1981. Estimates of secondary production of reef corals. *Proc. 4th Int. Coral Reef Symp., Manila.* **2**:369-374.

Lewis, J.B. 1989. Spherical growth in the Caribbean coral *Siderastrea radians* (Pallas) and its survival in disturbed habitats. *Coral Reefs* **7**:161-167.

Lewis, J.B. & Price, W.S. 1975. Feeding mechanisms and feeding strategies of Atlantic reef corals. *J. Zool. Lond.* **176**:527-544.

Lewis, J.B. & Price, W.S. 1976. Patterns of ciliary currents in Atlantic reef corals and their functional significance. *J. Zool. Lond.* **178**:77-89.

Lough, J.M. & Barnes, D.J. 1990a. Possible relationships between environmental variables and skeletal density in a coral colony from the central Great Barrier Reef. *J. exp. mar. Biol. Ecol.* **134**:221-241.

Lough, J.M. & Barnes, D.J. 1990b. Intra-annual timing of density band formation of *Porites* coral from the central Great Barrier Reef. *J. exp. mar. Biol. Ecol.* **135**:35-57.

Lough, J.M. & Barnes, D.J. 1990c. Measurements of density in slices of coral skeleton: effect of densitometer beam diameter, *J. exp. mar. Biol. Ecol.* **143**:91-99.

Lowry, O.H., Rosenbrough, N.J., Farr. A.L. & Randall, R.J. 1951. Protein measurement with Folin Phenol reagent. *J. biol. Chem.***193**:265-275.

Loya, Y, 1976, Skeletal regeneration in a Red Sea scleractinian coral population. *Nature, Lond.* **261**:490-491.

Macintyre, I.G. & Smith, S.V. 1974. X-radiographic studies of skeletal development in coral colonies. *Proc. 2nd Int. Coral Reef Symp., Brisbane* **2**:277-278.

Marsh, J.A. 1970. Primary productivity of reef-building calcareous algae. *Ecology* **51**:255-263.

Maxwell, W.G.H. 1968. Atlas of the Great Barrier Reef. pp. 258. Amsterdam: Elsevier scientific.

McCloskey, L.R. & Muscatine, L. 1984. Production and respiration in the Red Sea coral *Stylophora pistillata* as a function of depth. *Proc. R. Soc. Lond.* B **222**:215-230.

Meek, S.D. 1982. Structure, growth and regeneration in the asterocoeniid scleratinian coral, *Acropora formosa.* PhD dissertation, James Cook University, PP. 237.

Meyer, J.L. & Schultz, E.T. 1985. Tissue condition and growth rate of corals associated with schooling fish. *Limnol. Oceanogr.* **30(1)**:157-166.

Moore, W.S. & Krishnaswami, S. 1972. Coral growth rates using ^{228} Ra and ^{210}Pb. *Earth and Planetary Sci. Lett.* **15**:187-190.

Moore, W.S. & Krishnaswami, S. 1974. Correlation of X-radiography revealed banding in corals with radiometric growth rates. *Proc. 2nd Int. Coral Reef Symp., Brisbane.* **2**:269-276.

Moore, W.S., Krishnaswami, S. & Bhat, S.G. 1973. Radiometric determinations of coral growth rates. *Bull. mar. Sci.* **23**:157-176.

Muscatine, L. 1973. Nutrition of corals. In, *Biology and geology of coral reefs.* Vol 2. Biol 1. (ed. Jones OA, Endean R.), Acad. Press, 77-115.

Muscatine, L. & Porter, J.W. 1977. Reef corals: mutualistic symbiosis adapted to nutrient-poor environments. *Bioscience* **27**:454-460.

Muscatine, L., McCloskey, L.R. & Loya, Y. 1985. A comparison of the growth rates of zooxanthellae and animal tissue in the Red Sea coral *Stylophora pistillata. Proc. 5th Int. Coral Reef Cong., Tahiti* **6**:119-123

Noshkin, T.E., Wong, K.M., Eagle, R.J. & Gatrousis, C. 1975 transuranics and other radionuclides in Bikini Lagoon : concentration data retrieved from aged coral sections. *Limnol. Oceanogr.* **20**: 729-742.

Patton, J.S., Abraham, S. & Benson, A.A. 1977. Lipogenesis in the intact coral *Pocillopora capitata* and its isolated zooxanthellae: Evidence for a light-

driven carbon cycle between symbiont and host. *Mar. Biol.* **44**:235-247.

Pätzold, J. 1984. Growth rhythms recorded in stable isotopes and density bands in the reef coral *Porites lobata* (Cebu, Philippines). *Coral Reefs* **3**:87-90.

Potts, D.C., Done, T.J., Isdale, P.J. & Fisk, D.A. 1985. Dominance of a coral community by the genus *Porites* (Scleractinia). *Mar. Ecol. Prog. Ser.* **23**:79-84.

Porter, J.W. 1974. Zooplankton feeding by the Caribbean reef-building coral *Montastrea cavernosa. Proc. 2nd Int. Coral Reef Symp., Brisbane* **1**:111-125.

Porter, J.W. 1976. Autotrophy, heterotrophy, and resource partitioning in Caribbean Reef building corals. *The American Naturalist.* **110** (975):731-742.

Porter, J.W. 1985. The maritime weather of Jamaica: its effects on annual carbon budgets of the massive reef-building coral *Montastrea annularis. Proc. 5th Int. Coral Reef Congr., Tahiti.* **6**:363-367.

Porter, J.W., Muscatine, L., Dubinsky, Z. & Falkowsky, P.G. 1984 Primary production and photoadaptation in light- and shade-adapted colonies of the symbiotic coral, *Stylophora pistillata. Proc. R. Soc. Lond.* B **222**:161-180.

Roos, P.J. 1967. Growth and occurrence of the reef coral *Porites asteroides* Lamark in relation to submarine radiance distribution. Ph.D. Dissertation. University of Amsterdam.

Rosen, B.R. 1986. Modular growth and form of corals: a matter of metamers? *Phil. Trans. R. Soc. Lond.* B. **313**:115-142.

Schneider, R.C. & Smith, S.V. 1982. Skeletal Sr content and density in *Porites* spp. in relation to environmental factors. *Mar. Biol.* **66**:121-131.

Sebens, K.P. 1987. Coelenterata. In, *Animal energetics*, vol 1. (Ed. Pandian, T.J. & Vernberg, F.J.) pp. 55-120. Academic Press.

Shen, G.T. & Boyle, E.A. 1987. Lead in corals : reconstruction of historical fluxes to the surface ocean. *Earth and planetary science let.* **82**:289-304.

Shen, G.T. & Boyle, E.A. 1988. Determination of lead, cadmium and other trace metals in annually-banded corals. *Chemical Geology.* **67**:47-62.

Shen, G.T., Boyle, E.A. & Lea, D.W. 1987. Cadmium in corals : chronicles of historical upwelling and industrial fallout. *Nature Lond.* **328**:794-796.

Smith, D., Muscatine, L. & Lewis, D. 1969. Carbohydrate movement from autotrophs to heterotrophs in parasitic and mutualistic symbiosis. *Biol.Rev.* **44**:17-90.

Smith, S.V. & Kinzie, D.W. 1978. Calcification and organic carbon metabolism as indicated by carbon dioxide. In, *Coral reefs: research methods. Monogr. Oceanogr. Methodol. (UNESCO)* **5**:469-484.

Sorokin, Y.I. 1973. On the feeding of some scleractinian corals with bacteria and dissolved organic matter. *Limnol. Oceanogr.* **18**(3): 380-385.

Sorokin, Y.I. 1980. Experimental investigation of heterotrophic nutrition of abundant species of reef-building corals. *Dokl. Akad. Nauk. SSSR. Ser. Biol.* **249**:(1-6):1323-1326.

Sorokin, Y.I. 1981. Aspects of the biomass, feeding and metabolism of common corals of the Great Barrier Reef, Australia. *Proc. 4th Int. Coral Reef Symp., Manila* 2:27-32.

Stearn, C.W., Scoffin, T.P. & Martindale, W. 1977. Calcium carbonate budget of a fringing reef on the west coast of Barbados. Part 1 -zonation and productivity. *Bull. mar. Sci.* **27**:479-510.

Stephenson, T.A. 1931. Development and formation of colonies on *Pocillopora* and *Porites* Part 1. *Scient. Rep. Gt. Barrier Reef Exped. 1928-1929,* **3**(3):129-134.

Thompson, D. W. 1963. On growth and form. Vol.1 & 2. 2nd Edn. Cambridge at the University Press.

Titlyanov, E.A. 1981. Adaption of reef-building corals to low light intensity. *Proc. 4th. Int. Coral Reef Symp., Manila* **2**:39-43.

Titlyanov, E.A. 1987. Morphological differences of colonies of reef-building branching corals living in different light regimes. *Sov. J. Mar. Biol.* **13**(1):28-32.

Vandermeulen, J.H., Davis, N. & Muscatine, L. 1972. The effect of inhibitors of photosynthesis on zooxanthellae in corals and other marine invertebrates, *Mar. Biol.* **16**:185-191.

Veron, J.E.N. 1981. The species concept in the *Scleractinia of Eastern Australia. Proc. 4th Int. Coral Reef Symp., Manila.* **2**:183-186.

Veron, J.E.N. 1986. Corals of Australia and the Indo-Pacific. Angus and Robertson Publish.

Veron, J.E.N. & Pichon, M. 1982. Scleractinia of eastern Australia Part IV, Family Poritidae *Australian Institute of Marine Science Monograph series.* **5**

Weber, J.N., White, E.W. & Weber, P.H. 1975a. Correlations of density banding in reef coral skeletons with environmental parameters : the basic for interpretation of chronological record preserved in the coralla of corals. *Paleobiology* **1**:137-149.

Weber, J.N., Deines. P, White, E.W. & Weber, P.H. 1975b. Seasonal high and low density bands in reef coral skeletons. *Nature Lond.* **255**:697-698.

Weil, S.M., Buddemeier, R.W., Smith, S.V. & Kroopnick, P.M. 1981. The stable isotopic composition of coral skeletons : control by environmental variables. *Geochemica et Cosmochimica Acta,* **45**:1147-1153.

Wellington, G.M. & Glynn, P.W. 1983. Environmental influences on skeletal banding in eastern Pacific (Panama) corals. *Coral Reefs* **1**:215-222.

Wells, J.W. 1956 In, *Treatise on Invertebrate Paleontology*, (ed. Moore, R.C.), *Part F, Coelenterata,* 328-477.

Wijsman-Best, M. 1974. Habitat-induced modification of reef corals (*Faviidae*) and its consequences for taxonomy. *Proc. 2nd. Int. Coral Reef Symp., Brisbane.* **2**:217-228.

Wilkinson, C.R. & Cheshire, A.C. 1988. Cross-shelf variations in coral reef structure and function - influences of land and ocean. *Proc. 6th Int. Coral Reef Symp., Townsville* **1**:227-233.

Willis, B.L. 1985. Phenotypic plasticity versus phenotypic stability in the reef corals *Turbinaria mesenterina* and *Pavona cactus. Proc. 5th Int. Coral Reef Cong., Tahiti* **4**:107-112.

Willis, B.L. & Ayre, D.J. 1985. Asexual reproduction and genetic determination of growth form in the coral *Pavona cactus*: biochemical genetic and immunogenic evidence. *Oceologia* (Berlin) **65**:516-525.

Zar, J.H. 1984. Biostatistical analysis. 2nd Edn. Prentice-Hall, New Jersey, U.S.A.